GEOLOGICA ULTRAIECTINA

Mededelingen van het
Instituut voor Aardwetenschappen der
Rijksuniversiteit te Utrecht

No. 48

SEAFLOOR SPREADING PATTERN OF THE NORTH ATLANTIC BETWEEN 10° AND 40° N

A RECONSTRUCTION BASED ON SHIPBORNE MEASUREMENTS AND SATELLITE ALTIMETER DATA

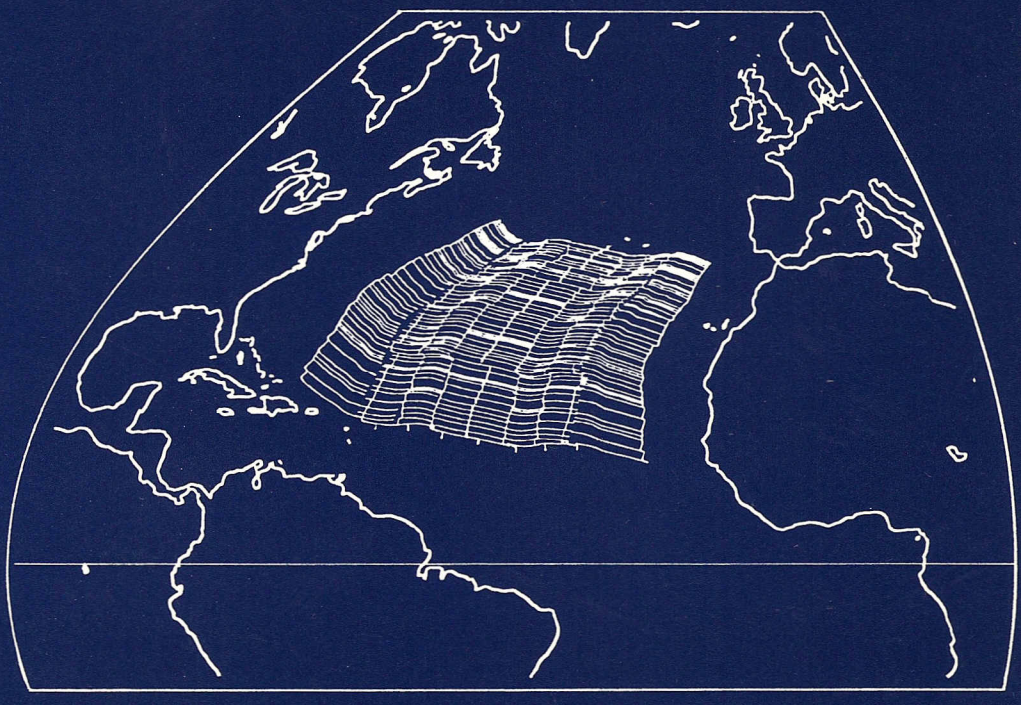

WALTER ROEST

STELLINGEN

1

Het gebruik van een totale separatiepool in plaats van een halfpool voor de rotatie van de huidige spreidingsrug naar een oude positie is principieel onjuist. De hierdoor veroorzaakte fout van ongeveer 15 km in de positie van de frakturezones in een rekonstruktie door Patriat *et al.* (1985) kan van grote invloed zijn op hun konklusie dat frakturezones zich niet stationair gedragen.

Patriat Ph., Segoufin J., Goslin J., Beuzart P. - *Earth Planet. Sci. Lett.*, **75**, 204-214, 1985
Dit proefschrift, hoofdstuk 4

2

Het vulkano-tektonische komplex van Royal Trough en Researcher Ridge & Trough is ontstaan ten gevolge van rek welke samenhangt met de differentiële beweging tussen Noord- en Zuidamerika. Het feit dat dit komplex zich uitstrekt ten noorden en zuiden van de Fifteen Twenty Fracture Zone vormt een aanwijzing dat frakturezones niet zwakker zijn dan de overige oceaanlithosfeer.

3

Het beschikbaar komen van Seasat-satellietwaarnemingen van de hoogte van het zeeoppervlak vormt een mijlpaal in het geofysisch onderzoek van de oceaan.

4

Door toepassing van het zwaartekrachtsfilter op de Seasat-satellietwaarnemingen van de gemiddelde hoogte van het zeeoppervlak worden de gegevens in het golflengte bereik van 30-400 km bij uitstek geschikt voor het bestuderen van het frakturezonepatroon.

Dit proefschrift, hoofdstuk 2

5

De gewoonte om de zgn. stagepolen te bepalen *tussen* magnetische isochronen komt veelal voort uit een gebrek aan topografische informatie. Ten onrechte zou gekonkludeerd kunnen worden dat er een werkelijke relatie tussen veranderingen in de relatieve beweging van platen en ompolingen in het aardmagneetveld bestaat.

6

Het woord stroomlijn (flowline) dat algemeen wordt gebruikt als men het over de sporen van het aangroeien van de oceaanlithosfeer heeft, is niet gelukkig gekozen aangezien het vervormingen in de oudere oceaanlithosfeer suggereert. Voorzover er al sprake is van stromen, treedt dit op tengevolge van thermische kontraktie in de jonge oceaanlithosfeer en wel loodrecht op de "stroomlijnen".

7

Het beschrijven van frakturezones met cycloïden in plaats van met kleincirkelsegmenten opent de weg naar de mathematische formulering van een kontinue baan van rotatiepolen.

Cronin V.S. - *EOS trans. Am. Geophys. Un.*, **67**, 1210, 1986

8

Reeds bij de zeer geringe lichtintensiteiten, die worden gebruikt bij het - psychofysisch - meten van de absolute drempel van het menselijk oog, treedt adaptatie op tengevolge waarvan de drempel verhoogd wordt.

9

Uit Hermans' uitspraak "Romanschrijven is wetenschap bedrijven zonder bewijs" mag niet worden afgeleid dat in de wetenschap wel altijd bewijs wordt geleverd.

W.F. Hermans, Het sadistische universum, Amsterdam, 1971

10

De fabrikant van software welke voor edukatieve doeleinden wordt gebruikt, zou zelf voor beveiligingen tegen illegaal kopiëren dienen zorg te dragen en niet de onderwijsinstellingen verantwoordelijk stellen voor de verspreiding van illegale kopieën door studenten.

11

De astronomische bedragen die schilderijen tegenwoordig op veilingen opbrengen (b.v. *Zonnebloemen* van Vincent van Gogh, Christie's, Londen, 30 maart 1987) maken het voor musea steeds moeilijker grote overzichtstentoonstellingen te organiseren, daar de verzekeringskosten bij bruikleen uit het buitenland navenant stijgen.

12

Genieten van het proces dat leidt tot een doel, dat is het geheim dat afrekent met de mythe van de grote beloning en de tijdsbesparing. Immers, telkens wanneer een doel is bereikt wordt het Niet Zo Leuk meer en stormen we weer af op het volgende en dan op het daarop volgende.

Naar: Benjamin Hoff, Tao van Poeh, Den Haag, 1986

13

Het principe van Zeno's paradox over Achilles en de schildpad gaat niet op voor het ledigen van een fles whisky.

14

Een bouwwerk is pas gereed als de laatste stelling is afgebroken.

Ad Stolk (pers. med.)

Stellingen behorende bij het proefschrift "Seafloor spreading pattern of the North Atlantic between 10° and 40° N".

Utrecht, 17 juni 1987 Walter Roest

GEOLOGICA ULTRAIECTINA

Mededelingen van het
Instituut voor Aardwetenschappen der
Rijksuniversiteit te Utrecht

No. 48

SEAFLOOR SPREADING PATTERN OF THE NORTH ATLANTIC BETWEEN 10° AND 40° N

A RECONSTRUCTION BASED ON SHIPBORNE MEASUREMENTS AND SATELLITE ALTIMETER DATA

SEAFLOOR SPREADING PATTERN OF THE NORTH ATLANTIC BETWEEN 10° AND 40° N

A RECONSTRUCTION BASED ON SHIPBORNE MEASUREMENTS AND SATELLITE ALTIMETER DATA

SPREIDINGSPATROON VAN DE NOORDATLANTISCHE OCEAAN TUSSEN 10° EN 40° N

EEN REKONSTRUKTIE GEBASEERD OP METINGEN OP ZEE EN SATELLIET-WAARNEMINGEN VAN DE HOOGTE VAN HET ZEEOPPERVLAK

(met een samenvatting in het Nederlands)

PROEFSCHRIFT

TER VERKRIJGING VAN DE GRAAD VAN DOCTOR IN DE WISKUNDE EN NATUURWETENSCHAPPEN AAN DE RIJKSUNIVERSITEIT TE UTRECHT, OP GEZAG VAN DE RECTOR MAGNIFICUS PROF. DR. J.A. VAN GINKEL VOLGENS BESLUIT VAN HET COLLEGE VAN DEKANEN IN HET OPENBAAR TE VERDEDIGEN OP WOENSDAG 17 JUNI 1987 DES NAMIDDAGS TE 2.30 UUR

DOOR

WALTHERUS ROBERTUS ROEST

GEBOREN OP 1 JUNI 1958 TE DORDRECHT

PROMOTOR: PROF. DR. B.J.COLLETTE

El desorden, la incoherencia y la variedad no son inaccesibles, pero es indispensable que los gobierne un orden secreto, que gradualmente se descubra.

Jorge Luis Borges, Otras inquisiciones

The state of chaos, incoherence, flux is not inaccessible, though it must be governed by a secret order that is gradually disclosed.

Contents

Chapter One

Introduction

1.1 The floor of the Atlantic Ocean between 10° N and 40° N

A detailed analysis of the pattern of fracture zone directions and seafloor spreading magnetic anomalies in the North Atlantic between 10° and 40° N will be carried out in order to reconstruct the history of the relative motion between Africa and North America. The present reconstruction forms a refinement of the reconstruction of the spreading pattern since anomaly 34 presented by Collette *et al.* (1984) and of that by Slootweg and Collette (1985) for the Cretaceous Magnetic Quiet Zone. These spreading histories are based on shipborne measurements carried out on the African plate. In the present study, data collected on the American plate will be included, as well as Seasat altimeter data.

Figure 1.1 shows a shaded relief of the study area, based on the Digital Bathymetric Data Base (DBDB5, 1984). It gives a good illustration of the regional structure of the ocean floor and the elements which are important for the understanding and the reconstruction of the spreading history. These elements are in the first place the curved Mid-Atlantic Ridge and the generally east-west trending oceanic fracture zones. Fossil fracture zones show directions which are (sub)-parallel to the direction of spreading at the time they were formed in the transform domain (Wilson, 1965). Their traces can be used as constraints for the construction of synthetic flowlines (Morgan, 1968).

The deepening of the ocean floor away from the spreading center reflects the depth/age relation of oceanic lithosphere (Parsons and Sclater, 1977). This means that the depth contours generally follow the isochrons, i.e. the lines of equal age. These isochrons can be accurately determined from the magnetic seafloor spreading anomalies (Vine and Matthews, 1963).

Furthermore one sees seamount groups, in general associated with a regional swell, and some island groups. A few seamount groups in the central North Atlantic are known to be related to differential movement between lithospheric plates. E.g. the Azores have been formed as a response to the differential motion between Africa and Eurasia (Searle, 1980; Srivastava and Tapscott, 1986); The volcano-tectonic complex of Researcher Ridge & Trough and Royal Trough finds its origin in the differential movement between North and South America (Roest and Collette, 1986; this study). Locations of other seamount groups should be considered as possible places for former plate boundaries.

Figure 1.1 - Shaded relief of the floor of the North Atlantic between 10° and 40° N. The bathymetry is based on DBDB5 (1985), and illuminated from the north-west. In addition, the depth contours are given at an interval of 1000 m.

1.2 Earlier reconstructions of the spreading pattern

Since the work of Heirtzler *et al.* (1968), several reconstructions of the relative motion of North America and Africa have been carried out (Le Pichon and Fox, 1971; Pitman and Talwani, 1972; Francheteau, 1973; Sclater *et al.*, 1977). Recent reconstructions are those of Collette *et al.* (1984), of Olivet *et al.* (1984), and of Klitgord & Schouten (1986). Archambault (1984) described the post-Eocene spreading history of the North Atlantic Ocean, as a refinement of the model of Olivet *et al.* (1984), who presented only one pole of rotation since anomaly 13. Slootweg and Collette (1985) reconstructed the spreading pattern in the Cretaceous Magnetic Quiet Zone on the African plate.

Most reconstructions are based on the fit of magnetic anomaly lineations mainly, and make no use of directions of fracture zones. This implies that changes in spreading direction are assumed to take place at the position of magnetic anomalies, which is not necessarily true. Collette *et al.* (1984) and Slootweg & Collette (1985) used fracture zone directions on the African plate as primary information for the calculation of poles of motion. Rotation angles were subsequently defined, using the magnetic lineations. In the present study, we will develop a method that allows the simultaneous use of fracture zone traces, as the primary data on spreading directions, as well as magnetic data in one model for the spreading history. Data on both the American and the African plate will be combined.

1.3 Data

The study started from the analysis by Collette *et al.* (1984) of seismic reflection and magnetic data obtained during the Kroonvlag Project and during detailed surveys, including gravity, carried out by the Vening Meinesz Laboratorium. As the greater part of the Kroonvlag measurements were carried out on board of ships going from The Netherlands to Surinam v.v., the data mainly cover the African plate. Only a few tracks were obtained by ships going to Caribbean Islands. It appeared that more data on the American plate were necessary to refine the spreading history. During the Nedlloyd Project in 1984 we obtained 3 additional tracks with seismic reflection and magnetic data, filling in large gaps between existing ship-tracks. These additional data allowed a correlation of fracture zone cross-sections between different tracks on the American plate, and a first revision of the spreading model of Collette *et al.* (1984).

In 1985, we obtained access to the Geophysical Data Records with the Seasat altimeter data (Lorell *et al.*, 1980). Several authors used altimeter data to study the step in the mean seasurface height over fracture zones in the Pacific Ocean for determining parameters concerning the thermal structure of the oceanic lithosphere (Crough, 1979; Detrick, 1981; Cazenave *et al.*, 1982 and 1983; Sandwell and Schubert, 1982a). No extensive use has yet been made of the high quality Seasat data for the reconstruction of oceanfloor spreading, although the data coverage provides an unique opportunity to do so. Comparison of the mean seasurface height with shipborne gravity and seismic reflection data over Atlantic fracture zones shows that the geoid only reveals the larger offset fracture zones. The construction of along-track gravity allows a much more accurate tracing of fracture zones from Seasat.

1.4 Outline of the study

In the first place, the study meant to provide additional information on the nature of the fanning of transform fault directions, first observed by Collette (1974). Roest *et al.* (1984) analysed GLORIA long range side-scan sonar data over five large offset transform faults in the area. They found a systematic deviation of their directions with respect to those predicted by the RM2 pole of Minster and Jordan (1978), varying from about 3° for Oceanographer Fracture Zone to about -4° for the Fifteen Twenty. The deviating transform fault directions, and the curving of fracture zones in the younger part of the lithosphere were related to thermal contraction in the horizontal plane, in combination with the fanning of the ridge push resulting from the sinusoidal shape of the ridge.

We started with an analysis of the pattern of transform faults and (fossil) fracture zones between the Fifteen Twenty and the Vema Fracture Zone. This showed that the curvature of the Fifteen Twenty Fracture Zone in crust younger than anomaly 13 and the deviation of its transform fault direction must, at least partly, be the result of a real change in spreading direction. The major evidence for this change in spreading direction was found in the fact that the distance between the Marathon and Fifteen Twenty Fracture Zone near anomaly 6 is about 15% less than at present, which is much more than can be explained by thermal contraction in the horizontal plane alone. The explanation is found in the geometric adjustment of the ridge segments and transform faults in this area, in response to a counter clockwise change in spreading direction (Figure 1.2). After the recognition of this change in spreading direction, which does not show in fracture zones farther north, the fossil fracture zone pattern on the American plate south of the Fifteen Twenty Fracture Zone was analysed further. From this analysis it was concluded that, although these fracture zones seem to follow the spreading pattern between North America and Africa as observed by Collette *et al.* (1984), they are in fact rotated over about 1-2° . This small rotation is the result of a recent (about 10 Ma B.P.) jump of the plate boundary between North and South America from a southern position towards a position near the Fifteen Twenty Fracture Zone.

This part of the study led to a first publication on the subject (Roest and Collette, 1986). The northward migration of the plate boundary between North and South America, as proposed in this paper, will be investigated further in the present study.

The next question was whether the fanning still exists when the direction of the Fifteen Twenty Fracture Zone is not considered. To answer this question, we calculated a new pole for the present daty relative motion between North America and Africa, based on magnetic anomalies and fracture zone data north of the Fifteen Twenty Fracture Zone. Using the data on both the American and African plate, we also investigated whether the deviating transform directions influence the trace of the fossil fracture zones, i.e. whether there is evidence for a difference in fracture zone distances east and west of the Mid-Atlantic Ridge, as predicted by Roest *et al.* (1984; also Collette *et al.*, 1984).

An other question concerned the reconstruction of the Cretaceous Magnetic Quiet Zone on the African plate by Slootweg and Collette (1985). These authors found evidence for a large clockwise change in spreading direction that took place about 100 Ma B.P., and which was followed by an even larger counter-clockwise change before anomaly 34. The rotation poles in this period are situated in the North Atlantic at about 43° N, west of Galicia Bank. This has major consequences for the reconstruction of the relative

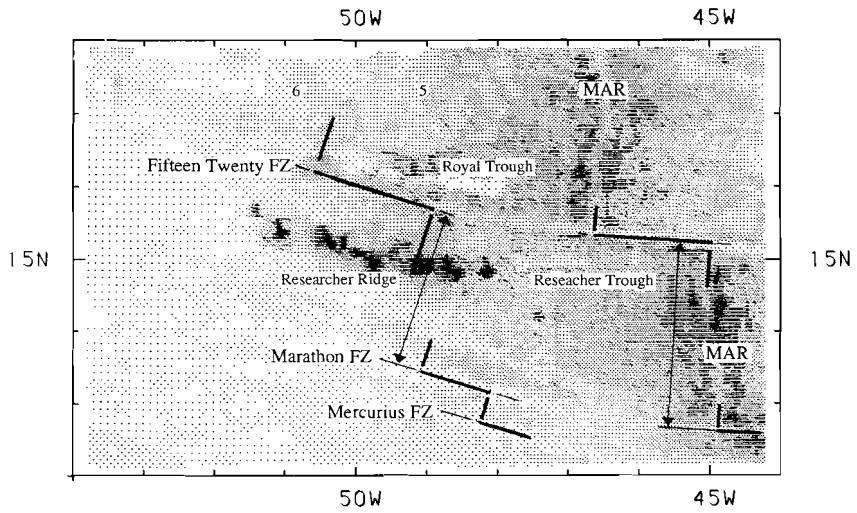

Figure 1.2 - A change in spreading direction near anomaly 5 resulted in a geometric adjustment of fracture zones and spreading elements in the area south of the Fifteen Twenty Fracture Zone. As a result, the present distance between the Marathon Fracture Zone and the Fifteen Twenty Fracture Zone is significantly larger than it was in the period between anomalies 6 and 5. (MAR: Mid-Atlantic Ridge)

motion between the Eurasian plate and Africa and, more specifically, for the differential movements of Western Europe (the end of the opening of the Bay of Biscay; the position of the plate boundary between Europe and Africa). The correctness of the reconstruction of the spreading in the Cretaceous Magnetic Quiet Zone was tested with the additional data on the American plate.

Several authors related the origin of the New England Seamount Chain and the Corner Seamounts to a hot-spot (cf. Duncan, 1984). An alternative explanation may be found in differential motion between parts of the major lithospheric plates. The same holds for the Atlantis-Meteor Seamount Complex, which was studied by Verhoef (1984). Verhoef and Collette (1985) proposed, as an alternative to the hot-spot model, that lithospheric fracturing is the origin of this extensional volcanic complex. The existence of a second order plate boundary, as a cause of this lithospheric fracturing was tested.

We will proceed this study in the following way. After a description of the different data sets that are used for the analysis of the spreading pattern, we discuss the morphology of fracture zones and their gravity signal.

A method is formulated for the combination of fracture zone directions and magnetic anomalies on both plates in the determination of the stage poles which describe the instantaneous relative motion.

After the analysis of the data and the presentation of the reconstruction, an evalutation of the accuracy of the rotation poles in relation with the accuracy in the data is given. Finally, we will discuss the results of the reconstruction in the light of the questions formulated above.

Chapter Two

Data

2.1 Introduction

Different types of marine and other geophysical data can be used to study the spreading history of an ocean. In the present study we used shipborne data (continuous seismic reflection data, precision depth recording, magnetic and gravity measurements) and satellite altimeter measurements, providing high quality data on the seasurface height.

In this chapter these data sets are described together with the way they are processed to provide an optimal set of documents to be used in the reconstruction:

- Seismic reflection profiles are used mainly for the recognition of oceanic fracture zone pattern. Following the results from the Kroonvlag project (Collette *et al.*, 1984), we will use high-pass filtered basement topography profiles.
- The Digital Bathymetric Data Base DBDB5 (1984) is used to provide a reliable regional framework for the reconstruction.
- Magnetic anomalies give information on the age of the ocean floor as well as on fracture zone trends (cf. Collette *et al.*, 1984; Twigt, 1980). Computer techniques will be used to construct contour maps of the magnetic anomalies.
- Shipborne gravity is used to delineate fracture zones in areas where thick sedimentary coverage obscures the basement relief associated with the fracture zones. In addition, the shipborne gravity data are used to calibrate the Seasat altimeter data.
- Seasat altimeter data are used to complete the fracture zone gravity anomaly pattern, especially in areas where no other data are available. The Seasat anomaly charts also provide a convenient reference for the reconstruction of the flowline pattern.

All processing, starting with digitizing, editing, profile plotting, computer gridding and contour-plotting, is done with the FELIX database and presentation system, which has been developed at the department of marine geophysics since 1974.

2.2 Bathymetry and seismic reflection data

The study of the central North Atlantic fracture zone pattern was originally started on the basis of the seismic reflection data and magnetic anomalies obtained during the Kroonvlag Project (Collette *et al.*, 1984). In the present study also the results of expeditions which were conducted as part of the Vaarplan (Twigt *et al.*, 1983; Slootweg and Collette, 1985; Verhoef and Collette, 1985), and of the Nedlloyd-project, are included.

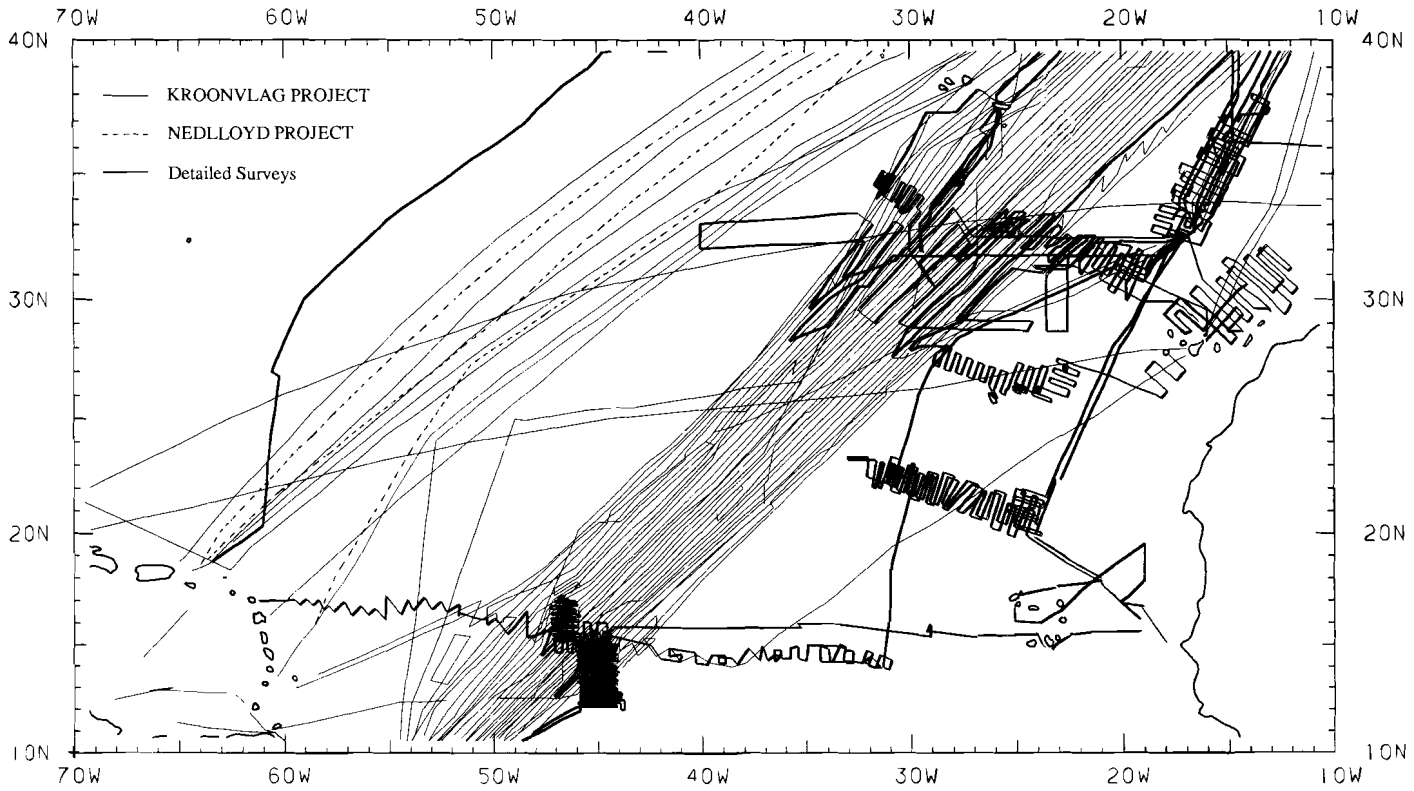

Figure 2.1 - Chart of tracklines along which seismic reflection data were recorded.

Figure 2.1 gives the trackchart of the different projects. Line drawings of the seismic reflection data along these lines have been digitized (Collette *et al.*, 1984). Due to the fact that the shiptracks are covering oceanfloor of different ages, and hence of different depths, presentation of the observed data projected along-track does not resolve the fracture zone pattern well. A high pass filter must be applied to eliminate the wavelengths related with the subsidence of older lithosphere. Although along-track filtering is possible, it was decided to subtract a regional surface from the data. The main advantage of this procedure is that a regional surface is more reliable than an along-track regional, and that it does not introduce artificial cross-over errors. The regional surface was constructed by interpolation of the oceandepth data on a grid, using the weightfunction method described by Slootweg (1978). The value of each grid-point was computed as a weighted mean of surrounding data. The weight function which appeared to produce a good result was the space-domain representation of a Butterworthfilter with a cut-off wavelenght of 60 nm and a roll-off of 6 dB/octave. Plate I displays the filtered basement topography. Topography deeper than the reference surface has been shaded.

Although the human eye is a good interpolator, an attempt was made to produce an alternative for Plate I in the form of an illuminated surface. Again a surface was constructed, which fitted the data. In contrast with the regional surface, in this case the along-track resolution had to be maintained. As the mean fracture zone trend in the Kroonvlag area is about 100°, an anisotropic filter was used with a long axis of 1.5 times in this direction. To enhance the fracture zone pattern, the directional derivative was calculated to imitate illumination. The type of structures that is enhanced in this way depends on the direction of illumination. Plate II gives a shadowgram for the basement topography with the direction of the artificial sun at 10°.

The Digital Bathymetric Data Base (DBDB5, 1984) gives ocean depth data in uncorrected meters on a 5' grid in latitude and longitude. Due to the grid distance, the resolution of the data base is less than that of the GEBCO sheets (e.g. GEBCO, 1982a & 1982b). A large advantage is that maps can be produced at any scale and projection, and with different contour intervals. Digital image processing techniques may be used to enhance different features (e.g. Heirtzler, 1985). Plate III is a normal contourmap of the study area, with a contour interval of 500 m.

2.3 Magnetics

Magnetic anomalies form a very important tool for the reconstruction of relative plate motion. Magnetic seafloor spreading anomalies make it possible to estimate the age of the ocean floor. Due to the age contrast over fracture zones, magnetic fracture zone anomalies can be expected. However, it is not only the magnetic contrast between crust of different age to both sides of the fracture zone that causes this magnetic fracture zone anomaly. Also in the Cretaceous Magnetic Quiet Zone (CMQZ), where no polarity reversals occur, fracture zones can be traced from their magnetic anomalies (Twigt *et al.*, 1983; Slootweg and Collette, 1985; Verhoef and Duin, 1986). Fracture zone valleys in the CMQZ are characterized by a higher than normal magnetization.

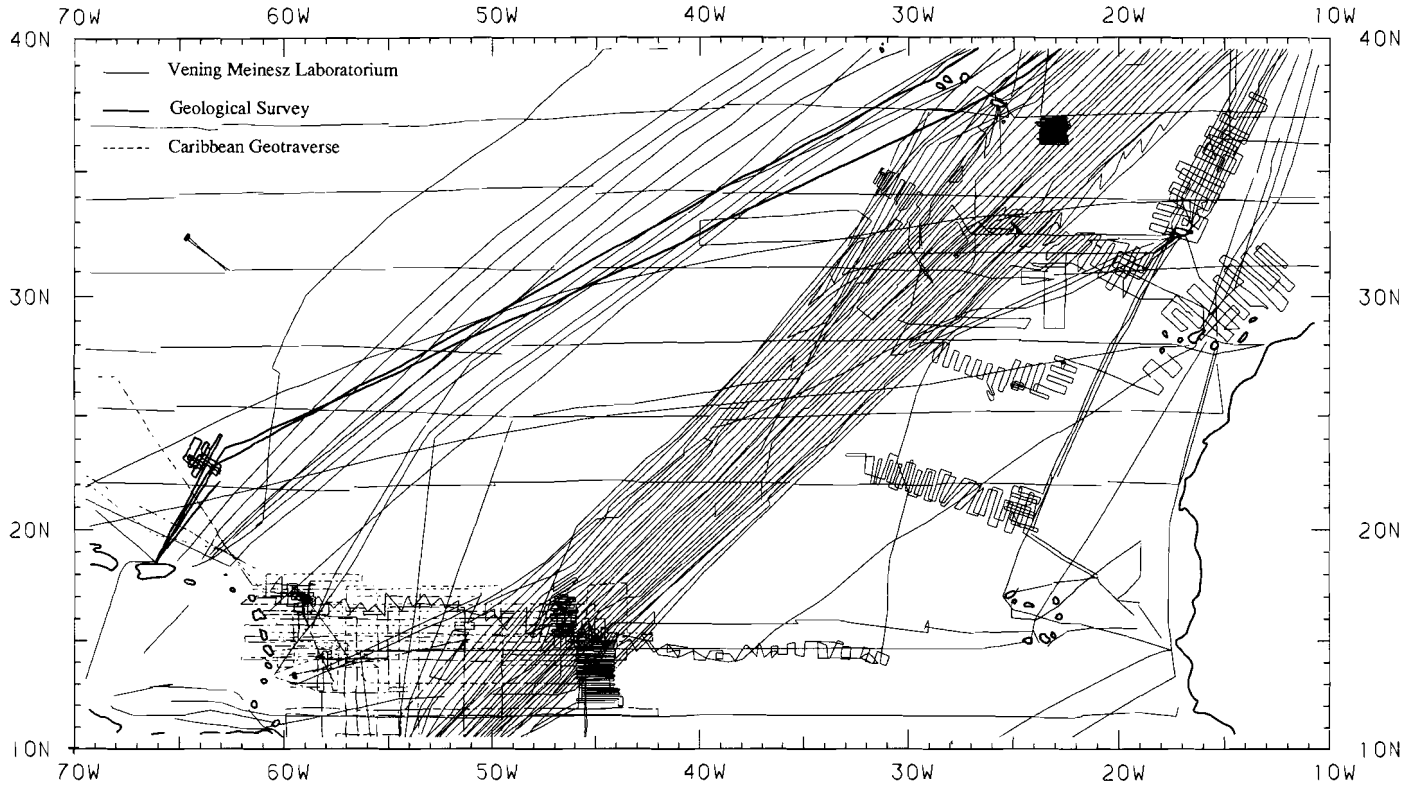

Figure 2.2 - Distribution of shiptracks with magnetic data.

Because of the interference of fracture zone and seafloor spreading anomalies, profile charts of magnetic anomalies can be difficult to interprete. A way to present magnetic anomalies avoiding this interference problem, is by contour map (e.g. Verhoef *et al.*, 1986).

Figure 2.2 gives the distribution of ship-tracks along which the total magnetic intensity was measured. The greater part was collected by the Vening Meinesz Laboratorium. Data of the Caribbean geotraverse, in the area between the Mid-Atlantic Ridge and the Caribbean subduction zone, and latitudes 10° - 20° N, were included (Peter *et al.*, 1973a & b). Furthermore the Dutch Geological Survey collected data during the Seabed Program (Kuypers *et al.*, 1984). The track-geometry of the Kroonvlag- project, with a trackspacing of about 30 km, poses a problem, when computer-contouring of the magnetic data is performed. Leveling problems, partly associated with the timedependent character of the magnetic field, are not fully resolved by the IGRF corrections. As there are almost no tracks intersecting, a cross-over analysis cannot solve this problem. A digital filter will be applied to reduce the artifacts which are due to the track-geometry.

The construction of the gridded dataset enables the correction of the magnetic anomalies for the fact that they are shifted with respect to their source, and the fact that the magnetic anomalies caused by N-S structures at lower latitudes are of relatively low amplitude (Schouten, 1971). The operator "reduction to the pole" (Le Mouel *et al.*, 1972), corrects not only for the direction of the magnetic vectors, but also for the amplitude effect. The operator gets directionally unstable at very low latitudes.

After application of the operator "reduction to the pole", a directional derivative (high-pass) filter was used, to enhance the individual magnetic anomalies.

Data processing

The data were edited, and reduced to magnetic anomalies, using the IGRF reference fields (IAGA, 1981). The latest IGRF fields (IAGA, 1986) differ from the former ones in the periods 1945-1965 and 1975-1990. The oldest data of the present data set are from the end of 1964 (Anomymous, 1967). For these data the differences are negligibly small. The definitive reference values for 1980 (the DGRF 1980) and the new IGRF 1985 would involve small changes which are not relevant for the present study.

The anomalies were computer contoured on a 3 nm grid, with the weight-function method (Slootweg, 1978). The weight-function used is the space-domain representation of a Butterworth filter with cut-off wavelength 30 nm and a steepness of 6 dB/octave. As the weigth-function in Figure 2.3 shows, the individual data points have influence on an area with radius of 18 nm. With an average track spacing of about 15 nm for the Kroonvlag data, there is only a small overlap of data in between two adjacent shiptracks. In Figure 2.4a an example is shown of the strong dependence of the contours of the track geometry. This is even more clear in the powerspectrum of the gridded dataset (Figure 2.5) in this area. Maxima in the power occur in the direction of about -45° and 135°, which is perpendicular to the shiptracks.

Directional filtering

One way to solve the problem of track biased contours is the use of a longer cut-off

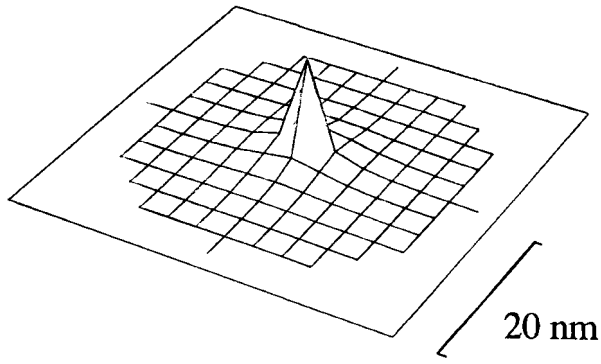

Figure 2.3 - Weight-function used in the gridding process. This weigth-function is the space domain representation of a Butterworth filter with cut-off wavelength 30 nm and a steepness of 6 dB/octave.

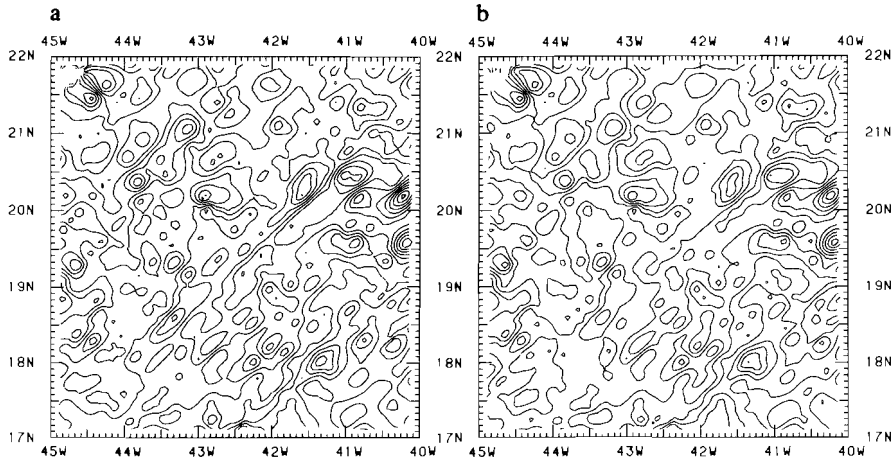

Figure 2.4 - (a) Detail of magnetic contours (contour-interval 25 nT), showing artifacts due to the distribution of tracks. (b) After application of a directional filter in the direction -45° and 135° and a half width of 10°.

wavelength in the gridding process. However, this would reduce the resolution of the data along-track. Inspection of the powerspectrum in Figure 2.5 shows that it must be possible to reduce the artifacts caused by the track- distribution by a directional filter. An example of such a filter, which is applied in the wavenumber domain, is given in Figure 2.6. After multiplication of the Fourier transformed gridded anomalies with a directional filter and inverse transformation, we obtain the anomalies displayed in

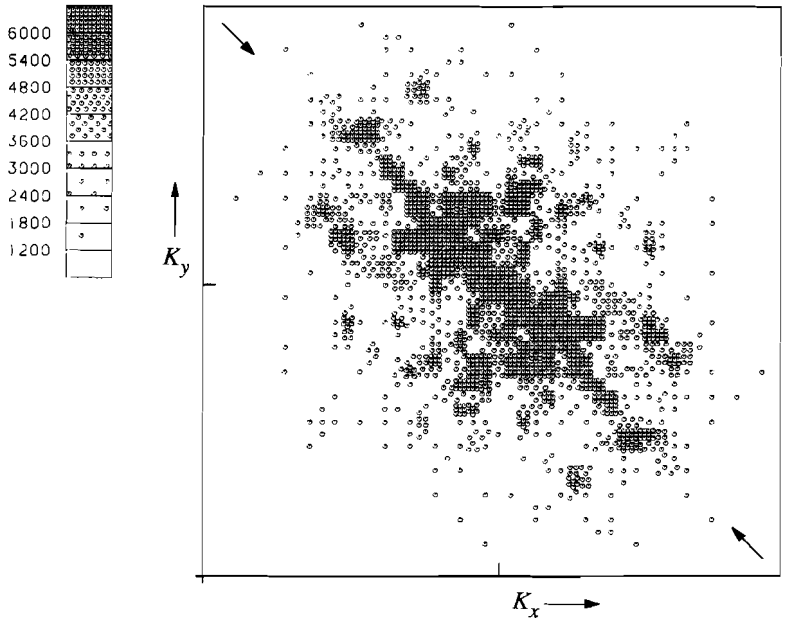

Figure 2.5 - The power spectrum of the gridded magnetic anomalies, shows peak values in directions -45° and 135°.

Figure 2.4b and the contour map shown in Plate IV.

Reduction to the pole

For a description of the theory of the reduction to the pole filter after Le Mouel *et al.* (1972) we refer to Verhoef (1984). To enhance the magnetic anomalies at lower latitudes, a reduced anomaly map was produced. The filter has as parameters the present and remanent inclination and declination. These parameters show a significant variation over the area. A solution would be to define relatively small subareas of e.g. 10°x10° and estimate the magnetic field parameters in the area from the paleo-pole positions and the present IGRF-fields. Due to limited computer facilities it was not possible to follow this rigoreous procedure. In this first product, the area was divided in 7 parts only. Paleo-pole positions were taken from Van den Berg (1979) and Irving and Irving (1982). The parameters for the reduction to the pole filter in the different areas are given in table 2.1. Plate V is a shadowgram of the reduced anomalies, illuminated from 280°.

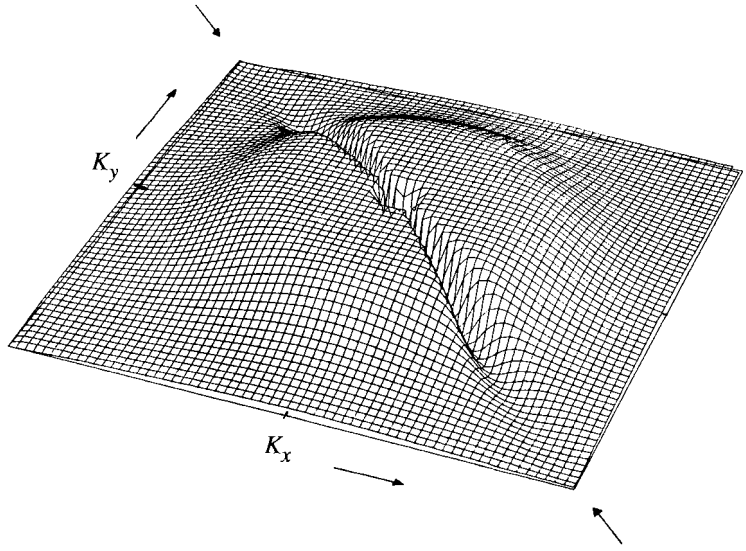

Figure 2.6 - Example of a directional filter combined with a band- pass filter. The directional filter is Gaussian shaped with the direction, the band-pass filter has a Butterworth roll-off.

Table 2.1: Mean magnetic field parameters in different areas, used in the reduction to the pole filter.

Latitude	Longitude	Present Field		Remanent Field	
°N	°W	Inclination	Declination	Inclination	Declination
35-50	0-20*	59°	-12°	46°	1°
35-50	19-32*	59°	-17°	54°	-2°
35-50	30-50	65°	-25°	50°	-8°
15-37	12-37	45°	-18°	65°	-20°
20-37	35-60	52°	-18°	38°	0°
5-22	35-60	42°	-17°	20°	-4°
5-25	55-65	45°	-14°	17°	-12°

*) see Verhoef *et al.* (1986).

Magnetic anomaly identifications

In a recent publication, Klitgord and Schouten (1986), presented a large dataset of seafloor spreading anomaly identifications. They re-examined and re-identified magnetic anomalies on both flanks of the Mid-Atlantic Ridge and digitized their positions at the tracks. The fact that their data-set was available to be included in the present study,

made it possible to reconstruct the spreading history in much more detail than before. Plate VI shows the magnetic seafloor spreading lineations from anomaly M4 (126 Ma B.P.) to anomaly 5 (10 Ma B.P.).

2.4 Gravity

The shipborne gravity data were collected by the Vening Meinesz Laboratorium, during the expeditions which were conducted as part of the Vaarplan. Detailed surveys which included gravity measurements were carried out in the area of the Fifteen Twenty Fracture Zone and the median valley N and S of it (Collette *et al.* , 1980 and in prep.). Kane Fracture Zone (Twigt *et al.* , 1983), and other fracture zones in the Cretaceous Magnetic Quiet Zone on the African plate (Slootweg and Collette, 1985) were investigated. A survey was carried out in the area of the Atlantis-Meteor Seamount Complex (Verhoef, 1984), and around the Canary Islands (Danobeitia, 1985).

The present study will not deal with the analysis of gravity data in terms of density structures, compensation mechanisms, lithospheric flexure *etcetera* . Instead the gravity data are used as an additional tool for the recognition of oceanic fracture zones (see Chapter 3).

Plate VII shows the observed gravity anomalies. As will be discussed in Chapter 3, the wavelength band between 50 and 200 km forms the most relevant part of the spectrum as far as the detection of fracture zones is concerned. Therefore, a long wavelength contour map (60 nm) was subtracted from the anomalies, which resulted in the enhanced short-wavelength anomalies of Plate VIII.

2.5 Seasat altimeter data

The Seasat spacecraft was launched in 1978 and recorded radar altimeter data in the period of July to October 1978 (Lame and Born, 1982; Tapley *et al.*, 1982; Lorell *et al.*, 1980). The satellite orbit is near-circular, with an inclination of 108°, a period of 101 minutes and an altitude of about 800 km. Figure 2.7 shows the Seasat ground-track-distribution for the central North Atlantic. There are two trends of the satellite tracks: tracks from NE to SW are descending tracks, whereas ascending tracks are orientated from SE to NW.

The radar altimeter - one of the five onboard sensors - was designed to measure the altitude between the satellite and the ocean surface to a 10 cm rms precision for 1-s averaged data. The distance between the 1-s averaged datapoints at the surface is 7 km. The radius of the footprint depends on the sea state and varies between approximately 1.2 and 6 km.

The accuracy of the Seasat altimeter, makes it possible to use the shorter wavelengths (25-500 km) of the seasurface height data for the study of the oceanic fracture zone pattern. Fossil fracture zones are characterized by a large basement relief, typically consisting of a valley and, to the older side of the axis, a high wall. This topography is superimposed on the depth/age step over fracture zones. Mulder and Collette (1984) showed that gravity anomalies in the wavelength band from 50 to 200 km are highly

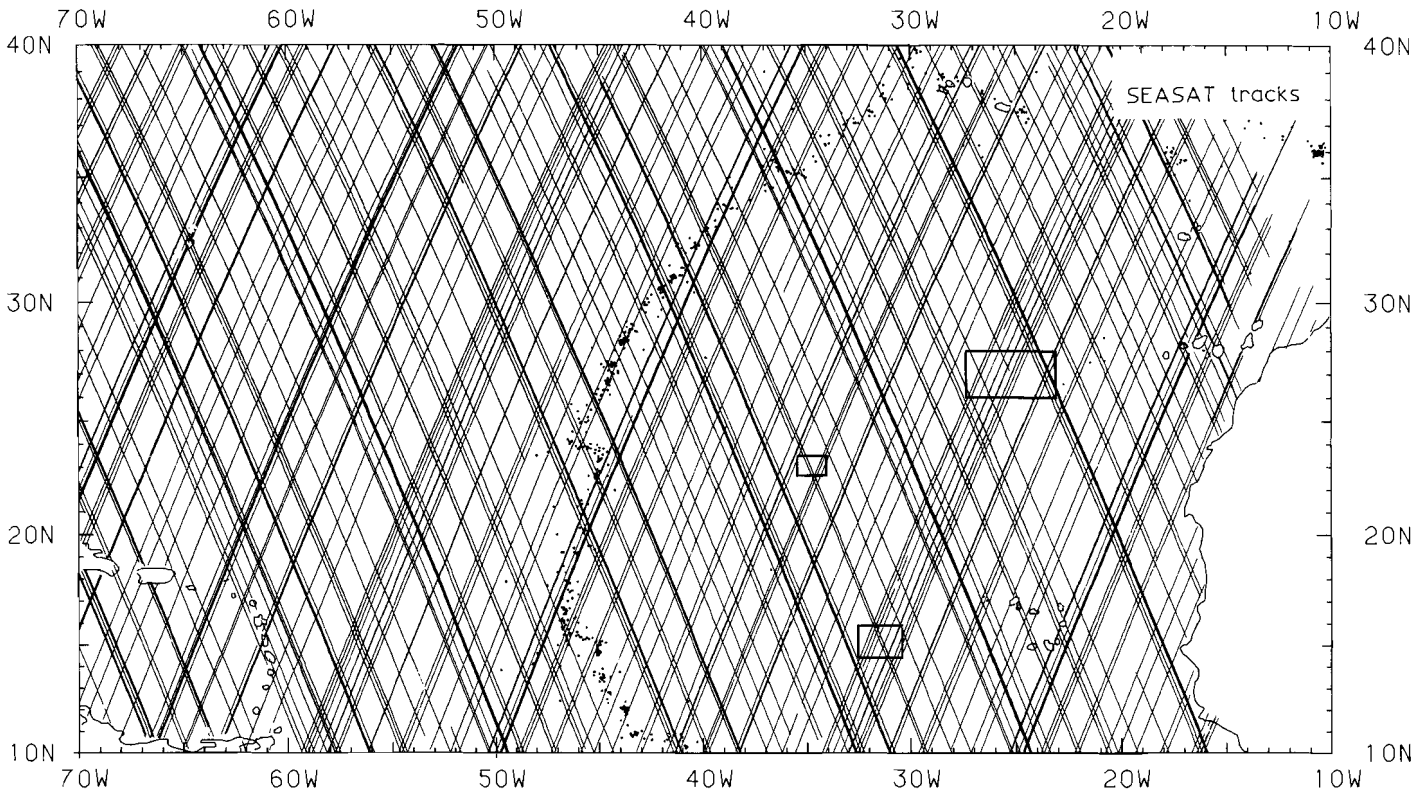

Figure 2.7 - Seasat ground track distribution. The boxes indicate the area's which are used to compare Seasat along-track gravity with shipborne data.

related to the fracture zone topography.

A large advantage of the Seasat data set is that it covers the whole study area. The intertrack spacing can, however, be as large as 120 km. To make full use of the resolution of the data, it was decided to process the data along-track, rather than to produce contourmaps. To enable the accurate identification of fracture zones from the Seasat data a high-pass filter had to be designed. This filter creates "along-track gravity". Modelling and comparing the Seasat derived gravity with shipborne gravity measurements and seismic reflection profiles showed that the Seasat along-track gravity data give an accurate definition of oceanic fracture zones.

Data editing

The Seasat altimeter data were provided on magnetic tape by J.G. Marsh of NASA. The geophysical data records (GDR) contained, besides the raw altimeter data (averaged over 10 measurement with a .1 s interval), all corrections which were applied to obtain the mean seasurface height above the reference ellipsoid (Lorell *et al.*, 1980). These corrections include track mode time tag correction, transit time correction, and ionospheric and tropospheric refraction effects. Mean seasurface height values in the geophysical data records were not corrected for ocean and solid earth tidal effects. Corrections for ocean tides with wavelengths from 500 to 1000 km, based on two different models, and for solid earth tides (20000 km) were provided separately in the GDR's. As the fracture zone signal is mainly restricted to wavelengths shorter than 200 km these additional corrections are ignored in the present study. Seasurface heights are referenced to a standard ellipsoid defined by a semimajor axis of 6378137 m and a flattening of 1/198.257 (Moritz, 1980).

As an indication of data quality a 7-bits flag was provided with each datapoint. Bits were set for large wave height (bad sea-state), large standard deviation of the mean, land, etcetera (Lorell *et al.*, 1980). In a first selection the sea/land flag was used to remove datapoints over land. Before further processing, all datapoints with a flag unequal zero were deleted, as it appeared that over 90% of these data were noisy or otherwise did not conform the surrounding data. Flags were mainly found in areas with sea-ice and bad weather conditions (mainly on the southern hemisphere), and close to the coast. All data were then checked visually, after conversion of the data to the data-handling and presentation system FELIX. During this inspection individual spikes and other spurious datapoints, which formed only a few percent of the data, were removed. In total, about 15% of the available datapoints were deleted.

Although the precision of the Seasat altimeter measurements is of the order of 10 cm, differences between different revolutions may exist of more than 1 m. These differences are caused by radial orbit errors with a typical wavelength of 40000 km (Tapley *et al.*, 1982) and are primarily resulting from errors in the gravity field model (Marsh *et al.*, 1986). Cross-over techniques can be used to reduce these errors to a 20 cm rms level (Rapp, 1983; Marsh and Martin, 1982). In this study we designed a high pass filter to calculate along-track gravity. In this case the radial orbit errors, like the tidal effects, are of no consequence.

Along-track gravity

To enable the accurate identification of fracture zones from the Seasat data Sandwell (1984) calculated the "along-track deflection of the vertical" in a study of fracture zones. For this he used the first derivative of the seasurface height in the direction of flight. This results into a 90° phaseshift of the signal with regard to the density disturbance.

A far better filter is obtained by calculating the "along-track gravity". Under ideal circumstances along-track gravity is the real free-air gravity as measured at the seasurface. It therefore can directly be compared to shipborne measurements. The flat-earth approximation for the two-dimensional case was used. The Laplace equation for the gravitational potential, U, of the anomalous mass:

$$\frac{\partial^2 U}{\partial x^2} + \frac{\partial^2 U}{\partial y^2} + \frac{\partial^2 U}{\partial z^2} = 0 \tag{2.1a}$$

is then reduced to:

$$\frac{\partial^2 U}{\partial x^2} + \frac{\partial^2 U}{\partial z^2} = 0 \tag{2.1b}$$

To first order U is related to the geoid height (N) above the reference plane z=0 (Brun's Formula, see Heiskanen and Moritz, 1967):

$$N = U / g_0 \tag{2.2}$$

where g_0 is the gravitational acceleration, and:

$$\Delta g = - \frac{\partial U}{\partial z} \tag{2.3}$$

with Δg the vertical component of the gravity anomaly. Combination of (2.1b), (2.2) and (2.3) leads to the following expression for the along-track gravity anomaly Δg:

$$g_0 \frac{\partial^2 N}{\partial x^2} = \frac{\partial \Delta g}{\partial z} \tag{2.4}$$

By taking the Fourier transform (FT), (2.4) can be used to calculate Δg from N:

$$FT(\Delta g) = - g_0 K \; FT(N) \tag{2.5}$$

with $K=\sqrt{k_x^2}$, the wavenumber in the direction of the track (Chapman, 1979).

In order to calculate along-track gravity with equation (2.5), standard FFT-techniques were used. Arcs with a length of about 3500 km were transformed in their totality, after subtraction of mean and trend. Tapering was used over the datapoints situated outside the study area. After multiplication with the absolute wavenumber and the gravitional acceleration, data were transformed back into the space domain.

As for the free-air gravity anomalies, an additional filter was used to isolate the gravity anomalies related to fracture zone topography. In this case we used a band-pass filter (15-200 nm, 12 dB/octave). In this way, the gravity effect of the subsidence of older oceanic lithosphere, and that related to regional depth anomalies are reduced. Short wavelength gravity anomalies oblique to fracture zones, as observed in the Pacific and there denoted as small scale mantle convection (Haxby and Weissel, 1986; Buck and Parmentier, 1986), are not affected by the band-pass filter. However, in the Atlantic Ocean this type of anomalies has not yet been observed.

Plate IX gives the along-track gravity for the descending revolutions in the Central North Atlantic. As the mean spreading direction in this area is WNW-ESE, the tracks are roughly perpendicular to the fracture zones. The expected correlation between the fracture zone signals on adjacent tracks is indeed present. However, also on the ascending revolutions (Plate X) the fracture zone signal is visible, although less clear. Due to the wavelength filtering, the Mid-Atlantic Ridge is not seen in Plates IX and X. Also the regional gravity anomalies related to depth anomalies (Cochran and Talwani, 1977; Verhoef, 1984) are lost. The median-valley is recognized on the ascending revolutions (Plate X) north of 25° N.

The method used in this study differs in the final product from that of Haxby *et al.* (1983; also Haxby and Weissel, 1986; Freedman and Parsons, 1986) who present maps of the Seasat derived gravity field. Haxby *et al.* (1983) first determined geoid height values on a grid and then applied equations (2.1a), (2.2) and (2.3). The advantage of their approach is that gravity anomalies over non-lineair structures are, in principle, also resolved. In the earlier version of their images (e.g. Haxby, 1983a & b) part of the resolution seems lost in the gridding process. In a study of the central east Pacific, Haxby and Weissel (1986) gridded the seasurface slope, instead of the seasurface height, in this way eliminating the radial orbit error. Gravity images constructed with this new approach look promising. Recently, Balmino *et al.* (1987) produced a database of free-air gravity anomalies from Seasat and GEOS-3, on a 15' grid.

Comparison with ship-borne Free-air Gravity

A number of authors compared Seasat altimeter data with shipborne measurements, to test its usefullness for marine geophysical research (e.g. Rapp, 1986; Balmino *et al.*, 1987). Haxby and Weissel (1986; see also Buck and Parmentier, 1986) compared Seasat altimeter data in the Pacific with shipborne measurements, in order to investigate the nature of a subtle lineated pattern of gravity anomalies oblique to fracture zone trends. Vogt *et al.* (1984) conducted "ground truth" marine geophysical measurements

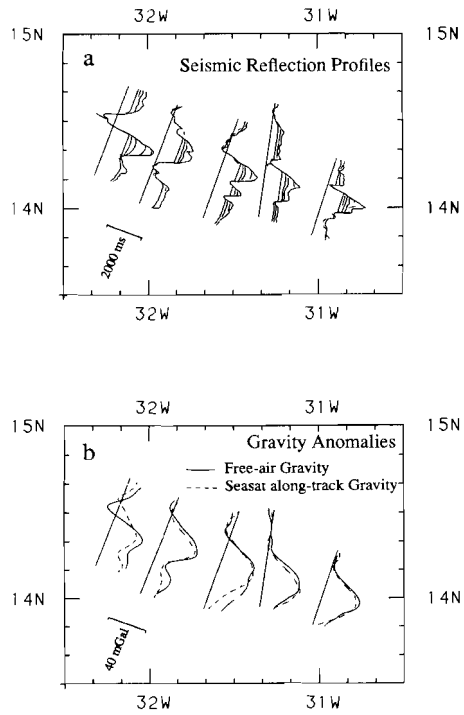

Figure 2.8 - (a) Seismic reflection profiles over the Fifteen Twenty Fracture Zone (offset: 7000 ms). (b) Seasat along-track gravity compared with shipborne measurements of free-air gravity. The position of the area is indicated in Figure 2.7. In this case a band-pass filter of 15-1000 nm was applied to the Seasat gravity data.

(gravity, magnetics and seismic reflection) along, in total, 9300 km of Seasat tracks in the Atlantic ocean. Good correlation exists between geoid height, vertical deflection, free-air gravity and seafloor topography. Diamant *et al.* (1986), used spectral analysis to study the isostasy of the Northern Bay of Biscay continental margin. They conclude that Seasat and marine gravity data yield identical admittance functions for wavelenghts greater than 100 km. The phase of the admittance for altimeter data is significantly deviating from zero for shorter wavelenghts.

In order to compare the Seasat derived along-track gravity with shipborne data, we selected two areas with a large track- density (see Figure 2.7). In both areas a large fracture zone is present, trending roughly perpendicular to the descending tracks. The Seasat along-track gravity based on the descending tracks was interpolated in the direction of the fracture zone, to obtain values along the ship-tracks. In Figure 2.8a, line drawings of the seismic profiles of the Fifteen Twenty FZ are shown. Figure 2.8b displays the observed free-air gravity, and the interpolated Seasat along-track gravity. Figure 2.9a and b give the same data for Tyro FZ. The amplitude of the along-track gravity is in good agreement with the shipborne data. Also the position of the negative

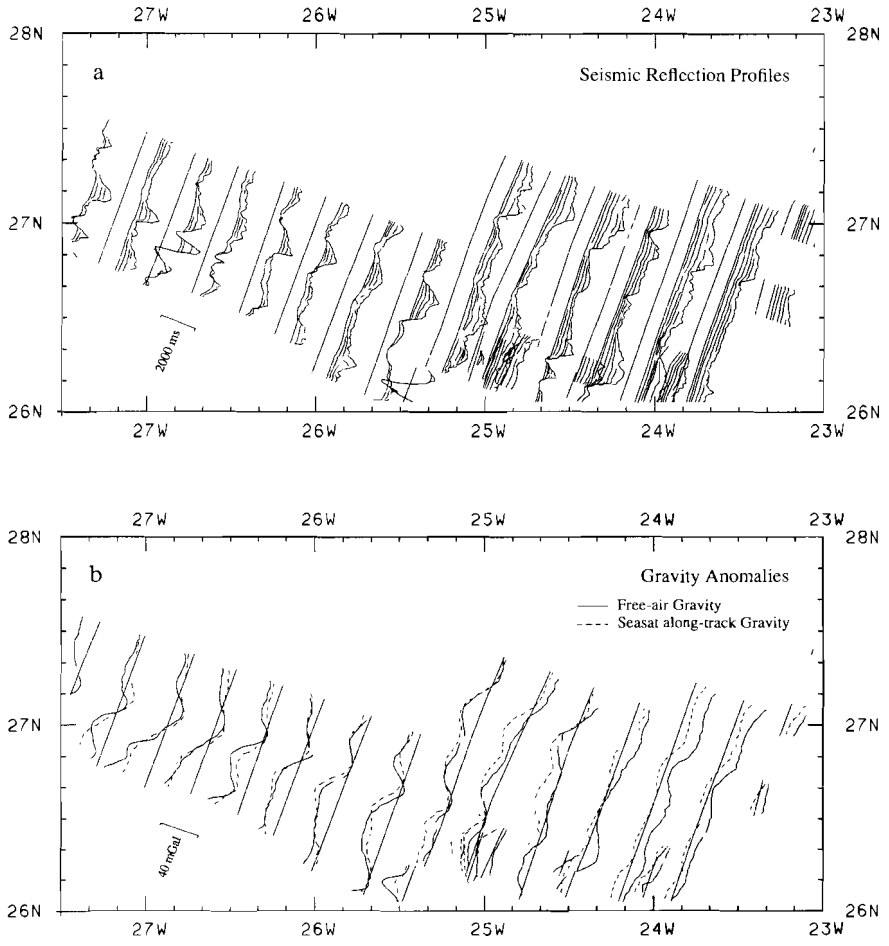

Figure 2.9 - (a) Seismic reflection profiles over the Tyro Fracture Zone (offset: 6000 ms). (b) Seasat along-track gravity compared with shipborne measurements of free-air gravity anomalies. The position of the area is indicated in Figure 2.7. As in Figure 2.8 a band-pass filter of 15-1000 nm was applied to the Seasat data.

gravity anomaly associated with the fracture zone valley is well resolved by the altimeter data. In the case of Tyro FZ several profiles show an offset of up to 20 mGal. This long wavelength deviation is a result of the along- track filtering process.

The overall accuracy of the along-track gravity is not always as large as Figures 2.8 and 2.9 may suggest. If a linear structure is crossed at an oblique angle α the amplitude of the Seasat derived along-track gravity will be in error. In Figure 2.10 this is demonstrated for both ascending and descending revolutions, crossing Kane FZ at 30° W,

where it trends about E-W. After multiplication of the amplitude with $1/\cos(\alpha)$ and projecting the profiles perpendicular to the fz a good accordance is achieved with the shipborne gravity.

Cross-over differences

Cross-over differences between the ascending and descending tracks given in Plate IX and X occur of over 50 mGal. They may partly be related to the fact that linear structures are crossed at different azimuths, as illustrated above. In general this means that the amplitude of the anomalies of both the ascending and descending tracks will be in error. The applied band-pass filter (15-200 nm for Plates IX and X) gives an additional cross-over error, because the spectra of ascending and descending tracks differ due to the different angles at which structures are crossed.

For this reason we checked whether systematic errors occurred in the position of (relative) minima and maxima on both sets of tracks. No measurable errors were found, which can be understood from the favourable geometry of the mainly E-W structures with regard to the flight directions.

Finally, large cross-over differences may also point to non-lineair structures. This is clearly seen at ridge-transform fault intersections, where both median-valley and transform fault anomalies are very poorly resolved.

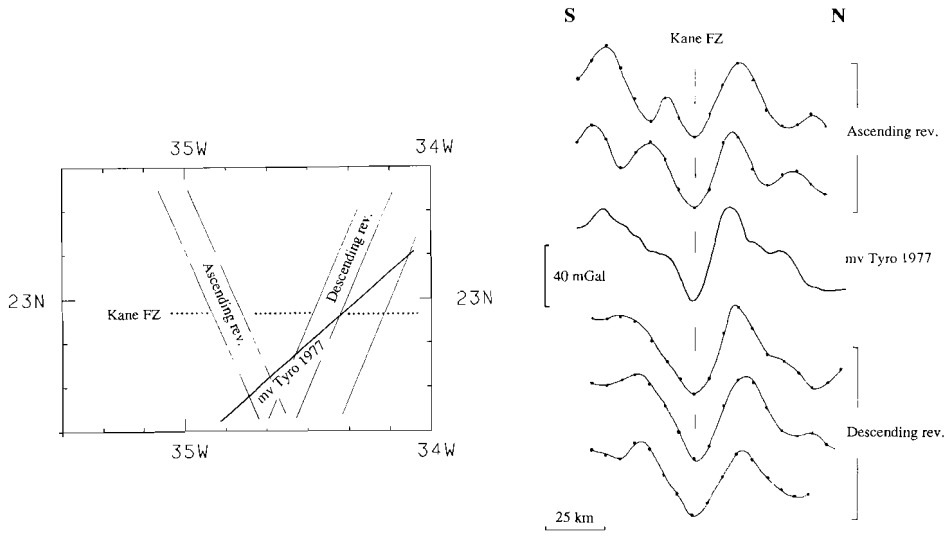

Figure 2.10 - Comparison of Seasat along-track gravity profiles with shipborne gravity. Profiles are projected perpendicular to the fracture zone trend. The amplitude of the Seasat along- track gravity is corrected for the azimuth. The position of the area is indicated in Figure 2.7.

Relation between gravity and bathymetry

In the preceeding section it was found that there is a good correlation between Seasat along-track gravity and shipborne gravity data. The next question is whether Seasat data can be used to predict bathymetry. Dixon and Parke (1983, cf. also White *et al.*, 1983) used Seasat mean seasurface data to detect uncharted seamounts. Dixon *et al.* (1983) and Watts *et al.* (1985) applied lineair response function techniques to predict bathymetric profiles from Seasat data. Again, this method proved to be useful for the detection of large seamounts and other large features.

We tried to produce bathymetry from the along-track gravity data in plates IX and X. Not taking into account isostatic compensation mechanisms, the gravity anomaly in the wavenumber domain g(k) is related to a density structure at depth z by the depth filter e^{-kz}, where k is the wavenumber. Figure 2.11 gives this filter as a function of the wavelength for different depths of the ocean floor. In Figure 2.12, the consequences of the depth filter are illustrated with a simple model. It appeared that the small-wavelength Atlantic fracture zone anomalies dissappear in the noise when of the inverse depth filter is applied. The signal to noise ratio is reduced due to the high-pass character of the filter. Additional uncertainties are related to the a priori unknown effects of isostatic compensation which have to be incorporated in the transfer functions.

We already mentioned the admittance study by Diamant *et al.* (1986), using Seasat gravity, shipborne gravity and topography. As illustrated by Gibert and Courtillot (1987) for the South Atlantic, the DBDB5 data (see Plate III) are in general not suited for such an approach. We estimate that the topography information in the Kroonvlag area may be sufficient for admittance studies. Also, the wavelengths longer than 200

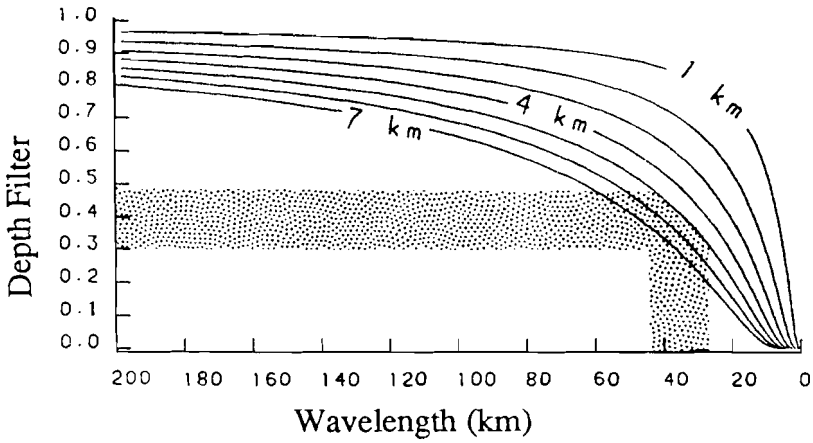

Figure 2.11 - Characteristic of the depth filter e^{-kz} as a function of wavelength for different ocean depths.The shaded band indicates expected filter effect for the south wall of the Vema Fracture Zone, discussed in section 3.5.

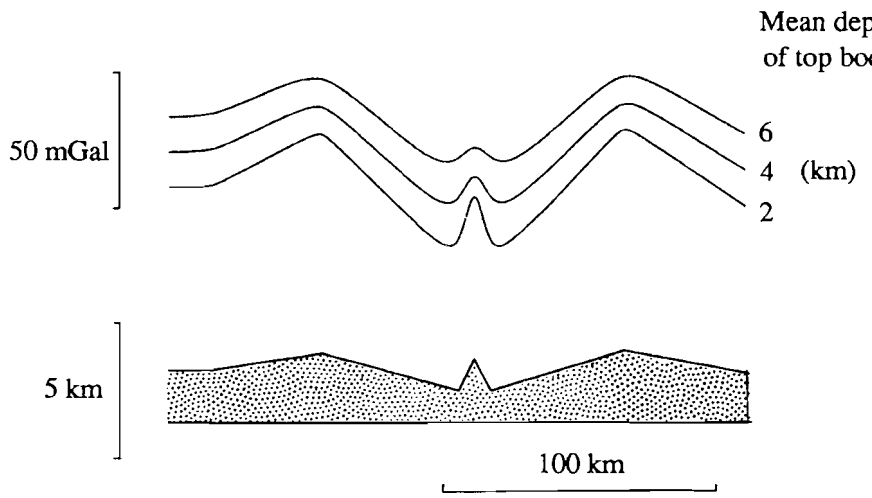

Figure 2.12 - Gravity anomaly over a model at different depths, illustrating the working of the depth filter. For larger depths, the short wavelength anomalies are reduced as compared to longer wavelength anomalies.

nm, which were filtered in Plates IX and X, can be expected to provide information on the occurrence of anomalies in the depth/age relation along fracture zones in the Atlantic. A map of Seasat along-track gravity filtered from 15-1000 nm (not reproduced) showed the existence of such anomalies. This subject won't be pursued any further in this thesis.

Chapter Three

Fracture Zones and their Gravity Signal

3.1 Introduction

Oceanic fracture zones belong to one of the most outstanding topographic features of the ocean floors. Fracture zones were first defined by Menard (1964). According to Menard and Chase (1970), fracture zones form narrow bands, characterized by an irregular basement relief, in addition to a regional difference in ocean floor depth to both sides, which difference is most clearly observed in the Northeast Pacific. Wilson (1965) first recognized the kinematic function of fracture zones as transform faults. Morgan (1968) introduced the concept that, in order to allow plate motion, transform faults have to follow small-circles about the pole of rotation. With the explanation of the relation between ocean floor depth and lithospheric age in terms of simple thermal models (McKenzie, 1969; Sclater and Francheteau, 1970), the regional difference in depth across a fracture zone was related to the age offset in the transform domain. Sibuet *et al.* (1974), deduced the lithospheric thickness from the gravity edge effect across the Mendocino Fracture Zone. Louden and Forsyth (1976) calculated the effect of thermal conduction over a fracture zone on the signature of the gravity edge effect. Sibuet and Veyrat-Peinet (1980) used the vertical temperature distribution in the lithosphere to construct a simple gravimetric model which is in close agreement with the free-air gravity anomalies observed over several Equatorial Atlantic Fracture Zones. More recently, the geoid step over the Mendocino Fracture Zone and others in the Pacific, was used to derive parameters for thermal models of the oceanic lithosphere (Crough, 1979; Detrick, 1981; Cazenave *et al.*, 1982 and 1983; Sandwell and Schubert, 1982a; Cazenave, 1984).

If the depth/age step over fracture zones were a consistent feature, this step could be used in the reconstruction of the spreading history. However, in the central North Atlantic the regional difference in ocean floor depth to both sides of fracture zones cannot always be recognized. This is partly caused by the complex fracture zone morphology. The closer spacing of fracture zones, which can be related to a lower spreading rate (Schouten *et al.*, 1985; Sandwell, 1986), may be another reason. Also interference of the fracture zone topography with the spreading topography, which is rougher in the Atlantic and Indian Ocean than in the Pacific, plays a role. Moreover, large depth anomalies, i.e. deviations from the depth-age curve, are found, which sometimes seem to be bordered by fracture zone traces.

An other topographic characteristic of fracture zones lends itself better for our purposes. Although fracture zones may have various topographic expressions, bathymetric maps of the Atlantic show them essentially as valleys. Frequently, the valleys are accompanied by parallel ridges. Fracture zones valleys form the deepest areas on the

axis and the flanks of Mid-Atlantic Ridge, but also in older crust (compare e.g. Plate III). In the abyssal plains, the valleys are elongate basement depressions. The Seasat gravity image made by Haxby (1983a) shows fracture zones as negative gravity zones, as does the along-track gravity in Plates IX and X. Therefore, this topographic and gravimetric feature will be used in the following.

One of the questions of the present study is whether or not the observed fanning of transform faults also affects the fossil fracture zone traces. Comparison of distances between fracture zones on the American and on the African plate may provide an answer to this question. Since an eventual difference may be of the order of 10-20 km only, an accurate definition of the position of the fracture zone axis is needed. Hence, it is necessary to know where the axis of the fracture zone is located relative to the position of the fracture zone valley or of the negative gravity anomaly over fracture zones.

To answer this question, we start with a description of the morphological model for Atlantic fracture zones as presented by Collette (1986). This model, based on many observations of active transform faults and fossil fracture zones, was used in the process of identification of fracture zones in the central North Atlantic.

3.2 Morphology of Atlantic fracture zones

Fracture zones in the Atlantic Ocean typically consist of an asymmetric valley with a wall to the older side of the fracture zone axis (Collette *et al.*, 1984). Sometimes, a marginal valley (Van Andel *et al.*, 1971) is found beyond the fracture zone wall, which valley may be larger than the axial fracture zone valley. Collette (1986; cf. also Collette *et al.*, 1984) relate the typical fracture zone topography to the way it is formed in the transform domain. The cross-section of a transform fault can be described as a graben, with uplifted walls to both sides. The origin of this graben is found in horizontal thermal contraction parallel to the ridge axis (Collette, 1974; Turcotte, 1974). The uplift of the walls is a result of upwelling of the viscous asthenosphere in response to the mass deficiency represented by the volume of the thermal crack. For a large offset transform, this uplift may go accompanied by warping, which leads to depressions, the marginal valleys. To account for the observed wavelength of e.g. the South Wall of the Vema Transform, Collette (1986) suggests that lithospheric thinning in response to heating from intrusions or friction occurs, causing a smaller elastic thickness.

The graben topography is superimposed on the topography related to the thinness of crust near fracture zones. This thinness was established be seismic experiments (e.g. Detrick and Purdy, 1980; White *et al.*, 1984; Mutter *et al.*, 1984).

The median valley can be modelled as the viscous response of the asthenosphere to the unloading by the spreading process (Collette *et al.*, 1980). The deepening of the median valley towards the intersection with a fracture zone follows as the end effect of this linear model. Collette and Verhoef (1987) studied the consequences of asymmetric viscous drag in a three- dimensional model of the ridge-transform intersection and arrived at an explanation of the anomalous shallow depth of the inner corner of the intersection.

The topography of inactive part of fracture zones results from the welding of the depressed axis of the median valley with the opposite high graben wall. In this way one gets the asymmetric valley with a high wall to the older side and, for very large offset

fracture zones, a marginal valley beyond the wall. If the welding of both sides along the fracture zone axis is perfect, the total step will remain intact. Indications that this is so are found in the fact that fossil fracture zones in old crust are still associated with a large basement relief. Moreover, there is no seismic evidence for motion along fossil fracture zones.

The 'typical' fracture zone morphology is not always found. Twigt *et al.* (1983) report on the variability of the cross- section of Kane Fracture Zone in the Cretaceous Magnetic Quiet Zone on the African plate. The fracture zone topography varies from the typical one with a high wall to the older side, to an a- typical cross-section where a broad valley is observed. Sometimes a minor ridge is found in this valley. Between 28° and 29°W, a major ridge occurs in the valley, and a double peak magnetic anomaly is observed. Twigt *et al.* (1983) relate the different fracture zone expressions to changes in spreading direction. Roest and Collette (1986) describe the limbs of the Fifteen Twenty Fracture Zone, and found a similar variability of the fracture zone cross-section. Moreover, they found a high degree of symmetry of the fracture zone expression on cross-section, observed east and west of the Mid-Atlantic Ridge.

The Atlantic fracture zone model depends on the existence of a median valley. If no median valley occurs, a different morphology - e.g. a simple depth/age step - can be expected.

3.3 Gravity over Atlantic fracture zones.

Mulder and Collette (1984) showed that gravity anomalies in the wavelength band from 50 to 200 km are highly related to the fracture zone topography. They modelled the gravity anomalies in this wavelength band both with a flat crust-mantle interface and with an interface following the basement topography. With a flat interface (or topographic correction only), negative anomalies remain over the valleys and positive anomalies over the ridges. If isostatic compensation is taken into account, e.g. by assuming that the crust-mantle interface to some degree mirrors the topography, the anomalies would become larger. If in the model the crust-mantle interface follows the topography, the anomalies become smaller. Therefore, the authors concluded that the fracture zone topography has a skew compensation, i.e. the high walls are resting on the depressed valleys and find their compensation under these valleys. They ascribe this to the origin of this topography as the non-isostatic process discussed above.

This skew compensation of fracture zone topography is confirmed by admittance studies over fracture zones by Diamant (1981) and Diamant *et al.* (1986), although the authors themselves do not recognize this feature as such. Several admittance curves from Diamant *et al.* (1986), calculated from gravity and bathymetric data over fracture zones, are shown in Figure 3.1. The curves illustrate that the admittance in the wavelength band of 50-100 km is too large, indicating that the gravity anomaly cannot be explained by isostatic models. There must be a high density body under the highs and a low density under the valleys.

The skew compensation of the high fracture zone wall is also confirmed by other observations. Robb and Kane (1975) modelled two gravity profiles over Vema Fracture zone, one in the transform domain, the other west of the western ridge-transform intersection. Evidence was found for an excess of mass under the Vema South Wall. Seismic

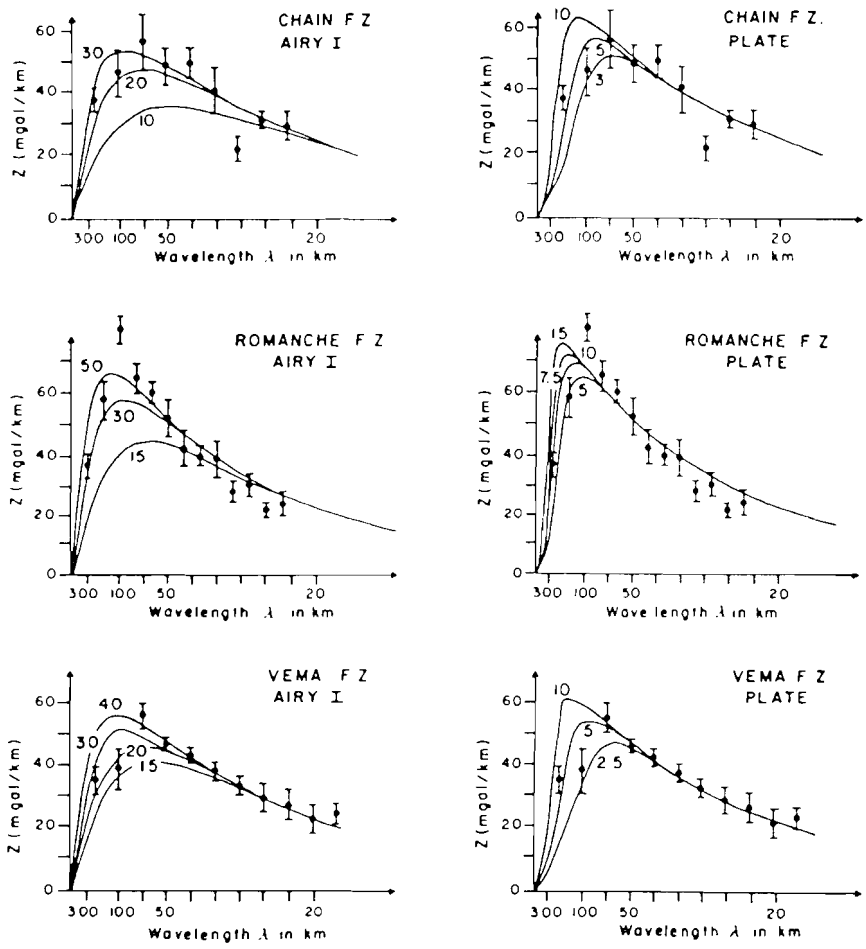

Figure 3.1 - Admittance curves taken from Diamant *et al.* (1986), over Equatorial Atlantic Fracture Zones. The admittance in the wavelength band between 50 and 100 km is too large as compared with the model curves (Airy and Plate model), indicating a skew compensation of fracture zone topography.

refraction studies seem to indicate that there is no thicker than normal crust under the fracture zone walls, it may even be thinner (cf. Whitmarsh and Calvert, 1986). In the fracture zone valley they find evidence for a serpentinite body. Louden *et al.* (1986) conclude from the upward warping of the seismic Moho under the Vema South Wall, that its origin is rather tectonic than an uplift by serpentinization (e.g. Francis, 1981). In this latter model, a deficiency of mass would occur under the wall, which is not in agreement with the observations.

Even in cases where the typical fracture zone topography is absent on cross-sections, a gravity low is usually observed. One of the reasons may be that gravity anomalies

over, essentially, linear structures are not very sensitive to short wavelength along strike variations in the topography. In other words, gravity as an integrated signal, gives a more continuous picture than topography. Furthermore, the gravity low over fracture zones is enhanced by the thinness of the crust which is observed near many large offset fracture zones (e.g. Detrick and Purdy, 1980; White *et al.*, 1984). More recently thinner than normal crust was also found at the Blake Spur Fracture Zone, which has only an offset of about 20 km (Mutter *et al.*, 1984). An explanation for the thinner crust near fracture zones may be found in inadequate magma supply from the central injection zone under a spreading segment toward the ends (Sinha and Louden, 1983).

3.4 Position of the fracture zone axis

As said before, fracture zones are characterized by valleys that are deeper than the neighbouring seafloor, and they have a negative gravity anomaly. These two observations are used in the identification of the fossil fracture zone pattern. For the reconstruction of the flowline pattern a positioning of the fracture zone at the deepest point, or at the location of the maximum of the negative gravity anomaly may be accurate enough. However, if we want to compare distances between fracture zones east and west of the Mid-Atlantic Ridge, in order to investigate the influence of fanning transform faults on the traces of fossil fracture zones, it is necessary to know more precisely the position of the actual fracture zone axis in relation to the observed valley. The model of Collette (1986) leaves room for a small distance between the deepest point of the fracture zone valley and the axis. The valley may be located to the younger side. The gravity anomaly over the asymmetric fracture zone topography would show a similar picture.

In order to quantify the possible difference between fracture zone axis and valley, we compared distances on the two plates, between valleys of pairs of fracture zones with a dextral and a sinistral offset. By taking two fracture zones with a limited distance in between, the theoretical effect of fanning transform faults and thermal contraction on the fracture zone distances east and west is limited to a few kilometers only, forming one of the inaccuracies in the determination of the position of the fracture zone axis (see also section 6.8). A good example is formed by the Kane and the Northern Fracture Zone between anomalies 33 and 25. Kane Fracture zone is a left lateral offset, and the Northern Fracture Zone is right lateral. No conclusive evidence for a different distance on either side of the ridge is found from the Seasat along-track gravity. The same is true for a set of fracture zones farther south, Luymes and Vidal Fracture Zones. It should, however, be noted that the sample distance of the Seasat data is 7 km, and the accuracy of localisation of fracture zones was estimated at about 5 km. This means the differences of a few kilometers are not likely to be detected. Within this marge, east-west differences in distances between fracture zone valleys seem not to exist.

In the following Chapters, the position of the deepest point of the valley or the maximum of the negative gravity anomaly will be taken as the actual axis of the fracture zone.

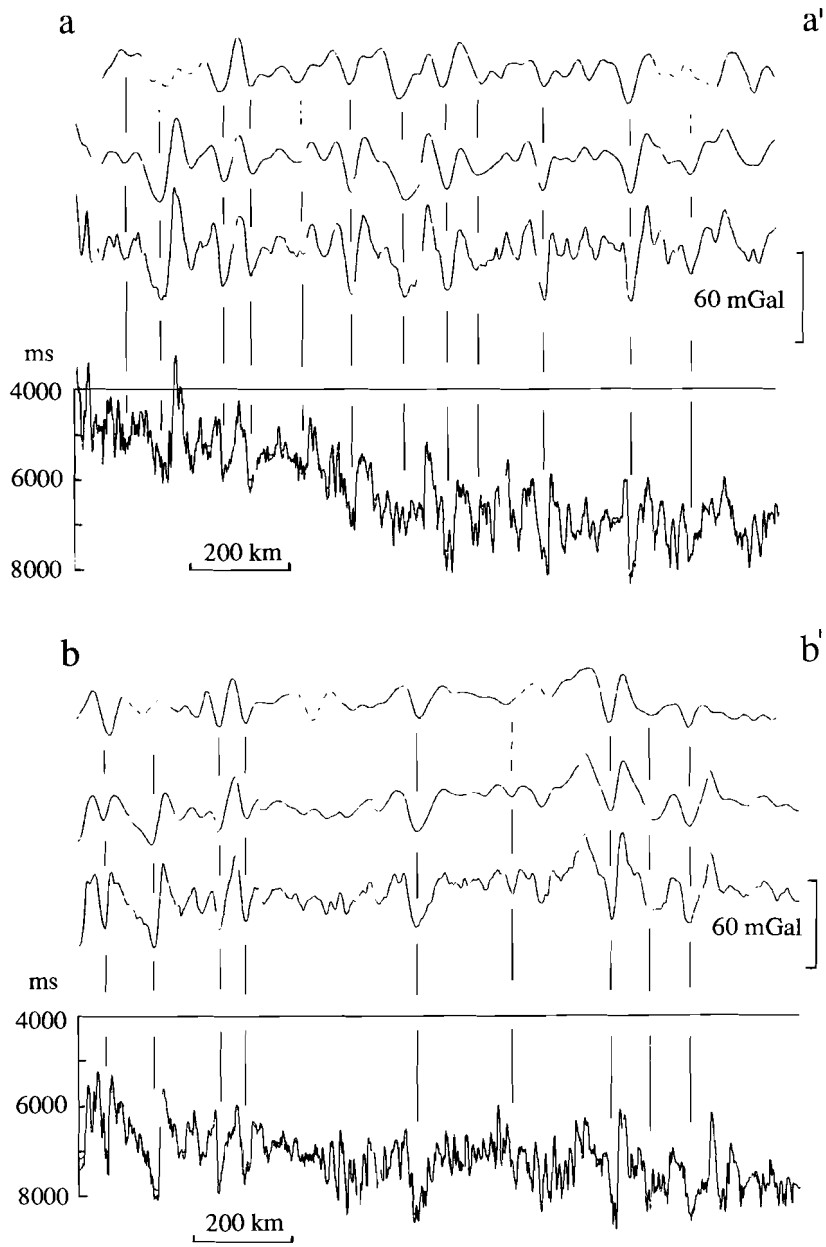

Figure 3.2 - (a and b) Comparison of shipborne data and Seasat along-track gravity along two profiles published by Mulder and Collette (1984). From bottom to top are displayed the seismic reflection profiles, observed free-air gravity, low-pass filtered (35 nm) free-air gravity and low-pass filtered Seasat along-track gravity, interpolated along the ships tracks. Where Seasat data are displayed as dashes, the distance to the shiptrack is too large to allow comparison.

3.5 Fracture zones from Seasat

The greater part of fracture zone studies with Seasat data deals with the Pacific Ocean. Pacific fracture zones are typically associated with a geoid step of 0.5-2 m, and the position of the steep slope gives an estimate of the position of the fracture zone axis. In the Atlantic, different conditions exist and the age step over fracture zones is less well observed both in the bathymetry and the geoid heigth. Comparison of the geoid height data with the basement topography in the Kroonvlag area led to the conclusion that the geoid step is highly obscured by the fracture zone topography. Following Vogt *et al.* (1984) we first applied only a high-pass Butterworth filter to the geoid height in an attempt to isolate the signal related to the fracture zone topography. This did not give the resolution needed for the identification of the fracture zones pattern. Calculation of the along-track gravity appeared to allow a much more accurate definition of the fossil fracture zones.

As an illustration of the ability to detect fracture zones from Seasat data, along-track gravity data were compared with the profiles published by Mulder and Collette (1984). The position of the two profiles is indicated on Plate VII. The track distribution is not ideal, as fracture zones are crossed at different angles, and Seasat and ship tracks are not parallel. Seasat data were interpolated on the ship-track, using a weight function (compare section 2.2) with a wavelength of 35 nm. Figure 3.2 shows a linedrawing of the seismic reflection profiles and the observed free-air gravity. A lowpass filter of 35 nm was then applied to the gravity in order to compare it with the Seasat derived gravity. Where the Seasat gravity is shown as dashes, the shiptrack is too far from the nearest Seasat ground track to allow a reliable comparison. Still, it is observed that all fracture zones identified by Mulder and Collette (1984) are clearly reflected in the Seasat along track gravity.

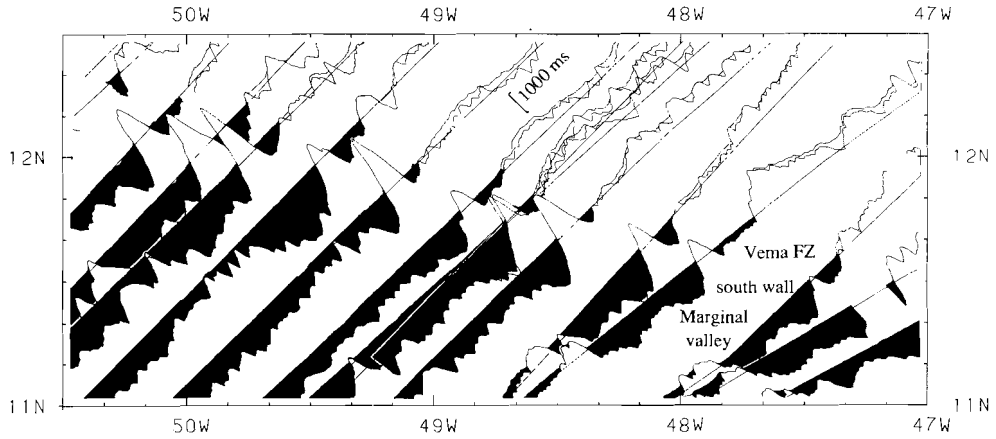

Figure 3.3 - Linedrawings of seismic reflection profiles over Vema Fracture Zone, on the American plate (offset: 6666ms). The fracture zone valley is situated to the north of the high wall, the marginal valley to the south of it (after Collette, 1986).

However, not all negative anomaly lineations should be associated with fracture zone axes. Figure 3.3 shows the prominent wall south of the western extension of Vema Fracture Zone, which has a marginal valley to the south of it (Collette *et al.*, 1984; Collette, 1986). Figure 3.4 shows a Seasat along-track gravity profile over this feature. The gravity anomaly over the wall is very small, which is mainly a result from the depth of the oceanfloor in this area. Figure 2.11 shows that the amplitude of the Vema south wall is reduced by 6 dB compared to the wavelengths larger than 150 km, which is the typical wavelength of the marginal valley. This means that the effect of the fracture zone valley and the high wall is drowned in the gravity expression of the marginal valley. This configuration can give rise to a wrong identification of the fracture zone axis.

3.6 Fracture zones as flowlines

A final comment regards the question how accurately fracture zones axes define the flowlines. The use of fracture zone directions for the determination of stage poles is in accordance with ideas of McKenzie and Sclater (1971) and Schouten and Klitgord (1982) who suggested that accreting plate boundaries have a memory. There are different opinions concerning the lengths of an offset in relation to the usefulness of fracture zones. Archambault (1984), following Olivet (1978), believes that large offset fracture zones are stable, and give the most accurate information on spreading directions. On the other hand, Klitgord and Schouten (1986) suggest that small offset fracture

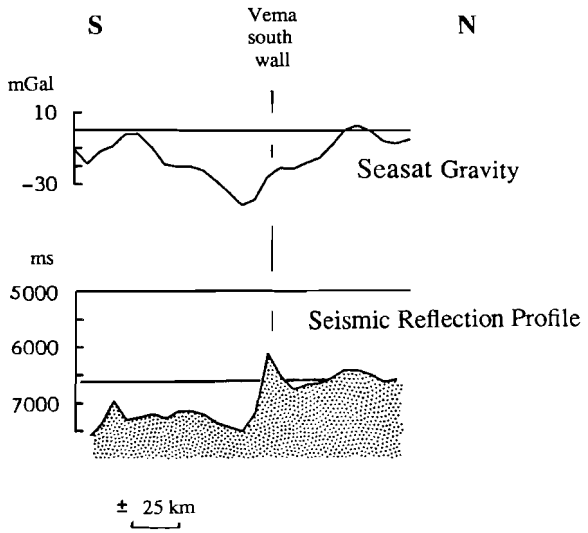

Figure 3.4 - Seasat along-track gravity over Vema Fracture Zone. Due to the large ocean depth in this area, the gravity anomaly of the south wall is drowned in that of the marginal valley.

zones produce coherent traces, whereas fracture zones with a large offset show complex structures in response to changes in spreading direction. Patriat *et al.* (1985) arrive at the conclusion that large offset fracture zones may be discontinuous, and cannot be used for the determination of rotation poles.

Although we agree with Patriat *et al.* (1985) that fracture zone offsets may vanish in the course of time, and that local reorganisations of the spreading axis (ridge jumps) occur, we conclude from the analysis of Collette *et al.* (1984), that the combination of fracture zone directions observed in a certain age zone makes the determination of accurate stage poles possible.

Oblique transforms cannot be used for defining flowlines since they are essentially non-steady state features. We distinguish two types of oblique transforms. The first type is the Kurchatov- type, which consists of a trace of irregular features off the spreading axis (e.g. Searle and Laughton, 1977). The second type consists of the so-called V-shaped structures which are symmetrical with respect to the ridge axis and which seem to trend systematically over a certain distance. Both types seem related to small offsets (<20 km). The symmetrical trending of V-shaped structures is related to asthenospheric flow from a hot spot (Johnson and Vogt, 1973; Vogt, 1974) or to absolute plate motion (Schouten *et al.*, in press). The latter authors associate the migration of the tip of the V-shape with the component of absolute plate motion parallel to the ridge axis.

Chapter Four

Method of the Reconstruction

4.1 Poles of rotation

The relative movement of rigid lithospheric plates on the surface of the earth can be described with Euler vectors of rotation. The intersection of the rotation axis with the earth's surface is called the pole of rotation. Distinction is made between two different types of poles: total separation poles and stage poles. A total separation, also named finite difference pole, gives the total rotation between corresponding isochrons on two adjacent plates. It can be used to reconstruct the relative position of the plates at the time to which the isochrons refer. Stage poles, or poles of (instant) motion, give the relative motion in or over a certain period of constant spreading. Small circles around these poles can be considered as flowlines, and can be compared with fracture zone trends.

We will introduce a new type of pole: the half poles, describing the total motion between the spreading center and a certain magnetic isochron or, for that case, between two arbitrary isochrons on one plate (cf. Figure 4.1). In this chapter, the relation between total separation poles, half poles and stage poles will be discussed. We will assume symmetric spreading.

In most published spreading histories, stage poles are calculated from a set of total separation poles without making additional use of fracture zone trends (a.o. Le Pichon and Fox, 1971; Pitman and Talwani, 1972; Francheteau, 1973; Ladd, 1976; Olivet *et al.*, 1984; Patriat *et al.*, 1985; Klitgord and Schouten, 1986). This method is only valid if no

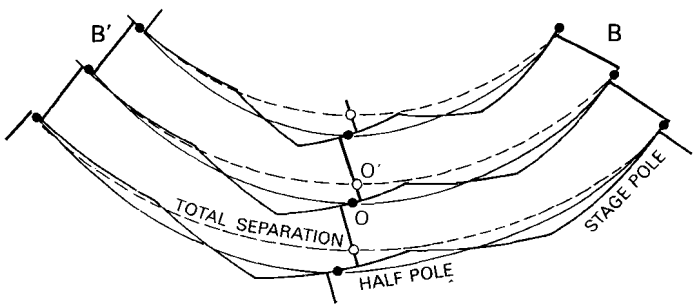

Figure 4.1 - Definition of total separation poles, half poles and stage poles.

changes in spreading direction occurred between the defined anomalies (Le Pichon *et al.*, 1973; Ladd, 1976; Dewey, 1975).

Collette *et al.* (1984) were the first to present a spreading history for the central North Atlantic, with stage poles defined between two changes in spreading direction observed on the African plate. Directions and lengths of fracture zone segments were used to obtain the position and rotation angle of the stage poles. The stage poles were related to identified magnetic lineations by specifying a rotation angle before and after each anomaly.

If changes in spreading direction took place between magnetic anomalies, the process of finding stage poles from total separation poles is not uniquely solvable. In section 4.6 we will show that the determination of half poles gives additional constraints. A method will be developed that makes it possible to incorporate both magnetic isochron data and fracture zone trends in the construction of a set of stage poles which accord to the half poles. This method is reducing the indeterminacy of the problem, and compensates for the influence which errors in individual stage poles may have on the total separation poles of well-defined magnetic anomalies.

4.2 Finite rotations

Firstly, the relevant mathematical formulation for finite rotation will be recapitulated. Linear algebra theory is used for the description of motion on a sphere, as is done in classical mechanics (cf. Goldstein, 1950). If S is a point on a sphere with radius 1, it may be expressed in cartesian coordinates (Figure 4.2):

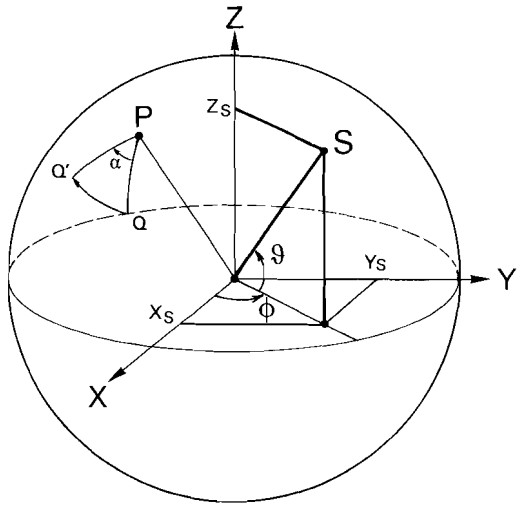

Figure 4.2 - Definition of the x, y and z component of vector $S(\theta,\phi)$, and of rotation angle α.

$$S = \begin{bmatrix} x \\ y \\ z \end{bmatrix} = \begin{bmatrix} \cos\theta \cos\phi \\ \cos\theta \sin\phi \\ \sin\theta \end{bmatrix} \tag{4.1}$$

with θ the latitude of point S, and ϕ its longitude. It should be noted that θ is used for the latitude, in contrast to the convention used by Goldstein (1950), who uses θ for the colatitude. A rotation on the sphere is an orthogonal transformation that can be specified by the position of the pole P (θ_p ,ϕ_p) and the rotation angle α. The angle of rotation α is measured clockwise (see Figure 4.2). The rotation matrix T will transform point Q to a point Q' on the sphere:

$$Q' = T \cdot Q \tag{4.2}$$

In general T can be split into three operations:

$$T = A^{-1} \cdot R \cdot A \tag{4.3}$$

where A is a transformation to the coordinate system where the rotation pole becomes (0,0,1). R is a rotation around this pole, and A^{-1} is the inverse of A.

The following expressions are found for the matrices A and R:

$$A = \begin{bmatrix} \sin\theta_p \cos\phi_p & \sin\theta_p \sin\phi_p & -\cos\theta_p \\ -\sin\phi_p & \cos\phi_p & 0 \\ \cos\theta_p \cos\phi_p & \cos\theta_p \sin\phi_p & \sin\theta_p \end{bmatrix} \tag{4.4}$$

$$R = \begin{bmatrix} \cos\alpha & \sin\alpha & 0 \\ -\sin\alpha & \cos\alpha & 0 \\ 0 & 0 & 1 \end{bmatrix} \tag{4.5}$$

As the rotation is an orthogonal transformation, A^{-1} can be obtained by transposing matrix A, i.e. $A^{-1}=A^t$.

From (4.3)-(4.5) we obtain the following expression for transformation matrix T, with x_p, y_p and z_p the x, y and z coordinate of the pole of rotation P:

$$T = \begin{bmatrix} \cos\alpha + (1-\cos\alpha)\, x_p^2 & z_p \sin\alpha + (1-\cos\alpha)\, x_p y_p & -y_p \sin\alpha + (1-\cos\alpha)\, x_p z_p \\ -z_p \sin\alpha + (1-\cos\alpha)\, x_p y_p & \cos\alpha + (1-\cos\alpha)\, y_p^2 & x_p \sin\alpha + (1-\cos\alpha)\, y_p z_p \\ y_p \sin\alpha + (1-\cos\alpha)\, x_p z_p & -x_p \sin\alpha + (1-\cos\alpha)\, y_p z_p & \cos\alpha + (1-\cos\alpha)\, z_p^2 \end{bmatrix} \tag{4.6}$$

The rotation pole $P=(\cos\theta_p \cos\phi_p\ ,\ \cos\theta_p \sin\phi_p\ ,\ \sin\theta_p)=(x_p\ ,\ y_p\ ,\ z_p)$ is invariant under transformation T. The combination of different rotations is now equivalent to the multiplication of the corresponding different transformation matrices T. The rotated position Q' of any point Q can be obtained be multiplication of its position vector with T (eq. 4.2).

4.3 Relation between total separation poles and stage poles

Every stage pole on one plate is related to the stage pole of the same age zone on the other plate. A rotation over the total separation pole which separates the two age zones tranports the stage pole of one plate to the other. In other words, there is only one stage pole for both plates at the time it is "active", but as both plates continue their movement in different directions in the more recent history, the reference systems become separated and one obtains a stage pole for each plate. With the knowledge of a complete series of stage poles for one plate it is possible to calculate the stage poles for the conjugate plate. It is important to note that the summation of stage poles on one plate give a half pole, that is in general not equal to the half pole on the other plate. The addition of all subsequent stage poles on both plates yields the total separation pole and is equal to the addition of the two half poles which describe the history of each plate.

The inverse process of finding stage poles from total separation poles is used in many reconstructions which are presented in terms of the relative positions of the involved plates at different times (a.o. Le Pichon and Fox, 1971; Pitman and Talwani, 1972; Francheteau, 1973; Ladd, 1976; Olivet *et al.*, 1984; Patriat *et al.*, 1985; Klitgord and Schouten, 1986). These reconstructions are based on magnetic anomalies and their total separation poles, sometimes additionally constrained by the superposition of fracture zone intersections on both plates. From a given set of total separation poles, stage poles can be calculated for both plates with the method of Le Pichon *et al.* (1973), if no change in spreading direction occurred between the identified anomalies. Figure 4.3 shows the configuration of two total separation poles ($P_{AA'}$ and $P_{BB'}$), and the way that the stage poles (P_{AB} and $P_{A'B'}$) for both plates are related to them. Several authors noted that, as the pole of instant motion is not necessarily equal to the pole of total motion in a period between two anomalies, stage poles computed in this way give, in general, only an approximation of the actual motion (Le Pichon *et al.*, 1973; Ladd, 1976; Dewey, 1975). Additionally, there is no reason that changes in spreading direction would take place exactly at the time of a certain anomaly and, especially when the age difference between two adjacent identifiable isochrons is large, intermediary changes in spreading direction are very likely.

Another disadvantage of the generally adopted procedure to calculate stage poles

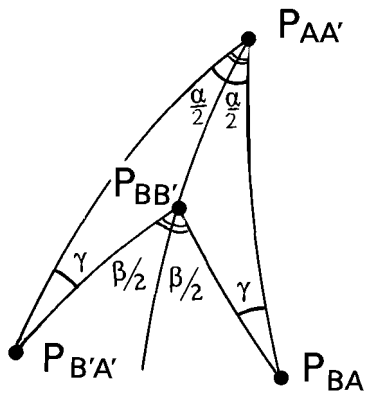

Figure 4.3 - Graphical determination of the positions of poles P_{BA} and $P_{B'A'}$ and their rotation angle γ, for given total separation poles $P_{AA'}$ and $P_{BB'}$ with angles α and β respectivily.

directly from the total separation poles, is that it does not give the possibility to include information on fracture zone directions. We will therefore develop a different method to find stage poles, using both fracture zone traces and magnetic anomaly data, and allowing changes in spreading direction between isochrons. The solution found when assuming constant stage poles between magnetic lineations only forms a special case of the more rigorous approach.

The fact that total separation poles are the sum of a set of stage poles, implies that a correction of one of the stage poles, e.g. when additional data become available, would change the (older) total separation poles. This means that in order to keep total separation poles fixed, correction of a stage pole always has to be compensated for by the adjustment of another stage pole.

When the number of stage poles involved is large, the number of possible adjustments is practically unlimited. The minimum number of stage poles needed to describe the spreading history of the central North Atlantic is 13, an estimate which is based on the combination of the history by Collette *et al.* (1984) since anomaly 34, and Slootweg and Collette (1985) in the period 34-M0. In order to reduce the number of degrees of freedom involved, the study area is divided into sub-areas or age zones, comprised by well defined isochrons. In each age zone there is only a small number of stage poles, and reconstruction of the spreading history of one age zone can be carried out independently of the spreading history before and after. Also, the final set of stage poles constructed in that way leaves the total separation poles of the well defined magnetic lineations fixed. This means that possible errors in individual stage poles do not have influence on the reconstruction as a whole.

4.4 Construction of total separation poles

If lithospheric plates behave rigidly, isochrons on two diverging plates keep their initial form. In that case rotation about the total separation pole makes coincide the two isochrons of the same age exactly. In practice, differences between the two separated isochrons will exist, but still it appears possible to define total separation poles very accurately when sufficient data are available.

Total separation poles are constructed using minimum criteria for the misfit between isochrons and fracture zone traces on both plates. For irregularly spaced data, the quantification of this misfit is discussed by Hellinger (1981). In practice, visual inspection of the superposition of isochrons appears to give good results, especially when data are available over the total length of the isochrons. The method of homologous points, as developed by Bonnin (1978), is very convenient for the calculation of total separation poles. This method allows a fast determination of the Euler pole in a graphical way. It starts with the definition of two homologous points on the respective isochrons on the different plates. Homologous points are points that coincided at the time that the isochron was formed. The next step in the reconstruction is the superposition of one point on the other, for which any pole of rotation can be chosen. For convenience, we will take the pole at a distance of 90° from both points (Figure 4.4). In the coordinate system of this great- circle pole the two homologous points are situated on the equator. Therefore, the rotation angle α that rotates one point to the other is equal to the great-circle distance between the two points:

$$\cos\alpha = \sin\theta_1\sin\theta_2 + \cos\theta_1\cos\theta_2\cos(\phi_2 - \phi_1) \tag{4.7}$$

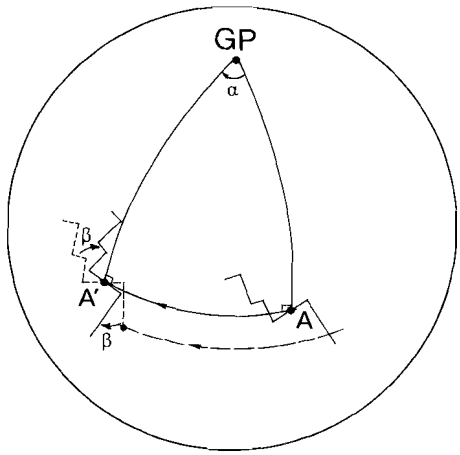

Figure 4.4 - The method of the homologous points: point A is rotated to A', using the great-circle pole. An additional rotation β around A' is applied to make the isochrons fit.

where θ_1 and θ_2 are the latitudes of the homologous points H_1 and H_2, ϕ_1 and ϕ_2 their longitudes. The position of the pole P is found from the vector product of H_1 and H_2:

$$P = (H_1 \, x \, H_{2)} / \sin\alpha$$

$$= 1/\sin\alpha \begin{bmatrix} \cos\theta_1\sin\phi_1\sin\theta_2 - \cos\theta_2\sin\phi_2\sin\theta_1 \\ \cos\theta_2\cos\phi_2\sin\theta_1 - \cos\theta_1\cos\phi_1\sin\theta_2 \\ \cos\theta_1\cos\phi_1\cos\theta_2\sin\phi_2 - \cos\theta_2\cos\phi_2\cos\theta_1\sin\phi_1 \end{bmatrix} \quad (4.8)$$

Rotation of one of the isochrons around the great-circle pole is the following step in the reconstruction. The fit must then be improved by a supplementary rotation a around the superimposed points (Figure 4.4). The final total separation pole is the summation of the great-circle pole and the additional rotation around the homologous points.

In practice, the application of the method depends on the possibility of identification of homologous points. In the central Atlantic Ocean, the longitude of these points can be accurately defined using the magnetic anomalies, the latitude by making use of the fracture zones. Moreover, different sets of homologous points can be used to test the variation in the resulting total separation pole. Finally, the method described by Stock and Molnar (1983), which is basically a sensitivity test, can be used to define the variation of the total separation poles in relation with the errors in the data.

4.5 Construction of half poles

Once the total separation poles for the selected magnetic lineations have been obtained, the lithospheric plates are divided in a number of age zones, as explained earlier. Equivalent age zones on both plates are brought together at their younger boundaries, as shown in Figure 4.5. In this way one is left with a limited number of reconstructed plate configurations. These are all equivalent to the configuration of two isochrons and the present spreading axis (Figure 4.5). Because we are still dealing with total rotations, the total separation pole for the reconstructed positions of the outer isochrons can be directly obtained from the total separation poles for the two isochrons before reconstruction (see section 4.3). In the following, we will deal with the problem of reconstructing the spreading history for the most recently formed part of the plates.

The plate configuration to be solved is given in Figure 4.1, where the total separation pole of the outer isochron is given. This total separation pole transfers homologous points from one isochron to the other, but does not necessarily make them pass through structurally equivalent points on the spreading axis. This would be the case if the total separation pole is equal to the stage pole, i.e. if no change in spreading direction occurred in the time that passed since the outer isochrons were formed. If one or more changes in spreading direction occurred, for each plate a different half pole is found that brings a point (0) of the spreading axis to the equivalent point (B, B') of the isochron (see Figure 4.1). Half poles represent the total motion between one isochron and the spreading center and, therefore, form an additional constraint.

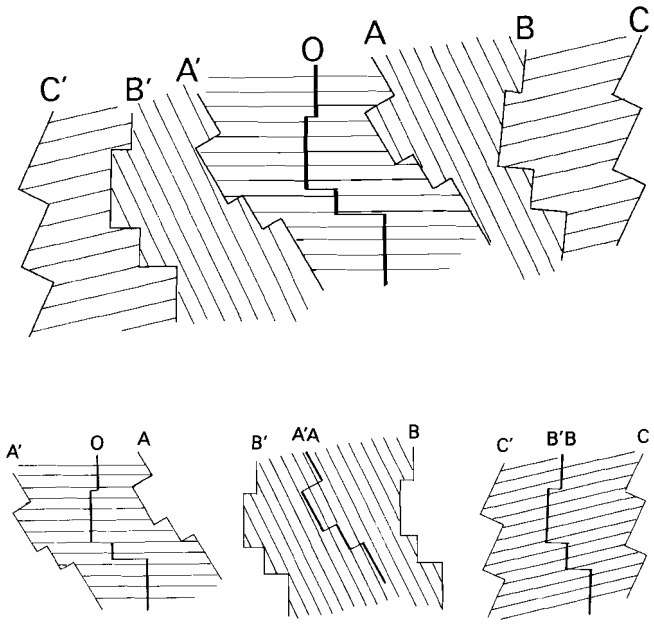

Figure 4.5 - Different age zones between selected isochrons (A, B and C) are reconstructed to the position of the younger isochrons, thus yielding three equivalent problems.

As for the total separation poles, for the calculation of the half poles the method of homologous points is used. However, the points are not homologous, but merely structurally equivalent. This difference is of no consequence for the method. The equivalent points are defined on a fracture zone which is continuous between the two isochrons on each plate. Half poles are calculated for both plates.

Using the two pairs of equivalent points B'-0 and 0-B (Figure 4.6), two great-circle poles are calculated, as a first estimation of the half poles. Their sum does not necessarily equal the total separation pole. An extra rotation around point 0 is needed to fulfil this condition. Under the assumption that the rotation angles for both half poles are equal, the extra rotation has to be equal for both plates. These extra rotations will result in a shift of the sum of the two half poles along a great- circle trough point 0 and the total separation pole for the outer isochron. The final solution is found, when the addition of the two half poles equals the total separation pole.

The assumption that rotation angles for both half poles are equal is valid, and then by approximation only, if the stage poles are not too far apart. Comparison of rotation angles for half poles on both plates, determined from published spreading histories (Le Pichon and Fox, 1971; Pitman and Talwani, 1972; Collette *et al.*, 1984; Klitgord and Schouten, 1986) showed that they seldom differ more than 0.01 °. Especially when only a few stage poles are involved, as is the case in the age zones defined, we conclude that the above assumption is justified for the study area.

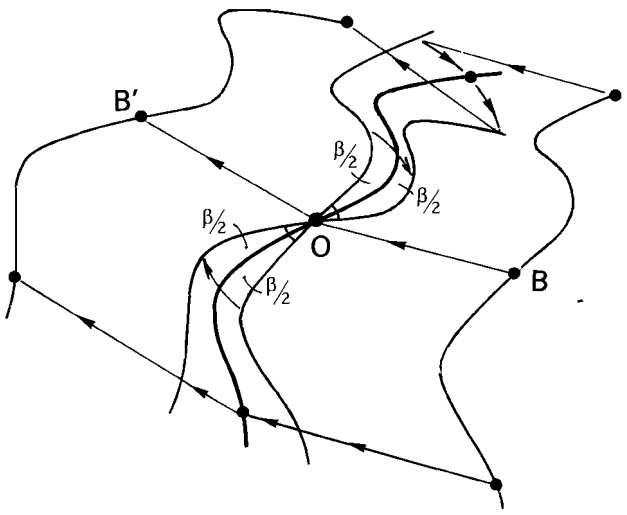

Figure 4.6 - The half pole P_{B0} is found as the summation of the great circle pole that rotates point B to point 0 and a rotation β/2 around point 0. The half pole $P_{0B'}$ is found in the same way.

The mathematical formulation for the calculation of both half poles is given below. Let T_{ts} be the matrix for the total separation pole, and T_{hw} and T_{he} the half rotations between the spreading axis and the western and eastern isochron, respectively. They fulfil the condition:

$$T_{hw} \cdot T_{he}^{-1} = T_{ts} \tag{4.9}$$

T_{he} and T_{hw} can be split in a rotation around the great-circle poles, T_{gpe} and T_{gpw}, and the extra rotation, T_{ad}, around the equivalent point on the spreading axis:

$$\begin{aligned} T_{he} &= T_{gpe} \cdot T_{ad}^{-1} \\ T_{hw} &= T_{gpw} \cdot T_{ad} \end{aligned} \tag{4.10}$$

so:

$$\begin{aligned} T_{ts} &= T_{gpw} \cdot T_{ad} \cdot (T_{gpe} \cdot T_{ad}^{-1})^{-1} \\ &= T_{gpw} \cdot T_{ad} \cdot T_{ad} \cdot T_{gpe}^{-1} \end{aligned} \tag{4.11}$$

Given the total separation matrix T_{ts}, and the two greatcircle pole matrices T_{gpe} and

T_{gpw} the supplementary rotation T_{ad} can be calculated from (4.11), as:

$$T_{ad} \cdot T_{ad} = T_{gpw}^{-1} \cdot T_{ls} \cdot T_{gpe} \tag{4.12}$$

The two half poles are finally found with (4.10).

4.6 Calculation of stage poles

The final step is the determination of the stage poles which on both plates fit the half pole and, therefore, the total separation pole. There is an infinite number of combinations of stage poles that fits a half pole. However, the circumstance that the resulting stage poles on the other plate have to fit the half pole for that plate, limits the solution. In case of only one change in spreading direction, one fracture zone direction is needed to obtain an exact solution.

The problem is illustrated in Figure 4.7a. Given a well- defined spreading axis (0) and two corresponding isochrons (B,B') on both plates. Using the method described above, we can calculate the total separation pole $P_{BB'}$, and the half poles P_{B0} and $P_{0B'}$. If the

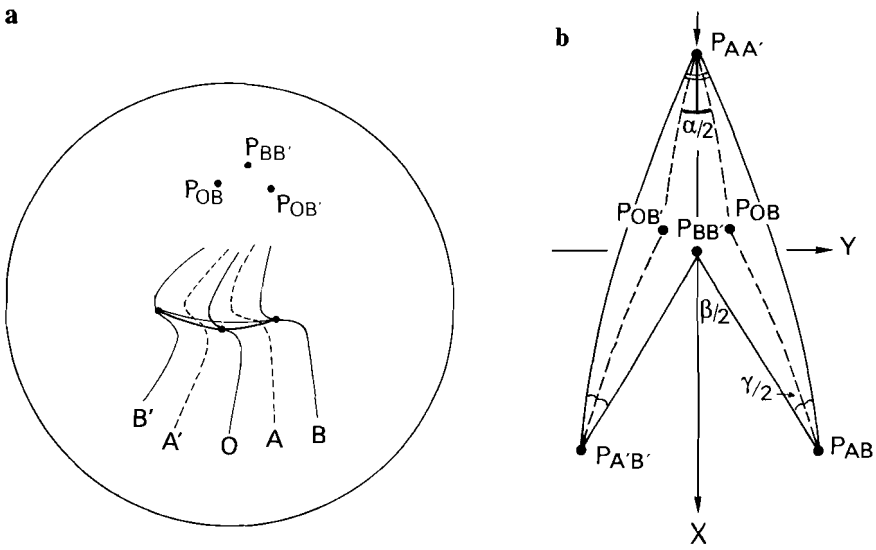

Figure 4.7 - (a) If the half poles P_{0B} and $P_{0B'}$ do not have the same position as pole $P_{BB'}$, at least one change in spreading direction occurred at the *a priori* not known isochrons A and A'. (b) Stereographic projection of the different pole positions and angles of rotation, in the coordinate system of pole $P_{BB'}$.

positions of these three poles are identical, the conclusion is that the direction of spreading was constant since anomaly B. The method, generally used, to calculate stage poles from total separation poles indeed uses the assumption that half poles between two subsequent isochrons are equal to the stage poles.

If the half poles for both plates are different, they are evidently not equal to a stage pole. This means that there was at least one change in spreading direction. For the description of the spreading pattern, we define auxiliar isochrons for the moment that a change of spreading occurred. In case that there was only one change at, say, auxiliar isochron A between 0 and B, one has to find a stage pole between isochron B and A, and a total separation pole of A and A'. These new poles have to obey the following conditions. -Stage pole P_{BA} summed with half the total separation pole of A result in the half pole from B to the spreading axis, P_{B0}. -In the same way $P_{B'A'}$ added to the half rotation A'A must give $P_{B'0}$. -Furthermore the pole $P_{B'A'}$ rotated over $P_{A'A}$ results in P_{AB}, as well as $P_{B'A'}$ rotated over $P_{B'B}$. -In the last place $P_{B'0}$ rotated over half the rotation AA' gives P_{0B}.

Figure 4.7b shows the position of the different poles in the coordinate system where pole $P_{B'B}$ is (0,0,1). The mathematical formulation is simplified, due to the symmetry in the pole configuration. The pole positions of the known total separation pole $P_{B'B}$ and the two half poles P_{0B} and $P_{0B'}$ are:

$$P_{BB'} = \begin{bmatrix} 0 \\ 0 \\ 1 \end{bmatrix} ; P_{0B'} = \begin{bmatrix} x_{hp} \\ y_{hp} \\ z_{hp} \end{bmatrix} ; P_{0B} = \begin{bmatrix} x_{hp} \\ -y_{hp} \\ z_{hp} \end{bmatrix} \tag{4.13}$$

The unknown stage poles of rotation are $P_{AA'}$, P_{AB} and $P_{A'B'}$:

$$P_{AA'} = \begin{bmatrix} x_a \\ y_a \\ z_a \end{bmatrix} = \begin{bmatrix} -\cos\theta_a \\ 0 \\ \sin\theta_a \end{bmatrix} ; P_{AB} = \begin{bmatrix} x_b \\ y_b \\ z_b \end{bmatrix} = \begin{bmatrix} \cos\theta_b \cos(\beta/2) \\ -\cos\theta_b \sin(\beta/2) \\ \sin\theta_b \end{bmatrix} ;$$

$$P_{A'B'} = \begin{bmatrix} x_b \\ -y_b \\ z_b \end{bmatrix} = \begin{bmatrix} \cos\theta_b \cos(\beta/2) \\ \cos\theta_b \sin(\beta/2) \\ \sin\theta_b \end{bmatrix} \tag{4.14}$$

The following expressions are found for the transformation matrices:

$$T_{AA'} = \begin{bmatrix} \cos\alpha + (1-\cos\alpha)\cos^2\theta_a & \sin\theta_a \sin\alpha & (1-\cos\alpha)\cos^2\theta_a \\ -\sin\theta_a \sin\alpha & \cos\alpha & \cos\theta_a \sin\alpha \\ (1-\cos\alpha)\cos^2\theta_a & -\cos\theta_a \sin\alpha & \cos\alpha + (1-\cos\alpha)\sin^2\theta_a \end{bmatrix}$$

$$T_{AB} = \begin{bmatrix} \cos\gamma + (1-\cos\gamma)x_b^2 & z_b\sin\gamma + (1-\cos\gamma)x_b y_b & -y_b\sin\gamma + (1-\cos\gamma)x_b z_b \\ -z_b\sin\gamma + (1-\cos\gamma)x_b y_b & \cos\gamma + (1-\cos\gamma)y_b^2 & x_b\sin\gamma + (1-\cos\gamma)y_b z_b \\ y_b\sin\gamma + (1-\cos\gamma)x_b z_b & -x_b\sin\gamma + (1-\cos\gamma)y_b z_b & \cos\gamma + (1-\cos\gamma)z_b^2 \end{bmatrix}$$

$$T_{A'B'} = \begin{bmatrix} \cos\gamma + (1-\cos\gamma)x_b^2 & z_b\sin\gamma - (1-\cos\gamma)x_b y_b & y_b\sin\gamma + (1-\cos\gamma)x_b z_b \\ -z_b\sin\gamma - (1-\cos\gamma)x_b y_b & \cos\gamma + (1-\cos\gamma)y_b^2 & x_b\sin\gamma - (1-\cos\gamma)y_b z_b \\ -y_b\sin\gamma + (1-\cos\gamma)x_b z_b & -x_b\sin\gamma - (1-\cos\gamma)y_b z_b & \cos\gamma + (1-\cos\gamma)z_b^2 \end{bmatrix}$$

(4.15)

The only equations that are available to solve the four variables (rotation angles α and γ, and the latitudes θ_a and θ_b) are:

$$T_{0B} = T_{AB} \cdot T_{\frac{1}{2}\,angle\ AA'} \tag{4.16a}$$

$$T_{0B'} = T_{A'B'} \cdot T_{\frac{1}{2}\,angle\ AA'} \tag{4.16b}$$

Equations (4.16a & b) give only three independent equations, since (4.16b) is the mirrored equivalent of (4.16a), and we are left with one adjustable parameter. We will take θ_a, the latitude of $P_{AA'}$, as parameter, and find the following expression for the rotation angle α of $T_{AA'}$ as a function of θ_a:

$$\alpha = \cos^{-1}\left(\frac{1 - 2(\sin\theta_{hp}\cos\phi_{hp})^2}{1 - (\sin\theta_a\sin\phi_{hp} - \cos\theta_a\cos\phi_{hp}\cos\theta_{hp})^2}\right) \tag{4.17}$$

Once that θ_a is known, α can be calculated with (4.17). $T_{AA'}$ is found from (4.15), and the matrices T_{AB} and $T_{A'B'}$ are calculated with equation (4.16a & b). The matrices define the positions of P_{AB} and $P_{A'B'}$, and the rotation angle γ.

θ_a, or pole $P_{AA'}$, is determined in the following way. As can be seen from Figure 4.7b, $P_{AA'}$ is situated on the great- circle through pole $P_{BB'}$ and the middle point of the arc defined by the two half poles P_{0B} and $P_{0B'}$. Depending on the position of pole $P_{AA'}$, the predicted directions of spreading will change. Thus, fracture zone directions can be used to establish the position of pole $P_{AA'}$ on the great-circle. Figure 4.8 shows that the pole $P_{AA'}$ is situated at the intersection of two great-circles, one of which is defined orthogonal to the direction of a fracture zone, which forms a small circle segment with regard to $P_{AA'}$, the other by the configuration of total separation pole and the two half poles.

The described method can be used to find three stage poles (the central stage pole and two conjugate older poles) when a total separation pole, two half poles, and a fracture zone direction is given. When more stage poles are involved, the way to proceed is to

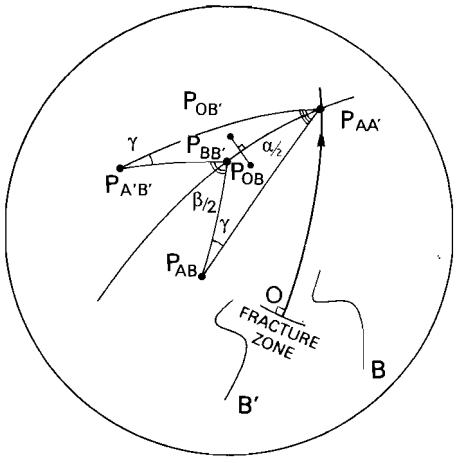

Figure 4.8 - The pole position of $P_{AA'}$ is found at the intersection of two great-circles, one of which is perpendicular to a measured fracture zone direction, the other defined by point $P_{BB'}$ and the midpoint of the two half poles P_{0B} and $P_{0B'}$.

first define auxiliar isochrons from the magnetic isochrons and the fracture zone geometry. Auxiliar isochrons are then treated as B and B' or 0 in equations (4.13)-(4.16).

4.7 Direct measurements of stage poles

A number of methods have been used to find stage poles directly from the actual data. Fracture zone trends alone (Wilson, 1965; Morgan, 1968; Le Pichon, 1968), or together with spreading rates determined from magnetic anomalies (McKenzie and Sclater, 1971; cf. Slootweg and Collette, 1985), can be combined to give the stage pole. Spreading velocities, expressed in cm/year, vary with the distance to the rotation pole; two measured isochron distances determine the position of the stage pole. If there is a longer period of constant spreading direction, poles of motion may be determined from the curvature of fracture zones (Phillips and Luyendijk, 1970).

The method, used in this study to find stage poles from the actual data is a modification of Le Pichon's (1968) method, described by Slootweg and Collette (1985). The root-mean-square misfit for both fracture zone directions and fracture zone segment lenghts with respect to predicted values, is calculated for different pole positions on a grid. The first search leads to the definition of a new search area with, if possible, a smaller grid-distance. The procedure can be repeated until the desired grid precision is reached. Each data point can be assigned a weight, according to its (subjective) accuracy. The procedure was developed to calculate stage poles for irregularly distributed fracture zone strike and spreading rate data, on one plate.

The fact that the stage poles on one plate in a two plate system are related to those on the other plate, makes it possible to combine data from both plates to calculate one stage pole. This is done by rotation of the data of one plate to the other with the total separation pole. Segment lengths are invariant under this rotation, but fracture zone azimuths change. The combined data set of two plates is used to give a stage pole for one plate. The equivalent pole on the other plate is obtained by rotating the stage pole back over the total separation pole.

Not only stage poles are better constrained by the utilisation of data on both plates. Comparison of azimuth data on one plate with data rotated from the other plate, provides a possibility to test the total separation pole used, independent of the stage pole which is computed from the same data.

4.8 Final remarks

In the present study, both total separation poles, and independently defined stage poles will be fitted into one model that gives an adequate description of the NOAM-AFRC relative motion. We outlined the procedure which is used to minimize the propagation of errors existing in individual poles. This chapter only considered the theoretical way to find total separation poles, half poles and stage poles. Errors in the isochron identifications and fracture zone data are not yet taken into account. The only approximation is made when half poles are calculated (section 4.5). In practice, the errors associated with this approximation are negligible. Different sets of points are used to test the precision of the calculated poles. Errors do not only depend on the accuracy of the data but also on their distribution in relation to the poles of motion. Also important are the stochastic aspects of the spreading process, the differences between fracture zones and actual flowlines, and the amount of later deformation that may be involved. This type of errors will be discussed with the presentation of the reconstruction in the next chapter.

Chapter Five

Reconstruction

5.1 General principles

The reconstruction of the central North Atlantic spreading history is performed following the principles outlined in Chapter 4, and based on the analysis of magnetic anomalies, seismic reflection data, Seasat gravity and shipborne gravity data. The fact that both magnetic isochrons and fracture zones are used in the analysis, makes the number of adjustable parameters so large, that it is necessary to divide the study area in age zones. Comparison of the shape of the different isochrons provided an additional, equally important, reason for this division.

The overall form of isochrons of different ages is not equal, what means that ridge reorganisation must have taken place. Reorganisation includes the disappearence and creation of offsets, the north-south jumping of fracture zones and the east-west displacement of parts of the spreading axis. East-west displacement of the spreading segments may be realized by ridge jumps or by asymmetric spreading. No evidence is found for asymmetric spreading of the Mid-Atlantic Ridge between 10° and 40° N as a whole, which means that neither of the two plates has been growing significantly faster in a certain period. A strong argument for the symmetry of spreading is found in the spreading history presented by Collette *et al.* (1984): although their stage poles were only based on African plate data, the resulting flowline pattern for the American plate is basically right. East-west displacements of the spreading segments will, therefore, be treated as ridge jumps.

A priori, there is no reason for the spreading axis not to be stable during a period with a constant spreading direction. For the moment being, we will assume that major reorganisations of the spreading axis are caused by changes in spreading direction. Periods of constant spreading direction allow an accurate measurement of fracture zone directions and, in combination with the magnetic anomalies, a precise definition of the acient spreading axis. Therefore, the isochrons used to define the different age zones, are selected in periods of constant spreading.

After the assessment of total separation poles for the selected isochrons, the half poles, which rotate reference isochrons to the adjacent ones, are obtained. Until that part of the reconstruction, not much use is made of the fracture zone traces and directions. The only condition is that total separation and half poles have to fit the recognizable fracture zones at their intersections with the selected isochrons.

For the final construction of the synthetic flowline pattern, a minimum number of stage poles is used. The set of stage poles that describes the relative movement of the American and African plates, has to obey the selected total separation poles and half poles.

The procedure followed to display the spreading pattern consisted of developing the ridge geometry from a chosen isochron to the next, accounting for the changes of form due to changes in spreading direction. In general the ridge geometry generated in this way, does not conform to the real isochron and a new definition of the ridge has to be taken. This means that a ridge jump is postulated at the place of this isochron, although we recognize that this is a simplification since reorganisation of the spreading axis is likely to have happened within the age zones. If the discrepancies, i.e. the ridge jumps, were large, the reorganisation was projected backwards in time to where a large change in spreading direction occurred.

For the realisation of the different steps, we choose for graphical methods. Synthetic flowlines were produced for different age zones and compared with the basic documents at a scale of 1:5961815 (1/5th of the scale of the GEBCO plotting sheets). The reason for this way of working lies in the difficulty of defining directions of finite fracture zone segments, which are always small circle segments, as long as their length has not yet been defined. Therefore, a numerical approach would be extremely tedious, if feasible. Also, the inhomogeneity of the data and their coverage necessitate the giving of a weight to each observation, which can only be done in a subjective way. Numerical correlations between profiles were tried, but proved inadequate. Therefore, visual correlation was the best tool.

After the presentation of the synthetic flowline and magnetic anomaly pattern, the accuracy of the reconstruction in relation to the basic assumptions will be discussed. For this purpose segments of fracture zones in chosen age zones, defined in length by the angles of rotation, were measured. The respective age zones were treated numerically (Tables 5.4-5.6). Even these data depend on the definition of the zone to which they refer and should be treated with caution.

5.2 Selected isochrons and their total separation poles

The reconstruction was started with the definition of a number of selected isochrons and their total separation poles. The isochrons were selected for their occurrence during longer phases of constant spreading direction and for their recognition over a large part of the study area on both plates. The magnetic anomalies M0, 33, 25 and 13 were chosen on these criteria. In addition, the present spreading axis was used in the analysis of the area between anomaly 13 east and west.

Anomaly M0 marks the beginning of the Cretaceous Magnetic Quiet Zone (CMQZ). The magnetic anomaly is well-defined on both the American and the African plate. There are no indications for a substantial change in spreading direction immediately before or after M0 (Slootweg and Collette, 1985). A detailed study of the magnetic anomalies M0-M4 near Kane FZ on both the American and the African plate (Rohr and Twigt, 1980) makes the total separation pole for anomaly M0 well constrained. This detailed analysis reduces the north-south error in the reconstruction of the magnetic isochrons. We use the total separation pole by Klitgord and Schouten (1986), which incorporates the results of Rohr and Twigt (1980).

A major change in spreading direction occurred just before anomaly 34 (Collette *et al.*,

1984; Slootweg and Collette, 1985). The first suitable magnetic anomaly after the CMQZ is therefore **anomaly 33.** The synthetic flowlines of Collette *et al.* (1984) show a constant spreading direction in a period of about 10 Ma, comprising this anomaly. The finite difference pole of Klitgord and Schouten (1986) was tested for its superposition of different FZ traces on both plates. No reason was found to modify it.

After anomaly 30/31 a counter clockwise change in spreading direction occurred of about 20°. The new direction seems to be stabilized at about anomaly 26, and ends just after anomaly 24. Magnetic **anomaly 25** is used as the next reference isochron. The finite difference pole of rotation was calculated with the method of the homologous points (section 4.4). Homologous points were defined on the isochrons on both plates, at the Kane FZ. The position of the total separation pole differs slightly from the result of Klitgord and Schouten (1986). Their pole does not superimpose the eastern limbs of Kane and Atlantis Fracture Zones on the western ones.

As the limit of the most recent period of central North Atlantic spreading history **anomaly 13** was chosen for a number of reasons. Firstly, the overall form of anomaly 13 differs from that of anomaly 25, indicating a reorganisation of the spreading axis between these anomalies. The spreading direction was essentially constant since anomaly 13. However, several authors reported small changes in spreading direction since anomaly 13 (Fox et al., 1969; Phillips and Luyendijk, 1970; Phillips *et al.*, 1975; Archambault, 1984). Anomalies 13 west and 13 east also comprise the youngest age zone (less than 37 Ma), for which deviations of the small circle pattern were reported by Collette *et al.* (1984). These deviations were modelled thermally (Roest *et al.*, 1984).

The total separation pole of Klitgord and Schouten (1986) was rejected as it posed problems in transforming directions of the African plate to the American (compare section 4.8). The fracture zone directions at anomaly 13 west showed, when rotated to the other plate, a systematic difference with the directions observed at anomaly 13 east. A shift of the total separation pole towards a position closer by, improved this misfit. In doing so, the fit of the magnetic anomalies north of Hayes Fracture Zone appeared to improve.

The total separation poles for anomalies M0, 33, 25 and 13 are given in Table 5.1

Table 5.1 - Total separation poles for the reference isochrons.

Anomaly	Age * (Ma)	Latitude (°N)	Longitude (°E)	Angle (°)	Source
M0	118	66.30	-19.90	54.25	Klitgord & Schouten (1986)
33	79	78.30	-18.35	27.06	Klitgord & Schouten (1986)
25	59	79.44	-0.97	18.16	this study
13	37	75.58	2.22	9.97	this study

*) According to the geomagnetic timescale by Lowrie and Alvarez (1981)

5.3 Determination of half poles

The total motion between two selected isochrons will be described with half poles. The procedure to construct half poles simultaneously for the two equivalent age zones on both plates, was given in section 4.5. We did not yet mention that the determination of half poles from the actual data may be obstructed by the fact that isochrons of different age in general do not have the same form. In a symmetric spreading process, the geometry of transform faults and ridge segments changes with a change in spreading direction.

To describe this geometric adjustment of the spreading axis, mid-points of spreading segments and transform faults are introduced. In this model, the overall form of the ridge is defined by the pattern of mid-points. Changes in spreading direction are supposed not to affect the configuration of mid-points, but only the direction of transform faults and ridge segments. In an orthogonal spreading process, the ridge geometry for any stage pole can then be found by drawing small circle segments at the position of transform fault mid-points, and great circle segments through the mid-points of spreading segments (Figure 5.1). For very large changes in spreading direction, this simple model does not always work, because mid-points of spreading segments may shift to the opposite side of a transform fault, thus creating a configuration that makes spreading geometrically impossible. In that case, also a "real" reorganisation of the configuration of mid-points has to be included, changing the overall form of the spreading axis.

As said before, several of those ridge reorganisations must have taken place, but no evidence was found for asymmetric spreading over the total length of the spreading axis. For the determination of the half poles, we will therefore adopt a model that is based on a symmetric spreading process. In a later stage, jumps of parts of the axis in response to large changes in spreading direction will be incorporated. However, this does not affect the half poles.

Reorganisation of the spreading axis by ridge jumps means that individual fracture

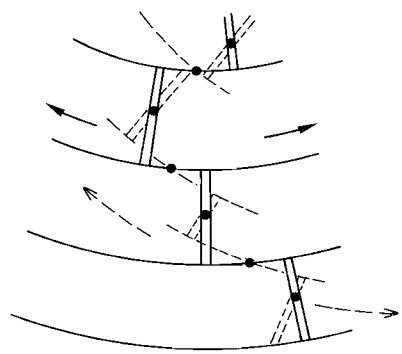

Figure 5.1 - An orthogonal spreading axis is formed by small circle segments through the midpoints of transform faults, and great circles through the midpoints of spreading segments. When changes in spreading direction are not too large, the configuration of midpoints remains stable.

zones may have asymmetric limbs on the two plates. For the construction of the two half poles in our symmetric model we, ideally, want to identify equivalent points on a fracture zone which is not affected by the reorganisation. Distances between the equivalent points, measured along the flowline, are then equal on both plates. Because the flowline is not *a priori* known, in practice the following approximation is made to identify equivalent points: if distances along flowlines are equal, the great-circle distances between start- and end- point of the flowlines on the two plates are also equal. It is difficult to give an exact estimation of the errors made by using this approximation. They depend on the number and the configuration of stage poles and their relative position with respect to the plate boundary under consideration. Modelling of the errors showed that the difference in the distance is of the order of a few kilometers only, for total distances of 500-1000 kilometers.

The procedure to define equivalent points was the following: first fracture zone segments were defined which are continuous between the two adjacent isochrons. Next, mid-points on the fracture zones were chosen. Finally that set of equivalent points was taken for which the great-circle distance between the pair of east points was equal to that of the pair of west points. When the calculated great-circle distances (eq. 4.7) between the two pairs of mid-points did not differ more than a few kilometers, they were accepted. Although minor reorganisations of the spreading axis near the chosen fracture zone cannot be precluded, the condition of equal distances between the two pairs guarantees an effective symmetric spreading. Moreover, different pairs of east and west points were used to test the accuracy of the half poles.

Once the equivalent points on two adjacent reference isochrons are defined, the half poles can be obtained in a straight forward way: great-circle poles are calculated for the two pairs of points (one set on each plate), the extra rotation is now to be applied around the younger points to find the two half poles that fit the previously defined total separation pole (compare section 3.5). Table 5.2 gives the different half poles for the periods M0-33, 33-25, 25-13, 13-1 on both the American and the African plate.

Table 5.2 - Half poles * for both the African and American plates. Pole positions are in the present day coordinate system, and refer to a rotation of the older magnetic anomaly to the younger one.

	AFRICAN PLATE			AMERICAN PLATE		
Period Anomaly	Latitude (°N)	Longitude (°E)	Angle (°)	Latitude (°N)	Longitude (°E)	Angle (°)
M0-33	55.879	-11.396	14.157	55.454	-29.658	-14.153
33-25	72.798	-36.330	4.466	74.792	-47.680	-4.465
25-13	83.630	-18.825	4.161	83.938	1.454	-4.162
13-1	75.416	2.996	4.983	75.752	1.510	-4.983

*) Half poles, calculated as described in section 3.5, give the real total motion between isochrons of different age and are not to be confounded with stage poles computed from total separation poles.

5.4 The stage poles

The following procedure was used to obtain sets of stage poles, or poles of motion, that both accorded to the fracture zone directions on both plates and to the half poles. The fit to the total separation poles of the reference isochrons was assured by the procedure described in section 5.3. In principle, the process of finding stage poles was one of trial and error. However, the fact that half poles were kept fixed reduces the number of degrees of freedom and hence makes the problem better determined. Moreover, errors in the individual stage poles are compensated for by the fit to half poles.

As a starting model the set of rotation poles by Collette *et al.* (1984) was taken, extended with the poles by Slootweg and Collette (1985) for the Cretaceous Magnetic Quiet Zone. Although they did not arrive at a small circle solution for the area comprised between anomaly 13 east and west, for which zone we propose a different interpretation, their rotation history since anomaly 34 gives a good description of the fracture zone pattern. Plate XI shows small circle segments around the different stage poles defined by Collette *et al.* (1984). In the whole procedure the aim was not to change significantly the synthetic spreading directions on the African plate, as given in Plate XI. However, rotation poles had to be modified as they did not fit the total separation poles of the selected isochrons and the half poles.

The first step was to calculate the misfit for each of the half poles, starting from the stage poles defined by the above authors. The deviations which resulted gave an indication of the way the pole positions should be changed to improve the fit. If possible, the pole positions were then adjusted by shifting them along the mean great-circle between the pole and the area of observation, in order to minimize changes in predicted directions. When necessary, a new pole was introduced, and the rotation angle of the neighbouring stage poles adjusted. Intermediary isochrons were used as an extra check on the stage pole positions. Stage poles which fitted well to the fracture zone directions, were used to calculate auxiliar isochrons at the position of changes in spreading direction. The method developed in section 4.6 was then applied to adjust stage poles in order to fit the half poles.

Where possible, the changes in the spreading direction were primarily identified from the shipborne data. The large distance between the Seasat tracks makes it difficult to accurately position a change in spreading direction from the along-track gravity data. Fracture zone directions were measured from Seasat data in the areas where no shipborne measurements were available, in this way enlarging the latitudinal coverage. This also allowed a comparison of fracture zone directions on both plates. The length of the fracture zone segments was not included as a separate parameter, but distances between adjacent magnetic lineations were used to estimate the distance of the pole. Data on the American plate, south of the Fifteen Twenty Fracture Zone, were not included in this part of the analysis, as they are influenced by the relative movement between North and South America (see Chapter 6).

Following Collette *et al.* (1984), the minimum number of stage poles was used that, in finite segments, provides an adequate description of the fracture zone pattern. Half poles that remained after the construction of intermediate isochrons were evaluated. If necessary an additional stage pole was introduced. Checks were done visually. In this way we arrived at 16 stage poles for a definition of the flowlines from magnetic anomaly M0 to present. A discussion of the accuracy of the method is given in section 5.5.

In the following, the analysis of the spreading pattern in the four age zones, separated

by the magnetic anomalies M0, 33, 25, 13 and 1, is presented.

Anomaly M0-33

The reconstruction of the flowline pattern between anomaly M0 and 33, is less well constrained. The absence of seafloor spreading anomalies in the Cretaceous Magnetic Quiet Zone means that no information on intermediate stages is available. In contrast, magnetic fracture zone anomalies are very clearly observed, as they are not obscured by magnetic reversals (Twigt *et al.*, 1983). Slootweg and Collette (1985, cf. also Slootweg, 1986) conclude, on the basis of fracture zone segments on the African plate, delineated from basement structure, gravity and magnetic fracture zone anomalies, and directions of spreading topography inferred from side looking seismics data, that at least 6 different stage poles are involved. Klitgord and Schouten (1986) have only one stage pole between anomaly M0 and 34, which pole resulted from the total separation poles of these two anomalies. Their stage pole does not give a good description of the actual fracture zones.

On the other hand, the stage poles by Slootweg and Collette (1985), predict wrong directions for the western (American) limb of Kane Fracture Zone. Analysis of available fracture zone and spreading topography directions showed that it is not possible to

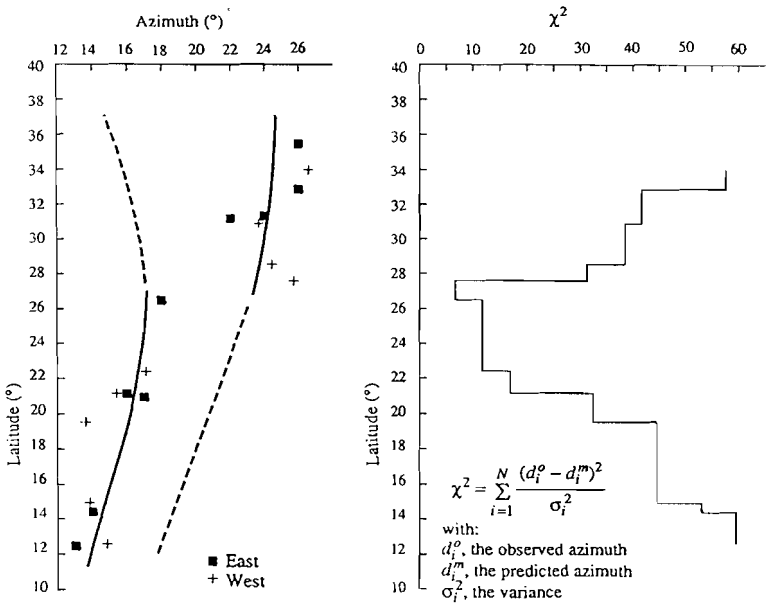

Figure 5.2 - Observed and predicted fracture zone directions in crust near magnetic anomaly M0 on both the American and African plates. Directions north of the New England Seamount Chain can not be combined with those to the south. The χ^2 curve shows a minimum near 27° N, but the 95% confidence interval extends from about 20° to 30°N.

fit the data of the areas north and south of Atlantis, or perhaps Cruiser Fracture Zone, into one model. Figure 5.2 is the combined set of fracture zone and spreading topography directions on both plates, identified in crust close to anomaly M0. It clearly shows that directions can be separated into two groups, and that a better fit can be obtained by assuming that a plate boundary existed in the area. Stein and Gordon (1984) discussed a statistical test of the improvement of the fit, when additional plate boundaries are introduced. They located plate boundaries by searching the position with the lowest value of χ^2, and used the F-ratio test to show the significance of the improvement of the fit.

Unfortunately, the small amount of data available in our case does not allow a very a rigorous approach. The χ^2 distribution shown in Figure 5.2 is calculated by the introduction of a plate boundary at different latitudes. The data north and south of this boundary are then used separately for the determination of a best-fit pole (cf. section 4.7). Figure 5.2 shows a minimum near 27° N. However, its confidence interval is very broad. Therefore, we propose that the most probable position for the plate boundary in this area, is close to the New England Seamounts. The precise differential motions of the area cannot be determined from the present data. We assume that an extension occurred of about 70 km, which affected the M0 isochron on the American plate. This extension led to the creation of the New England Seamounts. Anomaly 33 is supposed to have been left undisturbed. In order not to change the goodness of fit of M0, when using the total separation pole of table 5.1, we adjusted this total separation pole by application of a small additional rotation for the northern part of the area. This additional rotation resulted only in a shift of the rotated data in the general direction of the isochron. In this way, a total separation pole for M0, north of Cruiser Fracture Zone was found which lies at 65.903°N, 18.738°W. Figure 5.3 compares the superposition of the rotated and observed anomaly identifications (based on Rabinowitz *et al.*, 1979; Slootweg & Collette, 1985; and Klitgord & Schouten, 1986), for the two total separation poles. Due to the absence of large offsets, the fit of the anomalies is not seriously affected by the extra rotation for the northern part.

Next, the stage poles of Slootweg and Collette (1985) were modified to give a fit to the half poles and the fracture zone traces both north and south of the proposed boundary. In particular, their CMQZ3 pole at 49.8°N/124.5°E, which was not well constrained, appeared to be inconsistent with the overall motion between anomalies M0 and 33.

The impacts of the proposed relative motion in the area of the New England Seamount Chain will be discussed in section 6.6.

Anomaly 33-25

In the age zone comprised by the magnetic anomalies 33 and 25, a major change of spreading direction occurred. This counter- clockwise change was not yet observed in the reconstruction by Pitman and Talwani (1972). It was first recognized as an important change in spreading direction, in the trace of Kane Fracture Zone on both the American and the African plate (Rabinowitz and Purdy, 1976; Purdy *et al.*, 1979), and confirmed by the data in the Kroonvlag area.

The main difficulty in the reconstruction of this age zone forms the existence of two seamount complexes, which obscure the fracture zone pattern and the magnetic anomalies: on the American plate the Corner Seamounts, on the African plate the

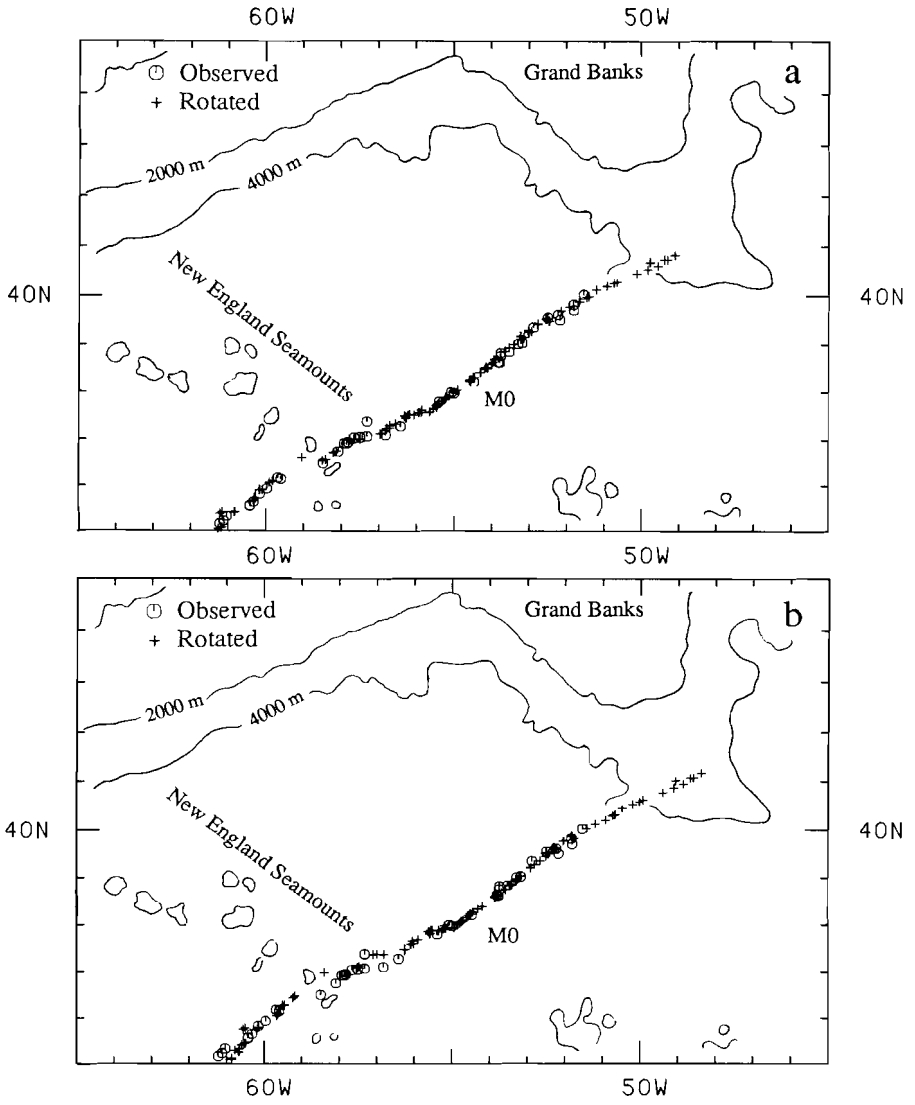

Figure 5.3 - Identifications of magnetic anomaly M0 on the American plate compared with those rotated from the African side with two different poles: (a) Using the total separation pole for the area south of the New England Seamounts; (b) Using the total separation pole for the part north of the New England Seamounts.

Atlantis- Meteor Seamount complex.

Verhoef (1984), corrected the observed magnetic anomalies in the Atlantis-Meteor area for the effect of the seamount anomalies, to make identification of the seafloor

spreading anomalies possible. The tracing of fracture zones from the seismic reflection data is difficult in this area, as the oceanic basement is often obscured by volcanoclastic sediments.

It appears that, although the area where reliable fracture zones directions can be established is limited in latitude (only between the Fifteen Twenty and Atlantis Fracture Zones), the reconstruction becomes fairly well constrained, when data on both plates are combined.

In chapter 6 we will discuss the origin of the two seamount complexes, in relation to the present reconstruction.

Anomaly 25-13

The next age zone is comprised by the magnetic anomalies 25 and 13. Here a gradual clockwise change in spreading direction occurred, which brings the spreading direction back to about what it was at the time of anomaly 33. No major problem occurred in the reconstruction of this age zone, although part of this area is still affected by the Atlantis-Meteor Seamount complex.

The magnetic anomalies 21 and 20 form the most outstanding magnetic anomalies in this age zone, giving additional constraints to the position of the stage poles.

Anomaly 13-1

The most recent rotational history of the central North Atlantic Ocean is more complex than the bathymetric data suggest at first sight. Detailed surveys of transform faults using GLORIA sidescan sonar and Seabeam, in combination with magnetic isochron data, led to a more complex picture. Roest *et al.* (1984) and Collette *et al.* (1984) noticed that the present transform fault directions do not conform to a small circle pattern about a pole of rotation that fits magnetic anomaly 5. Nor do they fit the RM2 model of present day plate motions by Minster and Jordan (1978). Roest and Collette (1986) arrived at the conclusion that the deviation of transform fault directions of the Fifteen Twenty FZ and the Vema FZ can be explained by the relative movement between North and South America. Still, it is not possible to find a total separation pole for anomaly 5 north of the Fifteen Twenty Fracture Zone, fitting the observed transform fault directions.

The solution to this problem was found in the introduction of a change in spreading pole between anomaly 5 and present. For that purpose anomaly 2' was analysed. Anomaly 2' was taken from Phillips *et al.* (1975) in the area near Oceanographer FZ and from W. Twigt (pers comm.; Collette et al, in prep.) immediately north and south of the Fifteen Twenty FZ. The pole given by Phillips et al, based on their observations near Oceanographer is too close to the study area, and does not give a good fit of anomaly 2' near 15°N (Figure 5.4b). In order to fit the observed transform fault directions, the pole should be situated at 1°S 133.5°E (Collette *et al.*, 1984). This pole is too far from the area of observation, and does not accord with anomaly 2'. The pole at 70°N 107°E is the most distant pole that still fits anomaly 2', and that predicts directions that do not deviate more than 1-2 degree in azimuth from the observed transform fault directions (Figures 5.4a and b). Identifications of anomaly 2' by Purdy et al. (1978) near Kane FZ

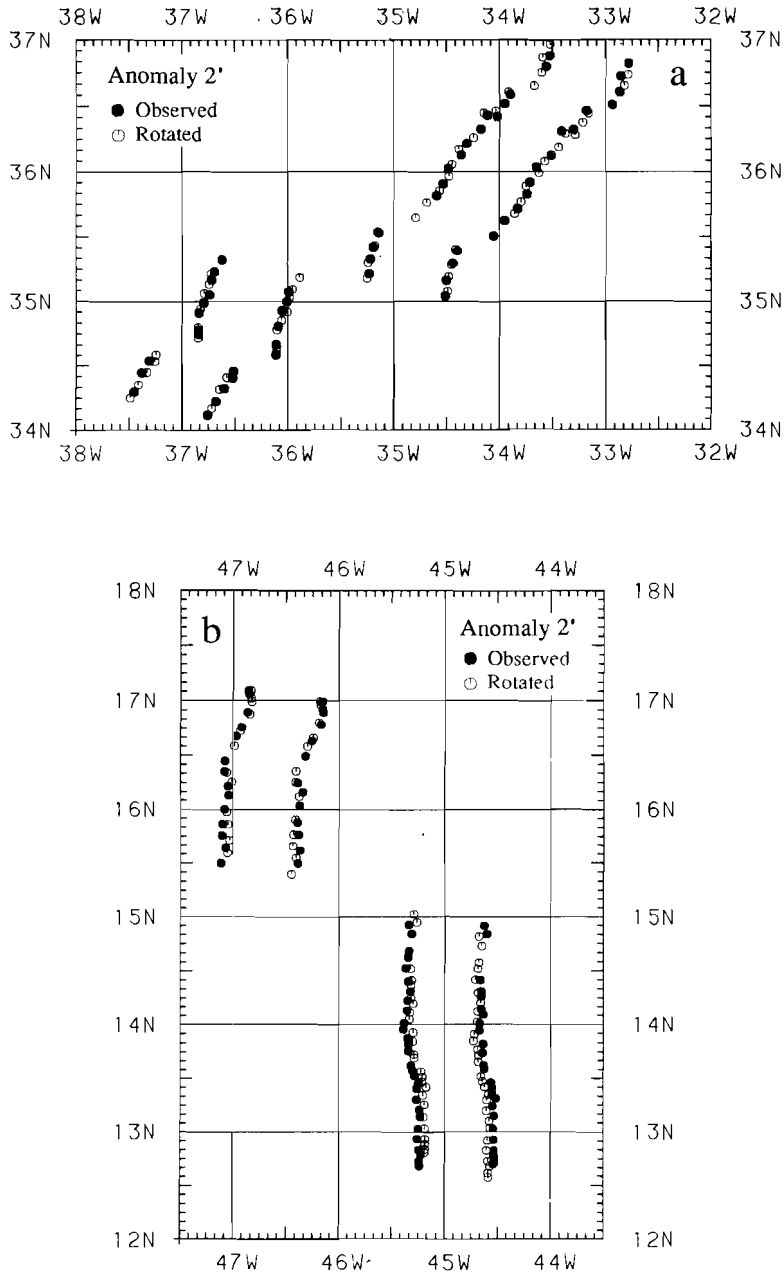

Figure 5.4 - The fit of magnetic anomaly 2'. The identifications are situated at the position of the positive anomaly. (a) The area near Oceanographer Fracture Zone (Phillips *et al.*, 1975). (b) The area north and south of the Fifteen Twenty Fracture Zone (unpublished data).

are also compatible with this pole at 70°N, 107°E.

Figure 5.4b shows a misfit of anomaly 2' south of the Fifteen Twenty, suggesting a slightly faster spreading velocity between South America and Africa. The differential movement between the North and South American plates will be discussed in chapter 6.

In order to fit the separation of anomaly 5, we have to compensate for the far distance of the present stage pole, by situating the preceding pole closer to the area. This rotation pole was located at 73.31°N and 8.83°W and gives a fairly well description of the fracture zones back to anomaly 6.

A final remark concerns the total separation pole of anomaly 6. The magnetic data north of 35° N do not allow a precise definition of this anomaly. The total separation pole gives a good fit for the area between the Fifteen Twenty FZ and Hayes FZ.

Spreading history

Table 5.3 shows the stage poles calculated between the Mid- Atlantic Ridge and magnetic anomaly M0. The stage poles will be refered to by the number of the most significant magnetic anomaly that falls in the period that the stage pole was active. With the stage poles of Table 5.3 we constructed a synthetic flowline and isochron pattern, which is shown in Plate XII. Ridge jumps are incorporated by the introduction of new starting points for the flowlines when necessary. This pattern will be discussed in section 6.2. We will now confine ourselves to a discussion on the accuracy of the different poles.

5.5 Accuracy of the reconstruction

The accuracy of rotation poles is, in general, indicated by their ellipses of 95% confidence. Information on the accuracy of the position of rotation poles is needed to calculate the influence of errors in the pole-positions on the calculation of motion of two plates with respect to a third plate.

In practice it is difficult to imagine the impact of an ellipse of confidence on the trustworthiness of the final result. In other words, it is interesting to know what the influence of a different pole position is in terms of synthetic flowlines and spreading rates. In our discussion on the accuracy of the reconstruction, the errors associated with the subsequent steps will be quantified, starting with the total separation poles, then the half poles and finally the individual stage poles. It will be stressed that the errors are not independent: a variation of one pole must be compensated for by an opposite correction of an other pole in order to obey the flowline pattern.

Total separation poles

If no later deformation of the isochrons occurred, errors in the total separation poles are caused by the inaccuracies in the magnetic anomaly identifications and fracture zone positions. The errors in the fracture zone and magnetic anomaly data of the selected isochrons are estimated to be at maximum 10 km to either side. That this is indeed a

Table 5.3: Central North Atlantic stage poles for the African and American plate. Rotation is defined from young towards old.

	AFRICAN PLATE			AMERICAN PLATE		
Period Anomaly	Latitude (°N)	Longitude (°E)	Angle (°)	Latitude (°N)	Longitude (°E)	Angle (°)
1 - 2'	70	107	-0.325	70	107	0.325
2'-	70	107	-0.575	70	107	0.575
- 5	73.318	-8.830	-0.333	73.866	-11.476	0.333
5 - 6	73.318	-8.830	-1.555	73.866	-11.476	1.555
6 -	71.005	-4.75	-1.523	71.497	-7.643	1.523
- 13	65.	-15.	-0.8	65.829	-19.543	0.8
13 -	65.	-15.	-1.	65.829	-19.543	1.
- 20	69.707	-16.927	-1.034	70.593	-19.656	1.034
20 -	69.707	-16.927	-0.557	70.593	-19.656	0.577
- 21	81.510	174.883	-0.2	80.098	134.899	0.2
21 -	81.510	174.883	-0.922	80.098	134.899	0.922
- 25	60.840	167.121	-0.718	59.494	143.873	0.718
25 -	60.840	167.121	-0.61	59.494	143.873	0.61
- 30	71.202	-47.681	-1.05	73.599	-62.191	1.05
30 -	71.202	-47.681	-0.15	73.599	-62.191	0.15
-	66.525	-27.980	-2.28	68.057	-42.501	2.28
- 33	58.06	-21.05	-0.6	59.157	-38.825	0.6
33 - 34	58.06	-21.05	-1.345	59.157	-38.825	1.345
South of Cruiser Fracture Zone						
34 -	59.20	-19.8	-2.22	60.119	-37.059	2.22
	44.505	-19.921	-1.5	45.940	-43.588	1.5
	48.5	-9.06	-2.16	47.693	-31.463	2.16
	58.504	-10.421	-2.5	57.195	-26.121	2.5
	57.5	-6.50	-4.0	55.273	-23.822	4.0
- M0	70.5	37.5	-0.57	54.589	15.818	0.57
North of Cruiser Fracture Zone						
34 -	55.02	-18.61	-2.66	55.90	-37.597	2.66
	43.4	-14.6	-3.14	44.0	-38.454	3.14
	59.4	-10.2	-2.58	57.645	-24.337	2.58
- M0	60.094	4.186	-4.40	54.472	-12.603	4.40

maximum may be illustrated by the fact that the mean distance between individual magnetic identifications on both plates and the idealized, orthogonal, isochrons is less than 5 km for each of the four selected isochrons. Also the position of the fracture zone axis was estimated to be accurate to about 5 km in Chapter 3.

We used the method of Stock and Molnar (1983) to calculate the variation in pole position when errors in the data exist. The method consists of the addition of so-called Partial Uncertainty Rotations (PUR's) to the best-fit total separation poles. A PUR can

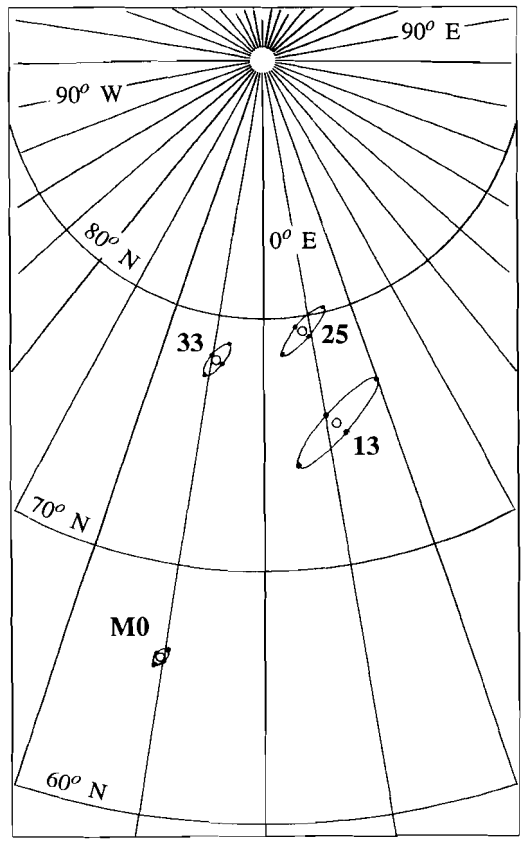

Figure 5.5 - Error ellipses of the total separation poles of the selected isochrons. The ellipses are drawn around the four poles that were obtained by addition of Partial Uncertainty Rotations, following the method of Stock and Molnar (1983).

be defined for the (practically) N-S uncertainty in fracture zone position. The pole of this PUR is chosen at 90° distance from the center point of the data and the total separation pole. The second PUR is an additional rotation around the center point of the data, and it gives an estimate for the error in the distance of the pole. The third PUR is orthogonal to the former ones. This PUR does virtually not change the position of the pole, but it provides an estimation of the accuracy of the angle of rotation.

In Figure 5.5 for each total separation pole the 4 poles that result from the addition of the different PUR's are given. The angle of rotation is accurate to about 0.1°. The error ellipse that can be drawn around the 4 poles defines the area where the total separation pole must lie, if the accuracy of the data is estimated correctly. The ellipses are very small, indicating that a small difference in the position of the total separation pole has already visible (± 10 km) consequences on the fit.

The ellipse for the total separation pole of anomaly M0 is calculated for the isochron

as a whole. It should be noted that the proposed total separation pole for the part north of the New England Seamounts lies outside the ellipse of M0 given in Figure 5.5, viz. about 1° to the south-east. Because the latitudinal extent of the area north of the proposed plate boundary is small, we will not discuss the accuracy of the poles in this part separately.

Half poles

After the calculation of the total separation poles for the selected isochrons, half poles were obtained. The determination of half poles is less well constrained than that of the total separation poles. The main reason for this is that isochrons between which the half poles represent the total motion, may have different shapes. If ridge jumps took place, the identification of the equivalent points may be wrong. To improve the accuracy, different pairs of equivalent points were used. Once that the equivalent points on the two isochrons are defined, the half poles are obtained in the straight forward way described in section 4.5. For a given total separation pole of the outer isochrons, the error in the equivalent point on the middle isochron is mainly perpendicular to the fracture zone direction because we identify the equivalent poles in such a way that the distance

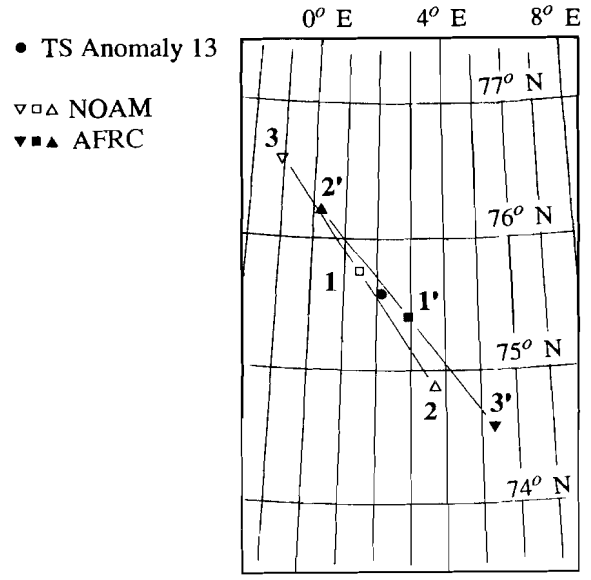

Figure 5.6 - The error in the half poles is mainly a result of a N-S error in the position of the equivalent points. As an example, the position of the two half poles 13-1 are shown with the consequences for their positions when the equivalent point on the present spreading axis is shifted 10 km to the north and south. The shift of the half pole for one plate is practically opposite to that for the other, because the summation of the two half poles has to yield the total separation pole.

between the isochrons on both plates at maximum differs a few kilometers. The variation of the half poles when an error of 10 km exists in the equivalent points can be calculated by the addition of a PUR for the fracture zone position. This error is then superimposed on the errors caused by the inaccuracy in the position of the total separation pole.

The errors of the two related half poles on the two plates are not independent, since the sum of the half poles has to fulfil the total separation pole. In Figure 5.6 this is illustrated for the total separation pole of anomaly 13 and the two half poles 13-1. The best half poles were found at the positions 1 and 1'. If an error of 10 km to either side of the fracture zone is introduced, the poles shift to position 2 and 3 and 2' and 3' respectivily. This error, which has to be considered as an absolute maximum has dramatic consequences for the position of the half poles relative to the total separation pole. For the half poles in the other age zones, which lie farther from the total separation pole since large changes in spreading direction occurred, the effect shows less.

Stage poles

In order to estimate the goodness of fit for the fracture zone directions, directions were measured and compared with the predicted values. Due to the large sample distance of the Seasat data and their large track distance it is very difficult to measure directions of the curved fracture zones accurately from these data. The reference isochrons 33, 25 and 13 formed the most suitable places for the measurement of fracture zone directions, since these isochrons fall in periods of constant spreading direction. Anomaly M0 is not used in this analysis since directions north and south of Cruiser Fracture zone cannot be combined due to the second order plate boundary, related to the New England Seamounts (see Figure 5.2). Figures 5.7a to 5.7c show fracture zone directions, compared with the model predictions. Directions on the American plate were transformed to the African plate using the total separation poles for the reference isochrons. The actual positions of the measurements, the observed directions and the predicted values from the integrated model poles of Table 5.3 and from best-fit calculations of the datasets as such, are also given in Tables 5.4-5.6 at the end of this Chapter. The RMS misfit for both the integrated model poles and the best-fit poles vary from 1.05 to 2.06. The difference between the two RMS values for each Table results from the circumstance that in the integrated model different constraints are taken into account. It is gratifying to notice that the differences are small.

The data in Table 5.4-5.6 were also used to calculate ellipses of 95% confidence for the three stage poles. This is done by contouring 2 x the RMS misfit of the best-fit pole (cf. section 4.7). The ellipses of confidence for the other stage poles are estimated in a way similar to that used by Collette *et al.* (1984). The sensitivity of the position of the stage pole to errors introduced in an artificial data set along isochrons is calculated. In this way the distribution of the data with respect to the pole can also be taken into account. The ellipse of 95% confidence for each stage pole is estimated as the mean of the ellipses found for different error distributions. The ellipses for the stage poles of anomaly 33, 25 and 13, if computed in this way, appear to be in good accordance with those obtained directly from the data. Figure 5.8 gives the stage pole positions with the ellipses of confidence for the different stage poles since magnetic anomaly 34.

No ellipses are presented for the stage poles for the Cretaceous Magnetic Quiet Zone.

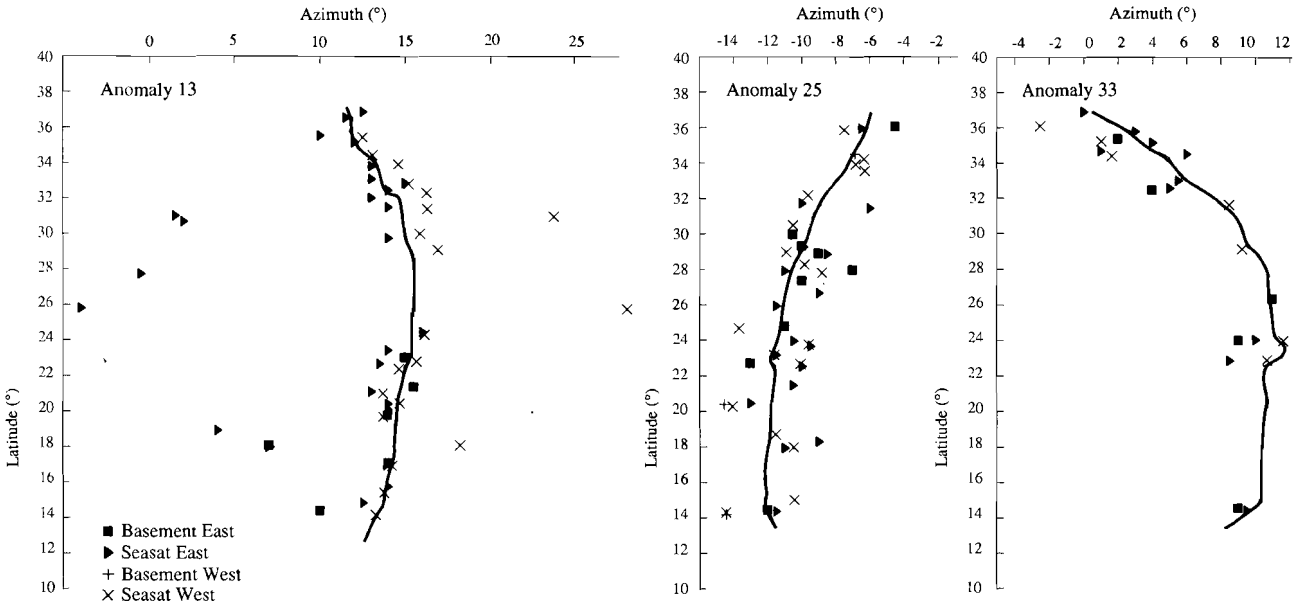

Figure 5.7 - Observed and predicted fracture zone directions at the position of different selected isochrons 13, 25 and 33. All directions are transformed to the African plate. The data are also listed in Table 5.4 to 5.6.

In principle, they are the same as those given in Slootweg and Collette (1985), which means that, due to the absence of magnetic isochrons, the incertainty is about twice as large as for the Cenozoic poles. Also, the New England Seamounts plate boundary adds to the uncertainty of the CMQZ poles.

The most important observation from Figure 5.8 then is that there is hardly any overlap between the ellipses of 95% confidence in the period between anomaly 34 and 13. This means that the number of stage poles for this period seems to be a fair minimum. On the other hand, stage poles since anomaly 13 have overlapping ellipses, only the present stage pole being practically disjunct. The change in spreading direction related to the difference in the stage pole of anomaly 5 and that of anomaly 6 is, however, clearly reflected in many fracture zones. The difference in spreading direction predicted by the poles of anomalies 6 and 13 is only minor. Analysis of the Seasat data on an oblique Mercator projection, with the total separation pole of anomaly 13 as north pole, showed that the synthetic flowlines in the period since anomaly 13 give a very accurate description of the fracture zones. Therefore, we feel that the ellipses of confidence for

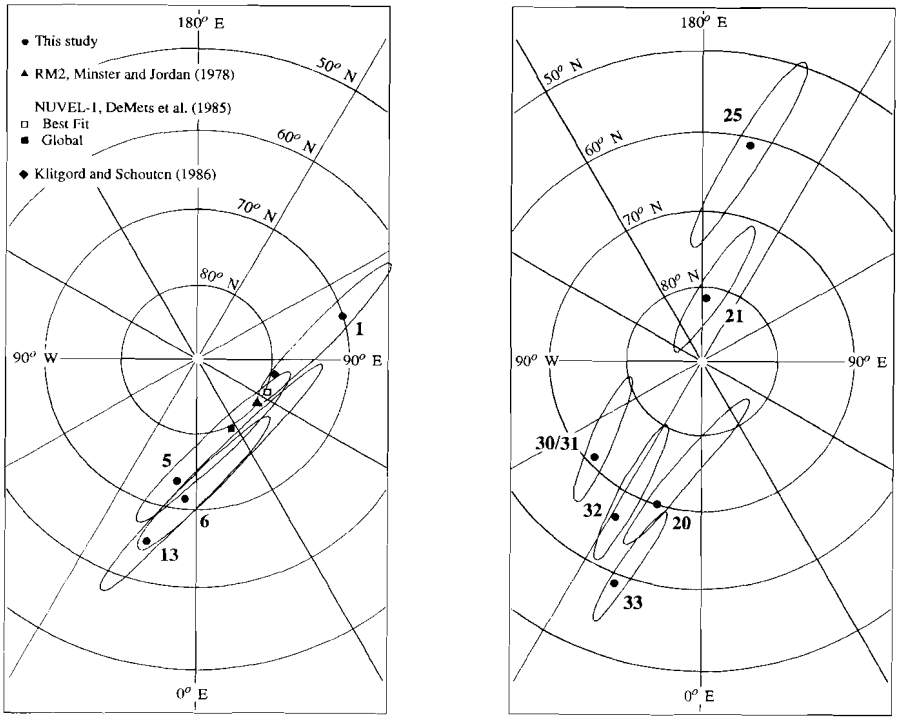

Figure 5.8 - Ellipses of 95% confidence for the different stage pole since magnetic anomaly 34. The poles are labeled with the number of a recognizable magnetic anomaly in that period. Also given are the present-day stage pole of the RM2 model (Minster and Jordan, 1978), NUVEL-1 (Demets *et al.*, 1985) and Klitgord and Schouten (1986).

stage poles 5, 6 and 13 may be significantly smaller than the maximum estimates given in Figure 5.8. Nevertheless, a good fit may possibly also be obtained when poles 6 and 13 are shifted in time.

Also displayed in Figure 5.8 are the poles for the relative motion between the North American and African plate of the global relative plate motion models RM2 and NUVEL-1 (respectively Minster & Jordon, 1978; and DeMets *et al.*, 1985), the best-fit pole of the NUVEL-1 dataset, and the most recent stage pole in the reconstruction of Klitgord and Schouten (1986). Only the pole of the global NUVEL-1 model lies outside the ellipse of confidence of the stage pole we obtained at 70°N/107°W.

Comparison of the stage poles for the African plate with those of Collette *et al.* (1984) shows that most of our stage poles lie in, or only just outside, the ellipses of confidence defined by these authors. The major discrepancy is found in the period of anomaly 34 and anomaly 33. The stage for anomaly 34 of Collette et al. (1984) is situated too closeby and is in their reconstruction compensated for by a stage pole for anomaly 33 which lies at a too far distance. Combination of these two poles to a single pole between anomalies 34 and 33 yields a pole close to our stage pole 33. A similar problem is found in the reconstruction of the Cretaceous Magnetic Quiet Zone by Slootweg and Collette (1985). The CMQZ3 pole of these authors is located too far away and is compensated for by poles situated too near. The present reconstruction of the Cretaceous Magnetic Quiet Zone shows a more gradual displacement of the stage poles.

It is also interesting to compare the stage poles from the present study with those of Klitgord and Schouten (1986). Since their stage poles are defined from magnetic anomaly to magnetic anomaly, these poles do not refer to the same periods in time as our poles. Therefore, we only compare the path of the stage poles for the African plate with time. Figure 5.9 displays the two paths of the stage poles since anomaly M0. It shows clearly that the stage pole paths of the two reconstructions have the same characteristics. However, comparison of the synthetic flowlines with the data shows that the fracture zones are better described with the stage poles derived in this study.

We conclude this chapter with a visualisation of the influence of the above described inaccuracies in the stage pole positions on the flowlines. The half poles are kept fixed in this exercise. The stage poles for anomaly 33, 25 and 13 are positioned at the four extremes of their ellipses. Intermediate poles were then calculated anew, to fit the half poles. These intermediate poles were only adjusted in the direction of the major axis of their ellipses of confidence. In this way an envelope was created that must contain all the synthetic flowlines that fit the fracture zone traces within the assigned errors. The result is shown in Figure 5.10. Due to the circumstance that the half poles are kept fixed, the envelopes narrow towards the selected isochrons. They are about 15 km wide in between. Possible errors in the half poles will broaden the envelopes.

Comparison with the actual data then learns that the width of the envelopes is of the right order to contain the identified fracture zone traces.

The goodness of the fit

The reconstruction of the spreading history in the central North Atlantic was carried out in a step-wise way. In the preceeding section, the inaccuracies associated with each step were discussed. We feel that the actual misfits between the data and the spreading

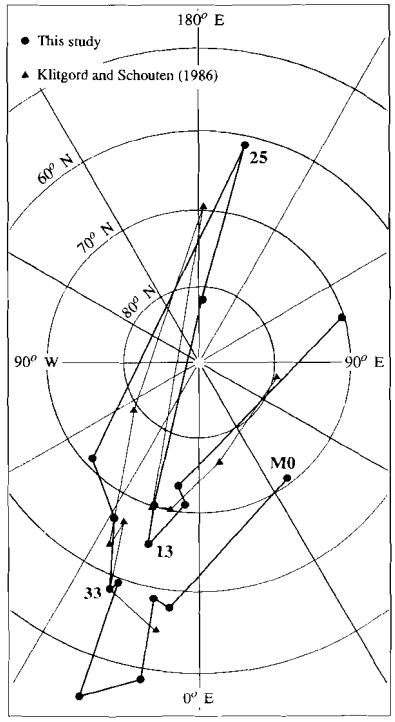

Figure 5.9 - Comparison of the path of the stage poles obtained in the present study with those of Klitgord and Schouten (1986). The position of the individual stage poles must be considered in relation with the ellipses of confidence displayed in Figure 5.8.

model can be fully explained by the inaccuracies in the identification of magnetic anomalies and fracture zone axes. The spreading process itself is also responsible for statistical variations.

No quantification was given of the overall goodness of the fit. However, we claim that the RMS error for the predicted fracture zone directions is less than 1-2°. We believe that the present data set does not allow a higher precision. When more data become available, the step-wise reconstruction followed in this study allows the incorporation of additional data in the different age zones, without consequences for the reconstruction as a whole. In this context we mention that further measurements in the Cretaceous Magnetic Quiet Zone on the American plate and on the African plate south of Kane Fracture Zone would be needed to reduce the uncertainties of the CMQZ poles and refine the analysis of the history of the New England Seamounts plate boundary.

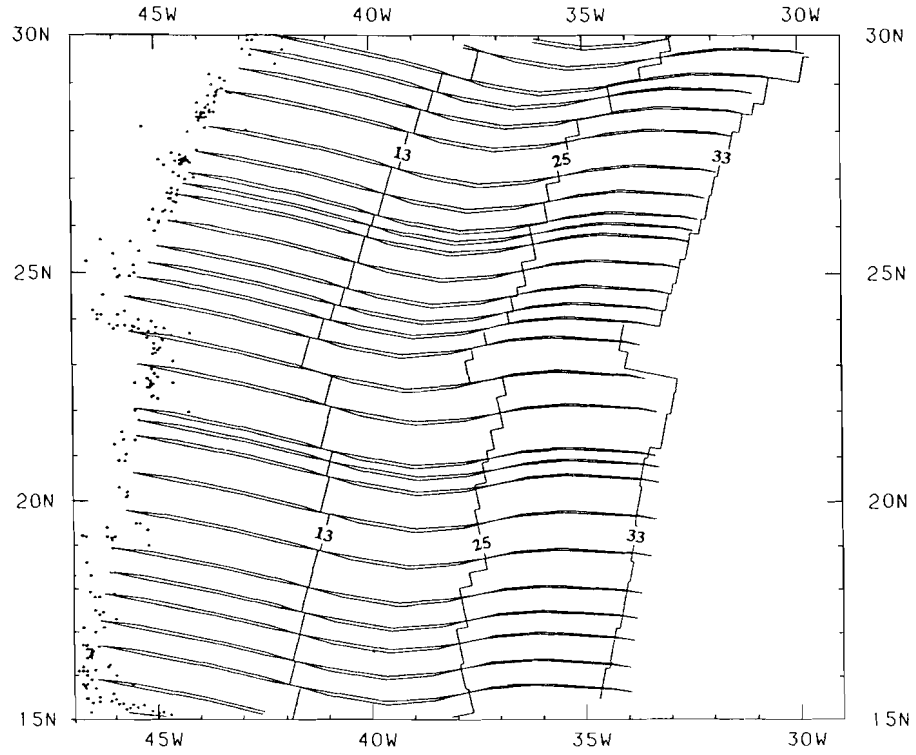

Figure 5.10 - Example of the consequence of variation of the stage poles positions inside their ellipses of confidence on the synthetic flowline pattern. The position of the stage poles for the selected isochrons is changed in order to alter the predicted directions and to create a zone that contains all possible synthetic flowlines. The flowlines are plotted to both sides of the anomaly 13 isochron. Jumps of the ridge are not taken into account in this illustration.

Table 5.4 - Observed and model fracture zone directions at anomaly 13 (37 Ma).

Latitude °N	Longitude °E	Observed	Strike (°) Integrated Model	Best-fit	Remark
					Basement Topography African Plate
23.05	-41.80	15.	15.5	15.3	
21.40	-41.15	15.5	14.8	14.6	
19.81	-41.28	14.	14.5	14.3	
18.11	-41.50	7.	14.2	14.1	v-shape
17.09	-42.26	14.	14.4	14.2	
14.42	-40.25	10.	13.0	12.9	
					Seasat directions African Plate
36.89	-28.49	12.5	11.6	12.0	
36.56	-28.84	11.5	11.8	12.1	
35.56	-29.33	10.	11.8	12.1	
35.17	-30.47	12.	12.6	12.8	
33.81	-32.12	13.	13.3	13.4	
33.08	-32.89	13.	13.5	13.6	
32.84	-34.14	15.	14.3	14.3	
32.46	-34.62	14.	14.4	14.4	
32.02	-35.02	13.	14.5	14.5	
31.49	-35.75	14.	14.8	14.7	
31.03	-35.89	1.5	14.7	14.7	v-shape
30.70	-36.30	2.	14.7	14.8	v-shape
29.75	-37.56	14.	15.3	15.1	
27.76	-39.09	-0.5	15.5	15.3	v-shape
25.83	-40.28	-4.	15.5	15.3	v-shape
24.47	-40.85	16.	15.4	15.2	
23.44	-41.24	14.	15.3	15.1	
22.70	-41.24	13.5	15.2	15.0	
21.11	-41.18	13.	14.7	14.6	
20.42	-41.15	14.	14.6	14.4	
20.11	-41.20	14.	14.5	14.4	
18.92	-41.34	4.	14.3	14.2	v-shape
18.02	-41.39	7.	14.2	14.0	v-shape
17.08	-41.82	14.	14.2	14.0	
15.74	-41.51	14.	13.8	13.7	
14.83	-41.48	12.5	13.6	13.5	
					Seasat direction American Plate
36.88	-37.26	15.	14.1	14.4	
35.94	-39.38	15.5	15.2	15.3	
35.45	-40.53	17.	15.7	15.8	
34.40	-42.18	17.5	16.3	16.3	
33.92	-43.24	18.5	16.7	16.7	
33.03	-43.83	18.5	16.7	16.7	
32.63	-44.36	26.	16.8	16.8	v-shape
31.69	-45.17	18.	16.9	16.8	
30.81	-46.47	19.	17.3	17.1	
27.58	-48.72	30.	17.2	17.1	v-shape
26.15	-49.73	18.	17.3	17.1	
24.66	-50.09	17.5	17.0	16.8	
24.23	-49.90	16.5	16.8	16.6	
22.85	-50.09	15.5	16.5	16.3	
22.29	-50.05	16.5	16.3	16.2	
21.54	-50.14	15.5	16.2	16.0	
19.92	-50.34	20.	15.9	15.7	v-shape
18.78	-50.70	16.	15.8	15.6	
17.27	-51.06	15.5	15.8	15.5	
15.97	-49.88	15	14.9	14.8	

Integrated model pole (African Plate) at 65°N, 15°W, RMS error 1.06°.
Best-fit pole (African Plate) at 66.25°N, 13.25°W, RMS error 1.05°.

Table 5.5 - Observed and model fracture zone directions at anomaly 25 (57 Ma).

Latitude °N	Longitude °E	Observed	Strike (°) Integrated Model	Best-fit	Remark
					Basement Topography African Plate
36.09	-25.40	-4.5	-6.1	-5.7	
29.97	-33.19	-10.	-9.7	-9.3	
29.35	-33.38	-10.	-9.8	-9.4	
28.92	-34.39	-9.	-10.3	-9.9	
27.99	-35.10	-7.	-10.6	-10.2	
27.40	-35.48	-10.	-10.8	-10.4	
24.82	-36.36	-11.	-11.2	-10.8	
22.75	-37.67	-13.	-11.8	-11.4	
14.48	-37.43	-12.	-12.0	-11.5	
					Seasat Direction African Plate
35.97	-25.57	-6.5	-6.2	-5.8	
31.73	-31.48	-10.	-9.0	-8.6	
31.47	-31.71	-6.	-9.1	-8.7	
29.25	-33.66	-10.	-10.	-9.6	
28.86	-34.37	-8.5	-10.3	-9.9	
27.94	-35.24	-11.	-10.7	-10.3	
26.68	-36.17	-9.	-11.1	-10.7	
25.96	-36.25	-11.	-11.1	-10.7	
24.01	-37.03	-10.	-11.5	-11.1	
23.70	-37.31	-9.5	-11.6	-11.2	
23.20	-37.62	-11.	-11.8	-11.4	
22.56	-37.66	-10.	-11.8	-11.4	
21.51	-37.15	-10.	-11.6	-11.2	
20.48	-37.29	-13.	-11.7	-11.3	
18.33	-37.69	-9.	-11.9	-11.5	
17.97	-37.78	-11.	-12.	-11.6	
14.39	-36.76	-11.	-11.7	-11.2	
					Basement Topography American Plate
36.40	-43.20	-3.5	-3.6	-3.2	
22.76	-54.37	-12.	-9.2	-8.8	
16.58	-54.70	-12.	-9.5	-9.1	
					Seasat Directions American Plate
37.68	-41.51	-4.	-2.8	-2.4	
36.12	-43.46	-3.	-3.7	-3.3	
35.83	-43.74	-3.5	-3.9	-3.5	
35.51	-44.56	-3.	-4.3	-3.9	
34.25	-47.20	-6.5	-5.6	-5.2	
32.65	-48.83	-7.5	-6.4	-6.0	
31.21	-50.51	-8.	-7.2	-6.9	
30.54	-51.32	-7.	-7.6	-7.2	
30.12	-51.82	-6.	-7.9	-7.5	
27.00	-53.31	-11.	-8.6	-8.2	
26.13	-53.94	-7.	-8.9	-8.5	
25.55	-54.04	-9.	-9.	-8.6	
25.05	-54.11	-7.5	-9.	-8.6	
22.66	-54.41	-11.5	-9.2	-8.2	
21.11	-54.64	-9.	-9.4	-9.0	
20.39	-54.88	-8.	-9.5	-9.1	
17.41	-55.09	-8.	-9.7	-9.3	
16.69	-54.32	-12.	-9.3	-8.9	

Integrated model pole (African Plate) at 60.84°N, 167.121°W, RMS error 1.57°.
Best-fit pole (African Plate) at 61°N, 166.4°W, RMS error 1.53°.

Table 5.6 - Observed and model fracture zone directions at anomaly 33 (79 Ma).

Latitude °N	Longitude °E	Observed	Strike (°) Integrated Model	Best-fit	Remark
					Basement Topography African Plate
35.40	-22.67	2.	2.2	1.2	
32.52	-25.57	4.	5.5	4.5	
26.38	-31.38	11.	10.2	9.2	
24.04	-33.72	9.	11.6	10.6	
14.58	-33.55	9.	9.4	8.6	
					Seasat Directions African Plate
36.90	-21.18	0.	0.2	-0.8	
35.82	-22.54	3.	2.1	1.1	
35.19	-23.38	4.	3.2	2.1	
34.71	-23.86	1.	3.7	2.7	
34.54	-24.43	6.	4.5	3.4	
33.04	-25.41	5.5	5.4	4.4	
32.61	-26.12	5.	6.2	5.1	
24.05	-33.16	10.	11.2	10.1	
22.90	-32.96	8.5	10.7	9.7	
14.43	-33.40	9.5	9.3	8.5	
					Seasat Directions American Plate
37.66	-46.15	4.	10.0	8.9	
36.86	-46.64	7.5	10.3	9.3	
36.16	-48.32	8.	12.1	11.0	
33.65	-51.52	14.5	14.4	13.3	
31.39	-54.27	15.	16.0	14.9	
26.51	-57.90	17.	16.9	15.9	
25.41	-57.77	16.	16.3	15.4	

Integrated model pole (African Plate) at 58.06°N, 21.05°W, RMS error 2.04°.
Best-fit pole (African Plate) at 58.75°N, 21.75°W, RMS error 1.75°.

Chapter Six

Discussion

6.1 Introductory remarks

In the preceeding chapter we presented a set of stage poles which describes the spreading history of the North Atlantic between 10° and 40°N. In the oceanic domain, these stage poles define a synthetic flowline and isochron pattern. This pattern can be used for prediction in areas where no data are available. Moreover, the rotation poles can be used for the reconstruction of the relative position of the North American (NOAM) and the African (AFRC) plate since magnetic anomaly M0 (118 Ma).

The reconstruction was started under the assumption that the lithospheric plates behave rigidly. An accurate flowline pattern makes it possible to test whether or not the NOAM and AFRC plates indeed behaved as rigid plates during the whole spreading history. When this is not the case, the existence of a, perhaps transient, second order plate boundary has to be introduced.

Conceptionally, there are two types of second order plate boundaries. The first type is associated with small deformation and fault zones, and does not necessarily have consequences on a larger, global scale. This means that the poles of motion for the two parts of a major plate with respect to a third are only slightly different, and the differential pole may be situated far away. Essentially, it forms the expression of a not entirely rigid behaviour of far away parts of the lithospheric plates. Stresses in the continents are released in a diffuse way (e.g. Rodgers and Sougy, 1984).

The other type of second order plate boundaries is of much more importance: the effects in the oceanic domain under consideration may be small, on a global scale the situation is different. In other words, the differential pole lies nearby and the type of differential movement varies rapidly off the ridge axis. As an example we point to the evolution of the plate boundary between Africa and Eurasia, which at present is a second order plate boundary from the Atlantic point of view. However, to the east the motion of the two plates results in a continuing first-order compression, forming the end phase of the disappearance of Thetys, the former ocean between Africa and Eurasia (e.g. Savostin *et al.*, 1986).

Second order plate boundaries are often characterized by abnormal topography, extensional volcanic complexes, and depth anomalies. There may be extension, shear or compression, and even a succession of different types of deformation along second order plate boundaries.

The present reconstruction shows evidence for the existence of at least three second order plate boundaries in the spreading history of the central North Atlantic. One forms the boundary between North and South America. This boundary migrated to the north, from a position south of the Four North Fracture Zone at the time of anomaly 13, to its

present position immediately north of the Fifteen Twenty Fracture Zone. The second boundary is the Azores-Gibraltar Plate Boundary, which is the present boundary between Africa and Eurasia. The Azores resulted from the differential, i.e. extensional movement in this area. The third boundary is presumably related to the origin of the New England Seamounts. It was active in the period between magnetic anomalies M0 and 33. Finally, the origin of the Atlantis-Meteor Seamount Complex and the Corner Seamounts as the possible expression of second order boundaries, will be tested in this chapter.

A different aspect of non-rigid plate behaviour is observed in the youngest part of the oceanic lithosphere. The directions of the active parts of the fracture zones, the present transform faults, show a systematic deviation from predicted values. Our reconstruction confirms the fanning of transform fault directions, reported by Roest *et al.* (1984; see also Collette *et al.*, 1984), but to a smaller extent: the effect seems limited to the transform domains, and does not affect the fossil limbs of the fracture zones.

We start our discussion with a description and evaluation of the spreading history. Before continuing with the remaining topics we will insert a synopsis of our findings on the morphology of fracture zones, as resulting from this study.

6.2 Spreading history of the North Atlantic between 10° and 40° N

The present model of central North Atlantic spreading differs fundamentally from earlier reconstructions by the fact that both fracture zones and isochrons on both plates have been used. It is especially the use of Seasat along-track gravity data, covering the whole study area, that makes the model very well constrained. We will not compare our results with all reconstructions that have been published since the early work of Heirtzler *et al.* (1968; see Le Pichon and Fox, 1971; Pitman and Talwani, 1972; Francheteau, 1973; Sclater *et al.*, 1977). These reconstructions do not yet include the significant change in spreading direction between anomalies 33 and 13, which was first recognized in the western part of the Atlantic in the trace of the Kane Fracture Zone by Rabinowitz and Purdy (1976) and became confirmed in the eastern part by Purdy *et al.* (1979), using also Kroonvlag data.

The more recent reconstructions are of Collette *et al.* (1984), who present the history since anomaly 34, based on African plate data, of Olivet *et al.* (1984), and of Klitgord & Schouten (1986). Archambault (1984) conducted a detailed study of the spreading process since anomaly 13, as a refinement of the model by Olivet (1978) and Olivet *et al.* (1984). Slootweg and Collette (1985) describe the spreading history during the Cretaceous Magnetic Quiet Zone on the African plate. In discussing our model of the spreading history, we will refer to these reconstructions.

Between magnetic **anomalies M0 and 33,** major reorganisations of the spreading axis must have taken place. The difference in the overall form of the two isochrons is large. In addition, we found evidence for differential movement on the American Plate. This differential movement, presumably related with the creation of the New England Seamounts, will be discussed in paragraph 6.6.

The magnetic anomaly M0 north of Atlantis Fracture Zone is very well covered, and

does not show many offsets (Rabinowitz *et al.*, 1979; Slootweg and Collette, 1985; Klitgord and Schouten, 1986; compare Figure 5.3). This suggests a spreading direction that is (almost) perpendicular to the overall direction of the isochron in this area. The spreading direction at the time of anomaly 33 is about 20° rotated in a counter clockwise way, which led to the creation of dextral offsets in the area to the north of Atlantis Fracture Zone. At anomaly 33, the offsets of Charis and Cruiser Fracture Zones exceed 50 km (Slootweg and Collette, 1985).

Not only a geometric adjustment to the new direction of spreading took place. Twigt *et al.* (1983) reported that between anomalies M4 and 34 the offset of Kane Fracture Zone increases from 15 to about 75 km. Moreover, it jumps to the south in response to a change in spreading direction before anomaly 34. The Northern Fracture Zone, about 75 km to the north, changes in the same period from a dextral into a sinistral transform.

In the area between the Kane and the Fifteen Twenty Fracture Zone, the overall form of the M0 isochron is not perpendicular to the direction of spreading and several offsets are found (Klitgord and Schouten, 1986; C.A. Williams, pers. comm.). However, at the time of anomaly 33 most of the offsets are reduced in response to the new, about E-W, direction of spreading. The Fifteen Twenty Fracture Zone itself, jumps to the south in a similar way as Kane Fracture Zone.

Olivet *et al.* (1984) report one large change in spreading direction at, what they call, pre-anomaly 34 (86-88 Ma). Klitgord and Schouten (1986) only have one stage pole between anomalies M0 and 34. Slootweg and Collette (1985) show that the spreading

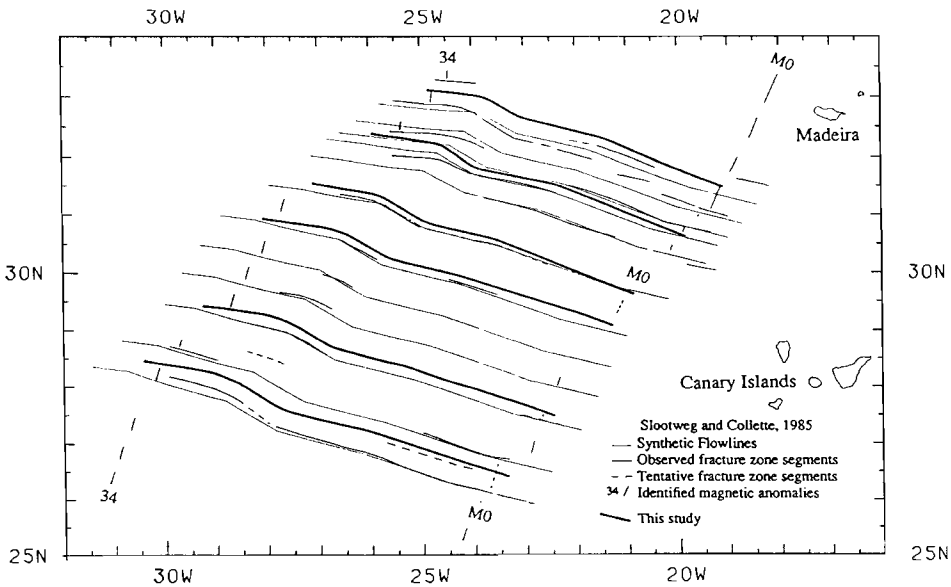

Figure 6.1 - Modified after Slootweg and Collette (1985). Comparison of observed fracture zone segments and synthetic flowlines of Slootweg and Collette (1985) and of this study. The flowlines of the present study are displaced to allow comparison with the fracture zone segments.

history between M0 and 34 is more complex. They identified a major clockwise change in spreading direction which occurred about 100 Ma B.P., and which was followed by a larger counter clockwise change just before anomaly 34. It might be hypothesized that the fracture zone data on the African Plate alone (Figure 6.1) can also be explained by jumps of fracture zones in response to only one change in spreading direction, as proposed by Olivet *et al.* (1984). This solution does not account for the fossil spreading directions revealed by the side-looking seismics data. However, when using data of two plates, it is possible to discriminate between the two models, since the signature of a jump of a fracture zone is symmetric on both plates, whereas a change in spreading direction gives an asymmetric pattern. Our reconstruction based on both the American and the African plate, confirms the findings of Slootweg and Collette (1985) and favours two large changes in spreading direction at the end of the Cretaceous Magnetic Quiet Zone. In Figure 6.1 the fracture zone segments observed by Slootweg and Collette (1985) are given, in combination with their synthetic flowlines and those resulting from the present study.

The implications of the large changes in spreading direction during the Late Cretaceous for the reconstruction of the relative movement between Eurasia, Iberia and Africa and the opening of the Bay of Biscay, need further to be investigated and will not be discussed here.

The period between magnetic **anomalies 33 and 25** is characterized by a gradual change in spreading direction, in a counter clockwise way. The related curvature of fracture zones in this age zone, since its recognition in the trace of Kane Fracture Zone, has been found in many other fracture zones in the area. It is also clearly reflected in the depth to basement map of the area west of the Mid-Atlantic Ridge, by Tucholke *et al.* (1982). Due to the inclusion of the data of the Kroonvlag Project on the African plate (Collette *et al.*, 1984), the curvature of the fracture zones is also seen in bathymetric maps (Perry *et al.*, 1981; GEBCO sheet 5.08, 1982b). The Seasat along-track gravity data provide additional information on the American plate, in areas where sediments cover the fracture zone topography.

The synthetic flowlines of Klitgord and Schouten (1986) shows only small deviations from the actual fracture zone pattern in this part of the ocean. Olivet *et al.* (1984) give one stage pole between anomaly 34 and 24. They recognize the above mentioned deviating directions of fracture zones, but relate them to intra-plate deformations. The authors use the fit of the Pico Fracture Zone and the Gloria Fault and consider the impact of different spreading directions on the reconstruction of the Pyrenees. They point to a possible relation with the Corner Seamounts and the Atlantic-Meteor Seamount Complex. We do not agree with their reasoning, as all fracture zones between the Fifteen Twenty Fracture Zone and the Azores-Gibraltar Plate Boundary show a consistent picture on both the American and the African plate. This forms clear evidence for the fact that the fracture zone directions are indeed related to real motions in the central North Atlantic. As far as the reconstruction of the North Atlantic is concerned, a refined history of the motion between North America and Eurasia including fracture zone directions is needed to derive a consistent reconstruction of the movement of Iberia and Eurasia.

Our reconstruction between anomaly 33 and 25 is mainly based on the analysis of Collette *et al.* (1984), and is in close agreement with the results of Klitgord and Schouten (1986). The curvature of the fracture zones is reflected in a change of the

position of the stage pole for the African plate over a distance of about 60°, from 58.06°N/21.05°W at anomaly 33 to 60.84°N/167.88°E at anomaly 25.

Additional reorganisations of the spreading axis that took place in this period, are small compared to those in the CMQZ. The most important jumps are found in the area south of the Kane Fracture Zone, where the total offset increased in response to the change in spreading direction. Intermediate isochrons suggest that the greater part of this reorganisation occurred before anomaly 30/31, but not enough data exist to prove this point.

An important observation concerns the distance between Kane and Atlantis Fracture Zones. This distance seems to be larger at anomaly 25 than it was near anomaly 33. In other words, between anomaly 33 and 25 Kane Fracture zone jumped to the south, whereas Atlantis Fracture Zone jumped to the north. The simple model of geometric adjustment of the spreading axis to a change in spreading direction, does not account for this difference. It may be due to difficulties of large offset fracture zone to adapt to a new direction of plate motion.

The two volcanic complexes in the age-zone, the Atlantis-Meteor Seamount Complex and the Corner Seamounts, will be discussed in section 6.7.

After the counter clockwise change described above, the period between **anomalies 25 and 13** is characterized by a clockwise change in spreading direction, which is clearly seen in the fracture zone pattern. One of the most outstanding fracture zones in this age zone is Atlantis Fracture Zone. With regard to the American plate this observation is new. The high wall to the north, which is the older side, is not yet seen on the GEBCO sheet 5.08 (1982b), but it shows in the Digital Bathymetric Data Base (DBDB5, 1984). The huge feature, with the accompanying marginal valley to the north, is identified on the seismic reflection profiles obtained during the Nedlloyd Project, and on the Seasat along-track gravity data. The eastern limb shows same features. The eastern limb of Kane Fracture Zone regains in this period a typical fracture zone cross-section, which was lost during the counter clockwise (opening) change in spreading direction before.

Olivet *et al.* (1984) describe the period between anomalies 24 and 13 with only one stage pole. They note the deviations of fracture zone directions and explain them in terms of intra-plate deformation, as in the preceeding period. The reconstruction of Klitgord and Schouten (1986) suffers from the fact that no imtermediate isochron data are used between anomalies 21 and 13. The large change in direction in their synthetic flowlines at anomaly 21 is not confirmed by the actual fracture zone data, which point to a more gradual change in spreading direction (cf. also Collette *et al.*, 1984).

In this study, three changes in spreading direction are introduced, together giving a good description of the flowlines. The stage pole for the African plate moves in a direction opposite to that in the preceeding period, and it is located at 65°N/15°W for the period comprising anomaly 13.

Only minor reorganisations of the spreading axis occurred in the period between anomaly 25 and 13.

The most recent period of the central North Atlantic spreading history is defined by **anomaly 13 east and west.** Although only small changes in spreading directions are observed in this period, the fit of both fracture zone directions and isochrons is difficult.

None of the published reconstructions gives a satisfactory description of the post-eocene spreading pattern. Collette *et al.* (1984) do not give a small circle solution for

this period. Olivet *et al.* (1984) determined one stage pole from the traces of the large offset fracture zones between anomaly 13 east and west. Deviations of fracture zones north and south of Atlantis Fracture Zone are ascribed to intra-plate deformation of the African Plate. Archambault (1984) used the total separation pole for anomaly 13 of Olivet (1978), which is equal to that of Olivet *et al.* (1984), as a boundary condition for a more detailed spreading history. However, the stage poles do not fit the identified fracture zones. One of the reasons is that the total separation pole of anomaly 13 does not make align the fracture zone traces of the two plates. Finally, the reconstruction of Klitgord and Schouten (1986) defines good fits for the total separation of anomalies 13, 6 and 5, but does not account for the fracture zone directions.

The important key to the reconstruction of the most recent spreading history of the study area was the recognition of the position of the present North America/South America plate boundary, just north of the Fifteen Twenty Fracture Zone (Roest and Collette, 1986). The discrepancy between the trace of the Fifteen Twenty Fracture Zone, and of fracture zones farther north is related to differential movement between the two American plates (see section 6.4).

Using fracture zone traces and magnetic anomalies between Luymes North and South Fracture Zones, near 18°N, and the Azores- Gibraltar Plate Boundary, we constructed four stage poles between anomaly 13 and the Mid-Atlantic Ridge. In this period, the stage pole gradually shifts to a more distant position and at present is situated at 70°N/107°E.

We remark that there remain systematic deviations of the transform fault directions with respect to the reconstruction, be it not so large as those observed by Roest *et al.* (1984). For a discussion of these discrepancies we refer to section 6.8.

6.3 Fracture zones

Before discussing the second order plate boundaries in the area, we summarize our findings concerning the morphology of fracture zones. The present study started with the identification of fracture zones with the model of Collette (1986) as the basic cross-section, typically consisting of a valley with a wall to the older side of the fracture zone axis. We pointed to the occurrence of a marginal valley that is sometimes present beyond the high fracture zone wall (e.g. Van Andel *et al.*, 1971), and may lead to a misidentification of the fracture zone axis. The accurate definition of fracture zones from the Seasat along-track gravity data became possible through a comparison with the large amount of seismic reflection data available on the African plate. The basic model of fracture zone morphology, and the recognition of the fact that a-typical cross-sections occur in response to changes in spreading direction, allowed an accurate interpolation of the fracture zone traces between shiptracks on the American plate using Seasat data, as well as an extrapolation of the fracture zone pattern in areas where no shipborne data are available.

Although a variety of fracture zone cross-sections is observed, no clear answer has yet been formulated concerning the question what type of fracture zone topography results from which type of changes in plate motion. There are two types of changes in spreading direction, which we will call 'opening' and 'closing'. The sense of a change in spreading direction is 'opening', when it leads to a leaky transform, as is the case for a

sinistral offset and a counter clockwise change in spreading direction. The spreading elements then become longer. The change of direction is spreading segments have to become shorter. We will try to arrange the different observations:

The **typical** fracture zone morphology, a **valley with a high wall to the older side,** is observed at both smaller (<20 km) and larger offset fracture zone. This cross-section seems to prevail in periods with a rather constant direction of plate motion. The length of the period needed may be related to the length of the transform, since the time it takes for a transform to adapt to a new direction of spreading is longer for large offsets. Textbook examples are found at the Fifteen Twenty Fracture Zone near anomaly 34 on the African plate, and since anomaly 5. Vidal and Snellius Fracture Zone show this expression in an exemplary way near anomaly 21. Collette (1986) used Luymes South Fracture Zone, near 18°30'N, to illustrate the change in cross-section which occurs when the Mid-Atlantic Ridge is passed.

An **extremely high fracture zone wall with a marginal valley** beyond it, is only observed at the large-offset fracture zones (> 100 km). It seems to follow an opening change in spreading direction at Kane FZ near anomaly 33 and at Atlantis FZ in the period between magnetic anomalies 25 and 20. The South Wall of the present transform domain of the Vema Fracture Zone may also be related to the creation of a leaky transform in response to a change in spreading direction. However, for the wall south of the western fossil limb of Vema Fracture Zone, between 46.5° and 51°W, such a relation is not obvious. From these observations it follows that not only the offset is an important factor controling the origin of a marginal valley. Also changes in seafloor spreading direction may play a role.

The occurrence of a **major ridge in the valley** of a fracture zone seems also a result from an opening type of change in spreading direction. Spreading segments have to grow by rift propagation, but for larger changes in spreading direction a small segment may be created temporarily in the transform domain. In the latter case, the fracture zone appears double. This cross- section is observed at Kane FZ in the Cretaceous Magnetic Quiet Zone over a lenght of about 100 km, where also the magnetic anomaly has a double signature. In the trace of the Fifteen Twenty Fracture Zone, a transverse ridge is observed on the African plate, following a counter clockwise change in spreading direction near anomaly 33. On the equivalent site at the American plate, Barracuda Ridge and Through are situated, which structure may have been deformed by the relative motion between North and South America. Atlantis Fracture Zone seems to be double before anomaly 13.

A-typical cross-sections may consist of a **broad valley,** sometimes with a **minor ridge** in it. At the Fifteen Twenty Fracture Zone, this type of topography is found between anomaly 25 and 6, where a gradual clockwise change in spreading direction is observed. For a sinistral offset this means that compression occurred in the transform domain, and extension beyond it. The fact that this configuration is much more complicated than the one that results from the opposite, opening, change in spreading direction, may account for a greater variety of fracture zone expressions. Also after an opening change in spreading direction may the fracture zone valley loose its typical character and become broad and ill-defined, e.g. Kane Fracture Zone near anomaly 25. In addition, we concluded to a small (about 10 km) southward jump of the fracture zone in this period, which may also help to explain its irregular shape.

Although there are exceptions, we conclude that typical fracture zone topography occurs when the spreading direction is constant or slightly opening. In these cases the graben-like structure of the transform can develop. Large opening may lead to a loss of typical topography and the origin of transverse ridges. (cf. also Tucholke and Schouten, 1986, who reported on morphological responses to extensional changes in spreading direction for Kane Fracture Zone). A closing type of change in spreading direction leads to irregular fracture zone topography.

We did not find evidence for adjustment fractures, as defined by Menard and Atwater (1968, 1969), with the possible exception of the latitudinal jump of Kane Fracture Zone near anomaly 34. The observations show a more gradual adaption of transform faults to a new direction of spreading. Even large offset transform faults give coherent traces. Therefore, a total of fracture zone directions in a certain period does provide accurate information on the real direction of spreading.

The V-shaped structures near 26°N at the Mid-Atlantic Ridge axis, originally described by Rona (1976) and Rona and Gray (1980) but interpreted differently by these authors, could be recognized clearly in the Seasat data over distances of about 200 km to the east and west. Rona and Gray (1980) relate the deviating directions to a reorganisation in response to changes in relative plate motion. Our reconstruction does not give rise to the proposed relation with relative plate motion, since no large recent changes of spreading direction occurred.

V-shaped traces are not only found in the most recently formed crust. The combination of fracture zone directions on both plates led to the recognition of V-shaped structures with deviating directions to both sides of the ridge. As an example, the deviating directions of several fracture zones near anomaly 13 are included in Figure 5.7 and Table 5.4.

6.4 The North America-South America Plate Boundary

No direct data exist on the present relative motion between the North and South American plate. The rate of motion is very small, and the fact that the Caribbean plate is overriding part of one plate, makes the configuration very complex (cf. Stein *et al.*, 1982). However, the second order plate boundary between North and South America can be inferred from observations of the motion of the two plates with respect to Africa.

Many authors propose the existence of a plate boundary between 10° and 20°N. Ball and Harrison (1970) placed the boundary near 20°N. Vogt and Perry (1981) suggested it to be situated at 13°45'N, whereas Le Douaran and Francheteau (1981) proposed a position near 13°N, where they observed a large axial depth anomaly. Bowin (1976) proposed that Barracuda Ridge and Through might be the place where of the plate boundary joins the Caribbean subduction Zone.

Also global models on present day plate motion include a differential motion between North and South America (Minster *et al.*, 1974; Minster and Jordan, 1978; Chase, 1978). The plate boundary is arbitrarely positioned at 15°N in these three models, but the position of the differential poles differs.

Collette *et al.* (1984) arrived to the conclusion that the plate boundary must be situated south of Vema Fracture Zone, as they observed a central North Atlantic

spreading pattern on the American plate between the Vema Fracture Zone and the Fifteen Twenty. A more detailed analysis of this area, and the transform fault directions of the two fracture zones, showed that the area south of the Fifteen Twenty Fracture Zone might have been rotated over 1° or 2°, with respect to the northern part. Therefore, Roest and Collette (1986) propose that the present plate boundary joins the Mid-Atlantic Ridge near 17°N, and that the present pole of differential movement between North and South America is located near 16°N/53.5°W, which is close to the boundary. Their reconstruction implies compression to the west of the pole, affecting Barracuda Ridge and Through. The volcano-tectonic complex of Researcher Ridge & Through and Royal Through is related to the extension that occurs east of the position of the pole of relative motion. This configuration is very similar to that of the Azores-Gibraltar Plate Boundary. Roest and Collette (1986) argued that before 7 Ma that the NOAM-SOAM plate boundary must have been situated farther south, i.e. south of Doldrums Fracture Zone.

The NUVEL-1 global relative motion data set (DeMets *et al.*, 1985) gives rise to the proposition of a plate boundary between the Fifteen Twenty Fracture Zone and the Kane Fracture Zone (S. Stein, pers. comm.). The pole of relative motion is similar to that of Roest and Collette (1986).

Recently, Bougault *et al.* (in press), analysed the composition of basalt dredged along the Mid-Atlantic Ridge between 12° and 17°N. They found indication for a 350 km long geochemical anomaly in the underlying mantle, centered around 14°N, which they relate to a developing mantle plume associated with, or responsible for the shift of the triple junction from 8°N to 14°N.

Thus, the present NOAM-SOAM plate boundary is most likely located near these latitudes. We suggest that it joins the Mid- Atlantic Ridge immediately north of the Fifteen Twenty Fracture Zone. Roest and Collette (1986) based their arguments for the northward migration of the plate boundary on a limited amount of data and commented that a more complex scenario cannot be precluded.

The Seasat along-track gravity gives the possibility to investigate this history of the plate boundary between North and South America. The study of the proposed migration of the NOAM- SOAM plate boundary started with the construction of a spreading history for the South Atlantic. We did not go back further than magnetic anomaly 34, since the fracture zone information provided by the Seasat along-track gravity data between M0 and 34 is very poor. This is partly due to the sedimentary coverage, but also to the existence of the Walvis Ridge and the Rio Grande Rise (Figure 6.2).

The most recent reconstruction of the relative motion between South America and Africa, is that of Sibuet and Mascle (1978). Their rotation poles for anomaly 13 and 34 are based on equatorial fracture zone trends, and on identifications of magnetic anomalies between 10° and 50°S, from Ladd (1976). Pindell and Dewey (1982) adopted these two poles in their reconstruction of western Pangea.

It appeared that the rotation poles of Sibuet and Mascle (1978) do not conform the fracture zone pattern, as inferred from Seasat data in the South Atlantic. We adjusted the rotation parameters by adding a small rotation to the total separation poles. This additional rotation was determined in such a way that it made the fracture zone segments on the two plates align, without materially changing the fit of the magnetic isochrons. For the most recent part of the South Atlantic spreading history, data of an aeromagnetic survey of the Mid-Atlantic Ridge south of Ascension Island are included (Brozena, 1986), and the data of a detailed survey of the Mid-Atlantic Ridge between

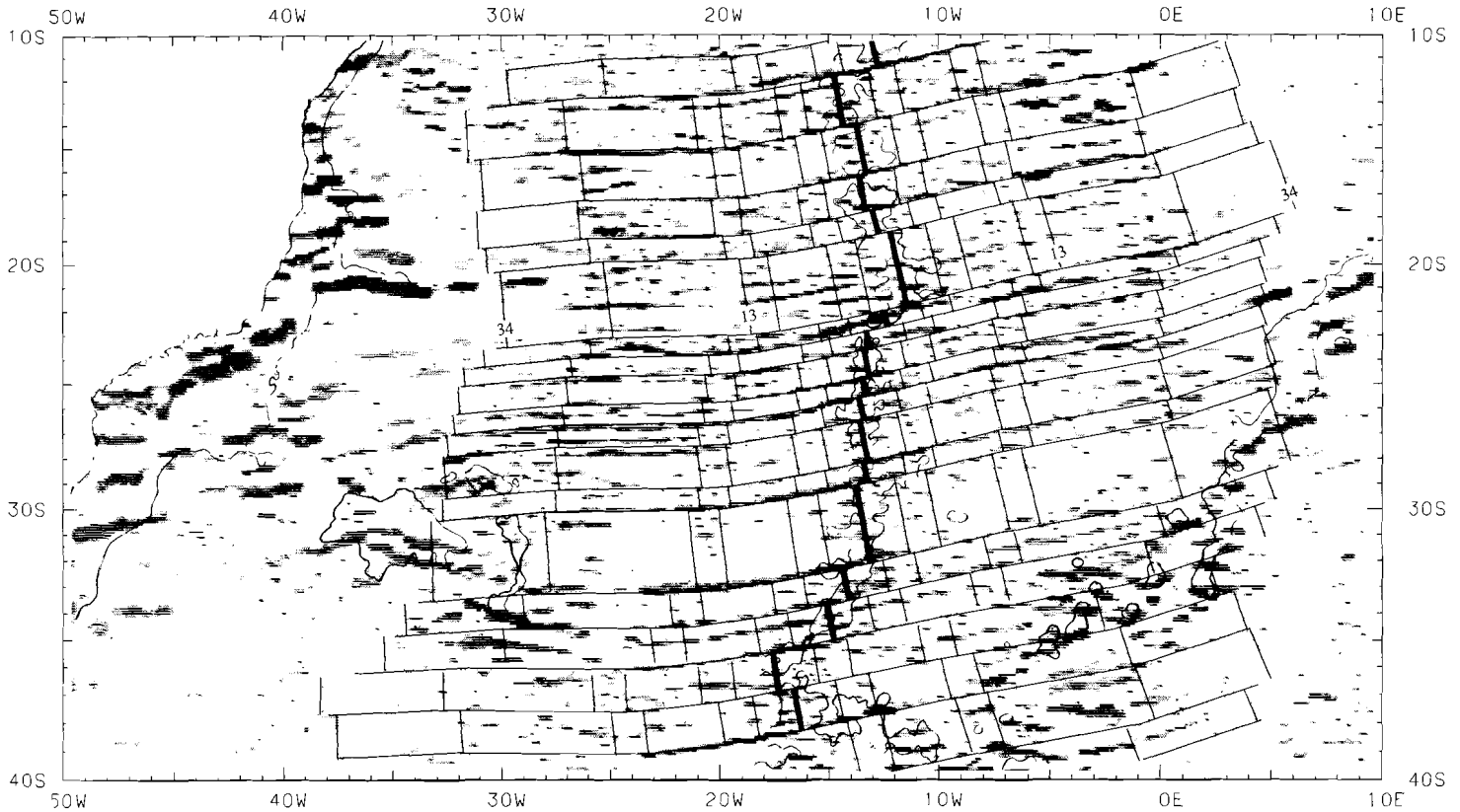

Figure 6.2 - Preliminary synthetic spreading pattern for the South Atlantic between 10° and 40 de S, overlying a shaded image of Seasat gravity. The 2500 m depth contour is shown to indicate the position of the Rio Grande Rise to the west, and the Walvis Ridge to the east of the Mid-Atlantic Ridge.

12° and 15° N (W. Twigt, pers. comm.; unpublished data,). Table 6.1 gives the, preliminary, total separation poles of anomaly 2', 13 and 34.

Table 6.1 - Total separation poles for the South Atlantic

Anomaly	Latitude (°N)	Longitude (°E)	Angle of Rotation (°)	Source
2'	62.0	-40.64	0.9	this study
13	57.66	-34.40	13.415	modified from
34	63.175	-34.67	33.816	Sibuet & Mascle(1978)

With the poles of Table 6.1 we determined the stage poles for the two plates, thereby accounting for observed fracture zone directions. Due to the absence of intermediate isochron data, the process of finding stage poles is less well constrained as in the central North Atlantic. To allow a more precise analysis of the fracture zone directions, the Seasat along-track gravity data were displayed at an oblique Mercator projection with the total separation pole of anomaly 2' as north pole. Since the South Atlantic stage poles are situated close to one another, fracture zone segments become fairly straight, and changes in spreading direction are observed more clearly. In this way, we noted a significant change in spreading direction between anomalies 34 and 13. The total separation pole of anomaly 13 was also divided in a number of stage poles, of which the most recent one has the same position as the total separation pole of anomaly 2'. The stage poles for the relative movement between South America and Africa are given in Table 6.2. Figure 6.2 displays the synthetic flowlines in the area between 10° and 40° S, merged with an image of Seasat gravity data.

Table 6.2 - African plate stage poles for the relative movement of Africa and South America.

Period	Latitude (°N)	Longitude (°E)	Angle of Rotation (°)
1 - 2'	62.0	-40.637	-0.45
2' -	62.0	-40.637	-1.12
	57.462	-36.214	-1.25
	52.896	-31.183	-2.71
- 13	63.396	-29.783	-1.2
13 -	71.484	-36.310	-5.8
- 34	60.223	-36.569	-4.5

The migration of the plate boundary is retraced by comparison of the synthetic flowlines for the North and South Atlantic with the actual fracture zones. Starting with the northern stage poles for the African plate (Table 5.3) and going south along the Mid- Atlantic Ridge axis, an increasing part of the most recent spreading history is replaced by stage poles of Table 6.2. Subsequently, the resulting stage poles for the American plate are calculated. This procedure implies that a boundary is assumed between North and South

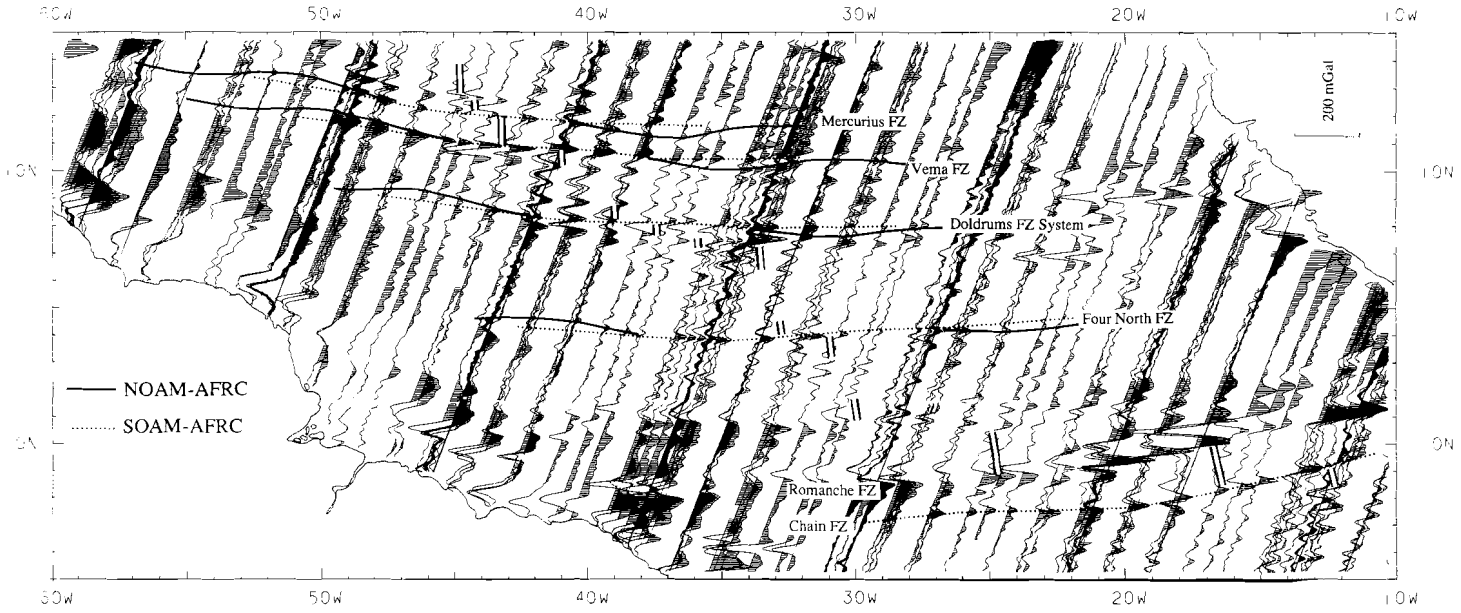

Figure 6.3 - Synthetic flowline pattern for the Equatorial Atlantic, overlying Seasat along-track gravity profiles. The migration of the plate boundary between North and South America is indicated by the transition from the northern flowline to the southern.

America, i.e. no differential movement in the African plate is taken into account.

Figure 6.3 shows the resulting flowline pattern, in relation to the observed Seasat along-track gravity. From this Figure, we conclude that the plate boundary between North and South America was situated south of the Four North Fracture Zone in the period between anomalies 34 and 13. From the present data, we cannot identify reliable fracture zone traces between Saint Paul Fracture Zone, at about 1°N, and the Four North. It seems impossible to fit the trace of Saint Paul Fracture Zone with part of the northern spreading history, although it is a tempting idea to identify the closeby Romanche Fracture Zone, which has a 950 km long transform (Parson and Searle, 1986), as the older plate boundary. Since anomaly 13, the plate boundary migrated to the north, passing the Doldrums Fracture Zone System. Vema Fracture Zone forms part of the southern spreading pattern since about 20 Ma, whereas Mercurius, Marathon and Fifteen Twenty Fracture Zones only seem to show the southern pattern 10 Ma. We remark that these ages are only estimates, as there is only a small difference in the spreading directions predicted by the northern and the southern stage pole in the period between 20 and 10 Ma B.P..

The determination of stage poles for the differential motion between North and South America from the stage poles of these two plates with respect to Africa is not very well constrained, since no intermediate isochron data are available in the South Atlantic. However, the present differential pole can be calculated accurately from the total separation poles of anomaly 2' north and south of the plate boundary. The stage pole for the relative motion between North and South America is situated at 16.5°N/51.9°W, which is close to the result of Roest and Collette (1986), and the angle of rotation is 0.64°. The position of the pole implies a N-S divergence of about 1 km/Ma at the ridge axis north of the Fifteen Twenty Fracture Zone, and a convergence of 1-2 km/Ma near Barracuda Ridge and Through. There is virtually no transcurrent motion along the present plate boundary. That no large transcurrent motion occurred in the history of the

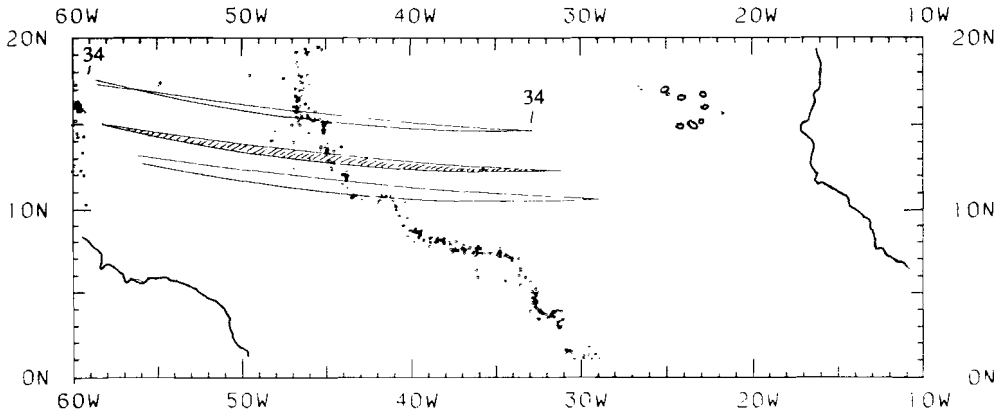

Figure 6.4 - Small circles about the total separation poles of anomaly 34 for the central North and for the South Atlantic. The shaded area gives in indication of the elongation of the spreading axis, which resulted from the differential motion between North and South America.

plate boundary since anomaly 34 can be concluded from total separation pole for the relative motion of North and South America since anomaly 34. This pole is located at about 11°N/59°W, and the total angle of rotation is 8.8°. The fact that this total separation pole is also situated close to the boundary between North and South American suggests that no large deviations from the present mechanism occurred. The configuration resulted in an actual growth of the length of the Mid-Atlantic Ridge, as illustrated schematically in Figure 6.4, where a small circle is shown around the total separation pole of anomaly 34 for the central North and for the South Atlantic. The small circles, starting from a common point at the anomaly 34 isochron on the African Plate intersect again near anomaly 34 at the American side of the ridge. The area in between the two small circles represents the actual elongation of the spreading axis.

6.5 The Azores-Gibraltar Plate Boundary

Comparison of the spreading history between North America and Eurasia, or more precisely the Iberian plate, with that between North America and Africa, must lead to the description of the differential motion along the Azores-Gibraltar plate boundary. The spreading history of the Northern Atlantic is recently described by Srivastava and Tapscott (1986), be it without having had the opportunity to use the new magnetic data presented by Verhoef *et al.* (1986). A profound analysis of these new data is needed to come to an accurate reconstruction of the motion along the boundary between the Iberian and African plates. Such an analysis falls beyond the scope of this thesis. We restrict ourselves to the following remarks.

Bonnin (1978) already noticed that the differential motion between the Iberian part of the European plate and the African plate must have been very small in the period between magnetic anomalies 34 and 13. Searle (1980) sketches the history of the development of the Azores Triple Junction, based on a differential movement since anomaly 13. A first test of the rotated set of central North Atlantic stage poles on the Iberian plate seems to indicate that the differential motion between anomaly 33 and 13 was indeed only minor, if existing at all.

A first estimation of the motion of the plates at the Azores Triple Junction may be obtained by the calculation of the total separation poles for Iberia with respect to Africa, using the present reconstruction and the results of Srivastava and Tapscott (1986). The result of this preliminary computation is given in Table 6.3.

Table 6.3 - Preliminary total separation poles for Iberia with respect to Africa (IBER-AFRC)

Anomaly	Latitude (°N)	Longitude (°E)	Angle of Rotation (°)
5	0.77	-5.69	0.70
6	20.96	-17.15	2.50
13	31.19	-19.32	8.08

There seems to be an indication for a progressive shift of the total separation pole towards the equator in the period since anomaly 13. However, one must be careful with this interpretation since the latitude of the differential pole is very sensitive for the angles of rotation of the two total separation poles from which it is calculated. For instance, a difference of 0.1° in the rotation angle of the total separation pole for anomaly 5 in the North Atlantic results in a difference of 8° in the latitude for the differential pole.

It should be noted that the IBER-AFRC pole for anomaly 5, which is given in Table 6.3, does not fit the observed direction of the Gloria Fault (Laughton *et al.*, 1972), which has been used by many authors as an indicator of the relative motion between Iberia and Africa. E.g. Minster and Jordan (1978) used the direction of the Gloria Fault in their present day plate motion model RM2, and found a pole at 25.2°N/21.2°W. Searle (1979) also calculated a pole based on the GLORIA side-scan sonar data of this fault. This pole is situated at 21.3°N/21°W and has a narrow but long ellips of 95% confidence, extending from 28°N to 45°S. The AFRC-EURA pole of the NUVEL-1 global relative plate motion model (DeMets *et al.*, 1985) is situated near 10°N/25°W. Like our pole for anomaly 5, this pole does not fit the observed direction of the Gloria Fault either.

It is clear that the stage poles for the older relative motion between Iberia and Africa are not very well constrained either. Therefore, it is not yet possible to describe the history of the Azores-Gibraltar plate boundary in detail. The preliminary results given in Table 6.3, indicate that also the stage pole of the motion between Iberia and Africa may have migrated from a position near 35°N/21°W at the time of anomaly 13 to the present position near the Equator. This present position might help to explain the E-W compressional mechanisms of earthquakes that occurred beneath southern Spain (Grimison and Chen, 1986).

6.6 Origin of the New England Seamounts

The New England (or Kelvin) Seamounts form a linear chain of volcanoes between 34°N/56°W and 40°N/68°W. The earlier explanations interpret the seamounts as the results of the occurrence of a major transform fault (Uchupi *et al.*, 1970; Le Pichon and Fox, 1971). Vogt (1973) did not observe offsets of magnetic anomalies north and south of the New England Seamounts, and concluded that no transform motion has occurred. Morgan (1971) was the first to relate the seamount chain to hot-spot activity. More recently Crough (1981) and Morgan (1983) argued that this hotspot is at present situated close to Great-Meteor Seamount, on the African plate. In all hot-spot models, the New England Seamounts are related to earlier uplift of the White Mountain Igneous Province, and to the later activity of the Corner Seamounts. This requires an eastward propagation of volcanic activity with time. Vogt and Tucholke (1979) concluded that the PSDP leg 43 data alone do not preclude synchronous volcanism, but that in relation with the White Mountain Province and the Corner Seamounts an age migration is required. Duncan (1984) found a linear rate of migration of volcanism of 4.7 ± 0.1 cm/y, from accurate ^{40}Ar-^{39}Ar ages determined from dredged and drilled volcanic rocks from 7 of the seamounts in the New England Seamount Chain.

Although we recognize the evidence for an age propagation of volcanic activity in

the area, we have several objections against the hot-spot model. In the first place, fracture zone directions on both the American and the African plate show two provinces, one north and one south of the New England Seamounts. These directions give rise to the proposition of differential motion in the area, leading to extension to the west of the Mid-Atlantic Ridge. As shown by Turcotte and Oxburgh (1973) a propagating crack (intraplate or interplate) may also lead to an age migration pattern. A second argument concerns the origin of the Atlantis-Meteor Seamount Complex on the African plate, which is in hot-spot models related to the New England hot-spot. Verhoef (1984) did not find an age migration pattern in this complex. However, his study on lithospheric flexure shows that the seamounts were not formed on the spreading axis, as is assumed in the hot-spot models. In addition, the lineations found in the individual seamounts in the Atlantis-Meteor Complex suggest a NE- SW extension of the area (see also section 6.7).

Besides the observations mentioned above, we have more general objections to the wide-spread use of hot-spot (mantle- plume) models as the only explanation for volcanic complexes. Thermal modelling shows that the fast rise of e.g. the Hawaiian-Emperor Chain can not be explained by conduction of heat alone (cf. Von Herzen *et al.*, 1982). In order to fit the observed heatflow data, the reheating of oceanic lithosphere must be confined to the lower half of it (cf. Crough, 1978). A model with an instantaneous thinning of the lithosphere with about 50% may fit the data, but there is no explanation for the occurrence of this thinning (cf. Von Herzen *et al.* 1982). We think that tectonic processes leading to fracturing of the lithosphere play an important role in the origin of "hot spot" volcanism and swells. It is possible that lithospheric fracturing is related to second order differential motions in the area. This model may also account for the spatial distribution of volcanism and oceanic swells.

The differential movement that is required for the fit of fracture zone directions north and south of the New England Seamount Chain is modelled by a differential pole that is situated far from the study area. This leads to a type of second order plate boundary that does not have great impacts for the reconstruction of other plates with respect to North America, i.e. the total separation pole for the area north of the New England Seamounts with respect to Africa is very close to that of the area to the south. The boundary is characterised by diffuse deformation. Extension occurs in the oceanic domain and, depending on the position of the pole of relative motion, compression may be involved at a greater distance. The present model links the White Mountain Igneous Province with the New England Seamount, both as extensional features. The differential movement proposed in Chapter 5, is only a first model for the origin of the New England Seamounts. If data of older lithosphere are included, it may be possible to calculate more precisely the mechanism and the amount of differential movement that took place. The origin of the Corner Seamounts is not explained by this model, as the differential movement is proposed to have occurred between anomalies M0 and 33. The possible origin of these seamounts and the Atlantis-Meteor Seamount Complex will be discussed in the following section.

6.7 A possible explanation for the Atlantis-Meteor Seamount Complex and Corner Seamounts

In several hot-spot models, the Atlantis-Meteor Seamount Complex and the Corner Seamounts are related to the hypothetical New England hotspot, which crossed under the Mid-Atlantic Ridge between 80 and 60 Ma B.P. As discussed above, Verhoef (1984) did not find any evidence for a hot-spot origin. But it appeared not possible to come to an unambiguous explanation for the origin of the Seamount Complex.

Verhoef (1984, cf. also Verhoef and Collette, 1983) observed that the complex essentially is a tensional feature. Several linear structures are found in the seamounts. These structures are more or less perpendicular to what the author interprets as transform zones which form the boundaries between the seamount groups. These boundaries seem to parallel the overall direction of the isochrons in this area, which may point to a relation with the thermal structure of the lithosphere. Verhoef and Collette (1985) conclude that the Atlantis-Meteor Seamount Complex is caused by lithospheric fracturing and following lithospheric rejuvenation.

The tension needed for the fracturing may find its origin in different processes. One of the explanations may be that extension occurred in response to a reorganization of the plate- boundary configuration. It should be noted that the Atlantis- Meteor Complex, as well as the Corner Seamounts, is situated on crust that is characterized by large changes in spreading direction. Between anomalies 33 and 25 a large counter clockwise change occurred, followed by a clockwise change between anomalies 25 and 13. Stresses thus may have been called into existence in response to plate interactions, leading to local failure of the lithospheric plates.

Another explanation for the extension that caused lithospheric fracturing, is found in thermal contraction in the horizontal plane. Part of this tension may be released in the transform domains of the large offset fracture zones (Roest *et al.*, 1984; Sandwell, 1984). This means that about 1% of the lateral extent may be left in older lithosphere, being 10-20 km. Verhoef and Collette (1985) argued that the total extension that may have occurred can also be estimated from the accuracy of the reconstruction by Collette *et al.* (1984), as this reconstruction did not reveal any inconsistancies related with the Atlantis- Meteor Seamount Complex. In this way, the possible extension is restricted to the same amount of 10-20 km.

Thirdly, the authors point to the resemblance of the zone from Atlantis-Meteor to Canary Islands with the Azores-Gibraltar Plate Boundary and with the former plate boundary in the area between King's Through and Galicia Bank. The Atlantis-Meteor Seamount Complex might, therefore, be the remnants of an ancient second order plate boundary. Slootweg and Collette (1985) recomputed the spreading history in the Cretaceous Magnetic Quiet Zone on the African plate assuming a hypothetical transcurrent fault from the Atlantis-Meteor Seamount Complex to the Canary Islands. They found no evidence for a large differential movement, but the occurrence of a small rotation may be hidden in the statistical errors of their reconstruction. Verhoef and Collette (1985) then conclude that, although lithospheric fracturing is the most likely cause of the Atlantis-Meteor Seamount Complex, no conclusive evidence exists whether the complex is the result of intra-plate or inter-plate tectonic activity.

An inter-plate mechanism must always show in the flowline pattern, whether the extension results from adaption to a new seafloor spreading direction or from the occurrence of a second order plate boundary. Our reconstruction since anomaly 33 does

not give rise to propose differential motions at the latitude of the Corner Seamounts and the Atlantis-Meteor Complex. The next question is whether a minor deformation would have been detected with available data. As stated in chapter 5, the fracture zone pattern north of Atlantis Fracture Zone is not very clear, which is partly related to the overprinting by the seamounts themselves, and to the presence of strongly reflecting volcanoclastic sediments (Verhoef, 1985). The latitudinal extent of the area north of both seamount complexes and the boundary between the central North and the North Atlantic spreading pattern is not more than 400 kilometers, which makes an independent determination of stage poles impossible. Instead, we will estimate the space that is available for an alternative reconstruction by assuming otherwise arbitrary mechanisms for the two hypothetical second order plate boundaries that may have existed in the area, one of which was related to the Corner Seamounts, and the other to the Atlantis-Meteor Seamount Complex.

There are several boundary conditions that have to be fulfilled by a reconstruction that incorporates differential motion. In the first place, the distance between Atlantis Fracture Zone and the Tydeman Fracture Zone (cf. Twigt *et al.*, 1979) at anomaly 33 is equal on both plates. Furthermore, we do not observe any deformation in crust younger than anomaly 13 (37.5 Ma). Moreover, the fit of intermediate isochrons may not be affected. A possible way to obey the boundary conditions is formed by introducing a differential motion on one plate that is practically mirrored from that on the other. The resemblance between the zone extending from Atlantis-Meteor to the Canary Islands with the Azores-Gibraltar Plate Boundary, led us to the adoption of a similar

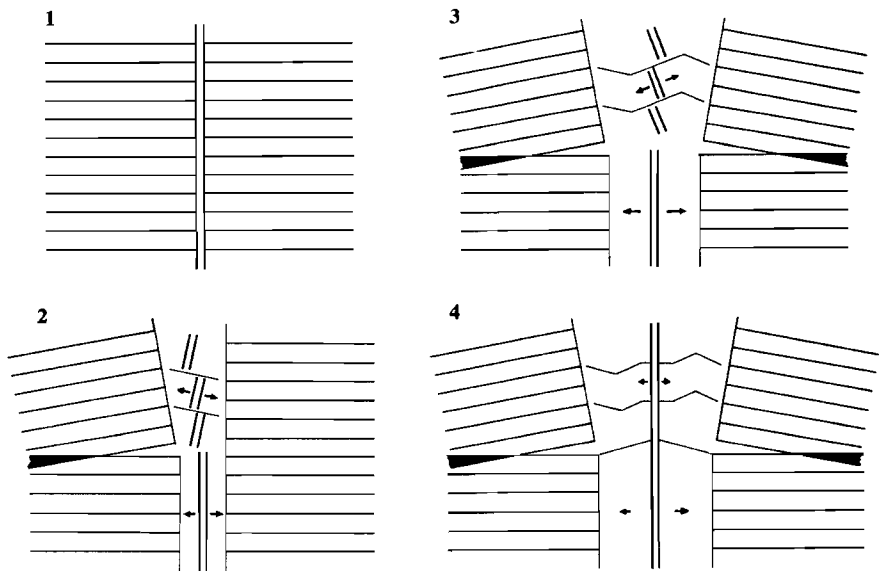

Figure 6.5 - Cartoon of a possible differential motion in the area of the Corner Seamounts and the Atlantis Meteor Seamount Complex.

mechanism of differential movement in this qualitative model, i.e. a pole of rotation that is close to the boundary and results in an elongation of the spreading axis. A cartoon of the mechanism is given in Figure 6.5, where first the Corner Seamounts are created, and later the Atlantis-Meteor plate boundary is active.

In order not to introduce a misfit of anomaly 33, the extension on both plates is parallel to the overall direction of this anomaly. The poles of differential motion are situated at 35°N/55°W for the American, and 30°N/15°W for the African plate. The angle of rotation is -0.5° and 0.5° respectively. Two scenarios were tested, one in which the American plate is firstly affected and next the African plate, the other in which this sequence was changed.

Figure 6.6 shows the synthetic flowlines for the two alternative reconstructions. We conclude that a model that incorporates differential motion at the latitude of the two seamount complexes is compatible with the data. An earlier activity of the Corner Seamounts gives a better fit than the model that first has differential motion on the African side. However, all kinds of intermediate models are possible. The extension is restricted to about 15 km only. At this point, the model is only qualitative. The difference between the rotation poles obtained with and without the additional plate boundaries may be significant for the reconstruction of the North Atlantic, and the differential motion between Africa and Eurasia. As stated above, there is evidence for the fact that the Azores-Gibraltar Plate Boundary was not active in the period between anomaly 33 and 13. Comparison of the observations in the area south of Kings Through with the central North Atlantic spreading history may provide a test of the alternative reconstruction.

For the moment being, we have shown that an alternative reconstruction is possible, but that the amount of extension that can have occurred is very small. Other explanations for the origin of the Atlantis-Meteor Seamount Complex and the Corner Seamounts cannot be precluded, as long as the deformation of the flowline pattern is only of the order of 10-20 km. This means that the occurrence of intra-plate factors like horizontal thermal contraction still may be the cause of the lithospheric fracturing and the subsequent volcanic activity.

6.8 Transform domain directions

Transform domain directions provide information on the present- day relative motion. Collette (1974) first observed a systematic deviation of these directions, as compared to the predicted values. The fanning of transform-fault directions in the central North Atlantic was confirmed by the GLORIA observations of Oceanographer, Hayes, Atlantis, Kane and Fifteen Twenty Fracture Zones (Roest *et al.*, 1984). The finding was explained in terms of horizontal thermal contraction and a fanning of the ridge push force caused by the curvature of the Mid-Atlantic Ridge. The present reconstruction shows that the transform domain of the Fifteen Twenty Fracture Zone belongs to the spreading system between South America and Africa. With the four transform fault directions that remained, it was possible to calculate a pole of motion that is in accordance with anomaly 2', and does only give small deviations of transform fault directions. Table 6.4 gives the transform fault directions of the five major offset fracture zones, based on Roest *et al.* (1984), and the values predicted from the present

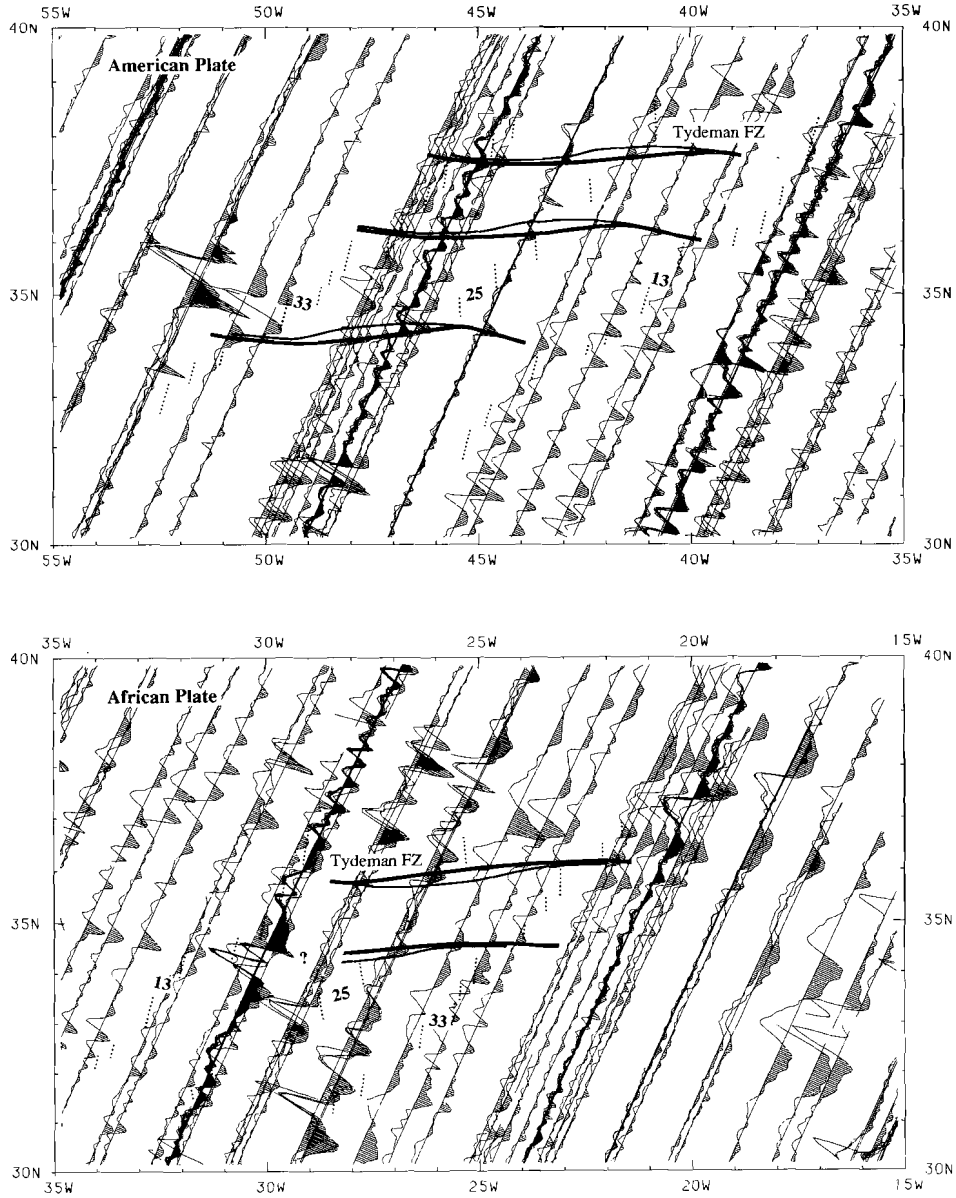

Figure 6.6 - Comparison of alternative synthetic flowlines for the area north of the Atlantis-Meteor Seamount Complex and the Corner Seamounts, when differential motion is included. The thick flowline refers to the case that differential motion first takes place on the American plate and later on the African side of the ridge; the thin flowline results when this order is changed.

reconstruction.

Table 6.4 - Present day transform fault directions, based on GLORIA sidescan sonar data (Roest*et al.*, 1984), and values predicted with the stage pole at 70°N/107°E.

Transform	Observed		Predicted	Difference with	
	Overall	Mean		Overall	Mean
Oceanographer	104.5°	107.°	103.°	1.5°	4.°
Hayes	104.5°	103.°	102.5°	2.°	0.5°
Atlantis	101.5°	100.5°	100.5°	1.°	0.°
Kane	98.5°	99.5°	99.°	-0.5°	0.5°
Fifteen Twenty	95.5°	95.5°	99.°	-4.° *	-4. ° *

*) This difference is caused by the NOAM-SOAM relative motion.

Table 6.4 shows a small, but systematic difference between observed and predicted values. There is also a significant difference in the mean trend of individual lineations, and the overall trend of the Principal Transform Displacement Zone (PTDZ). The fact that the PTDZ forms a narrow, well defined, band suggest that it gives a good indication of the actual motion. Individual lineations may show different, *en echelon*, directions oblique to the spreading direction. In contrast to the model of Roest *et al.* (1984; see also Collette *et al.*, 1984) we think that the observed fanning of transform fault directions must be a local transform domain effect, for the analysis of spreading pattern to both sides of the ridge did not show a measurable difference in distances between fracture zone traces on the two plates. This means that the fanning of transform faults has no cumulative effect on the traces of fossil fracture zones. A local deviation of the fossil limbs cannot be precluded since there remains an uncertainty of a few kilometers in the position of the fracture zone axis with respect to the deepest point of the valley. The fanning of the transform fault directions results in an additional inaccuracy. Deviations of transform fault directions of 1-2° can be explained by the 1- 2% horizontal thermal contraction of ocean floor with a lateral extent of a hundred kilometers only. The observations still point to the importance of horizontal thermal contraction in the transform domain, and even as the cause of transform faults, as proposed by Collette (1974) and Turcotte (1974). Recently Sandwell (1986) studied the relation between fracture zone distances and spreading rate, and came to the conclusion the transform faults relieve thermal stress. The horizontal thermal contraction explains the graben-like cross-section of transform faults, as observed by Collette (1986). The present interpretation agrees with that of Collette *et al.* (1984) who state that transform faults are intrinsically leaky. Therefore, small opening changes in spreading direction do not affect the typical cross-section of transform faults. A closing change in spreading direction introduces a component of compression, and leads to an a-typical expression of fracture zones.

Chapter Seven

Summary and Conclusion

The history of the relative motion between North America and Africa is recorded in the floor of the central North Atlantic Ocean. The resulting pattern of magnetic anomalies and fracture zones in the area between 10° and 40° N was analysed using shipborne measurements and Seasat altimeter data. This analysis led to the reconstruction of the spreading history since magnetic anomaly M0.

The reconstruction differs in the first place from earlier reconstructions in the fact that it makes use of both the fracture zone traces and the magnetic lineations on both the African and the American plate. Secondly, the large amount of data used allows a better precision than could be achieved before. The study means to provide an answer to the questions formulated in **Chapter 1.** One of these questions concerns the nature of the fanning of transform fault directions. The evolution of the plate boundary between North and South America forms a second aspect. Another question is related to the origin of different seamount complexes in this part of the ocean.

Chapter 2 deals with the different datasets that were used for the analysis of the spreading pattern. Seismic reflection data form the primary tool for the recognition of fracture zones. In areas where the basement structure is irregular or obscured by sediments we also used gravity data. These gravity anomalies are highly related to fracture zone topography in the wavelength band of 50-200 km. Seasat altimeter data in this wavelength band appeared to be accurate enough to make the identification of fracture zones possible. To make full profit of Seasat mean seasurface height data a high pass filter was applied, producing gravity. The Seasat along-track gravity thus obtained is in good accordance with shipborne gravity measurements, and allows an accurate tracing of fracture zones in areas where no other data are available.

The seismic reflection and gravity data are displayed along the track. The interpretation of magnetic anomalies along profiles is often difficult, due to the interference of seafloor spreading anomalies with magnetic fracture zone anomalies. In addition, magnetic anomalies are shifted with respect to their source. The construction of a gridded data set, and the subsequent display of contours allows a more objective analysis. Moreover, a reduction to the pole filter can be applied to correct for the different directions of the magnetic vectors. A shadowgram technique, suggesting artificial illumination, was used to further enhance the seafloor spreading anomalies. The magnetic dataset was extended with the magnetic anomaly identifications published by Klitgord and Schouten (1986).

The morphology of Atlantic fracture zones and the signature of the related gravity signal are discussed in **Chapter 3.** The identification of fracture zones is based on the

morphological model of Collette (1986). This model relates the typical fracture zone topography, a valley with a high wall to the older side of the fracture zone axis, to the way it is formed at the intersection of the transform fault with the median valley. This process is non-isostatic, as is confirmed by the observed gravity anomalies over fracture zones. A deficiency of mass exists under the valley, a mass excess under fracture zone walls. Within the accuracy of the measurements, we could not detect a systematic shift of the fracture zone axes relative to the position of the deepest point in the valleys or the maximum of the negative gravity anomalies. Therefore, the position of the valley and the related negative gravity anomaly was used in defining the fracture zone axes.

In **Chapter 4,** a method was developed to combine fracture zone traces and magnetic anomaly lineations in the reconstruction of the spreading history. This method starts with the definition of a small number of well recognizable magnetic anomalies and their total separation poles. We used the magnetic anomalies M0, 33, 25 and 13 east and west of the Mid-Atlantic Ridge, and the present spreading axis. A new type of poles is introduced, the half poles, describing the integrated spreading on each plate in the period between two selected isochrons. If changes of seafloor spreading direction occur, the positions of the half poles differ from the position of the total separation pole. The eight half poles thus obtained, form the basic framework for the spreading history. The individual stage poles, giving the instantaneous motion at any time, have to satisfy the half poles. In this way it is possible to use fracture zone directions for the calculation of independent stage poles, the errors of which do not propagate into the whole spreading history.

The reconstruction and a discussion of its accuracy are presented in **Chapter 5.** The reconstruction shows that the spreading history of the central North Atlantic is essentially symmetric. Small changes in spreading direction only result in a simple geometric adjustment of transform faults and spreading elements. Larger changes in spreading direction give rise to local reorganisations of parts of the spreading axis by ridge jumps and displacements of fracture zones. To account for this type of reorganisations, a new idealised isochron was defined at each of the four selected isochrons.

A minimum number of stage poles was used, that still gives an accurate description of the data. The analysis of the accuracy of the reconstruction showed that most ellipses of 95% confidence of subsequent stage poles are disjunct, indicating that indeed a minimum number of poles is used.

The important changes in the direction of spreading at the end of the Cretaceous Magnetic Quiet Zone, observed by Slootweg and Collette (1985) on the African plate, are confirmed by the data on the American plate. Also the deviating spreading direction near anomaly 25, which was first observed in the trace of Kane Fracture Zone, is clearly reflected in the synthetic flowlines.

The more accurate a reconstruction is, the more questions arise concerning the origin of deviations with respect to the first order relative motion between the major plates. As discussed in **Chapter 6,** these deviations may find their origin in the non- rigid behaviour, or even the break-up, of lithospheric plates.

Indications for non-rigid behaviour of the oceanic lithosphere are found in the youngest part of it, where transform faults show significant deviations from small-circles about the present stage pole. The reconstruction confirms the fanning of transform fault

directions reported by Roest *et al.* (1984). The deviations are smaller than reported earlier, because the present Fifteen Twenty Fracture Zone does not belong to the central North Atlantic spreading pattern but to the South Atlantic. The fanning of the other large offset transform faults with respect to the directions predicted by the present-day stage pole is limited to about 1°-2°. The effect is a local phenomenon and has no measurable consequences on the traces of fossil fracture zones. Thermal contraction in the horizontal plane causes the transform faults to be intrinsically leaky, and allows motion that does not parallel small-circles. The thermal contraction also explains the graben-like cross-section of transform faults.

A different type of non-rigid behaviour is described in terms of second-order plate boundaries. These boundaries show only minor deformations in the oceanic domain but may, depending on the position of the pole of differential motion, have large consequences on a global scale.

The present study gives rise to the proposition of differential motion along the New England Seamount Chain. This second order plate boundary was active in the period between magnetic anomalies M0 and 33. The position of the differential pole was arbitrarely chosen at 90° distance to minimize the consequences of the relative motion on a global scale. The present reconstruction relates the White Mountains Igneous Province with the New England Seamount Chain. The extension that occurred may be as large as 70 km near anomaly M0 and reduces going westwards. This explanation can account for the observed age migration of volcanic activity and offers an alternative for the generally used hot-spot models.

The present second order plate boundary between North and South America and its history since anomaly 34 was studied in more detail. It is shown that the plate boundary was situated south of the Four North Fracture Zone in the period between anomaly 34 and anomaly 13, and then started migrating to the north. The mechanism of the differential motion remained the same during this evolution, i.e. the stage pole remained close to the plate boundary, which resulted in extension near the spreading axis and compression to the west. There is no evidence for large transcurrent motion. The stage pole for the differential motion between North and South America is now situated near 16.5°N/51.9°W and has an angular velocity of about 0.2°/Ma. The present position of the plate boundary comprises the volcano- tectonic complex of Researcher Ridge & Trough and Royal Trough, which is an extensional feature. Compression may have affected Barracuda Ridge & Trough.

The Azores-Gibraltar Plate Boundary seems only to have been active since anomaly 13. Several authors suggested that before that time, back to anomaly 33, the Iberian Plate essentially acted as part of the African plate. This was confirmed by a first comparison of the magnetic data on the Iberian plate with synthetic isochrons. The present reconstruction gives rise to the proposition of a migration of the stage pole for the differential motion between Africa and Eurasia from a position near the plate boundary at anomaly 13, to a present position near the equator.

Several authors related the Corner Seamounts and the Atlantis- Meteor Seamount Complex to the New England hot-spot. This model implies creation of several of these seamounts at the ridge axis. The model is partly contradictory on the actual track of the hot- spot and remains vague on its present position. Verhoef (1984) studied the Atlantis-Meteor Seamount Complex and showed that no clear age migration pattern exists. Moreover, a 3-dimensional lithospheric flexure study proved that the seamounts are not created at the ridge axis. As an alternative to the hot-spot model, Verhoef and

Collette (1985) proposed an extensional origin, explaining the Atlantis-Meteor Complex as a result of lithospheric fracturing. The authors could not answer the question whether the tension that created the fracturing was an intra-plate or inter-plate feature. In the present study, we tested the inter-plate explanation, viz. a relation with a second order plate boundary. This analysis showed that there may have been a differential motion at the latitude of both seamount complexes, but the extension must have been restricted to about 10-20 km. If the Atlantis-Meteor Seamount Complex is, like the Azores, the result of a second order plate boundary, the Canary Islands may form part of this boundary, with shearing movements relieving compression east of the pole of rotation, as suggested earlier by Verhoef and Collette (1985).

Concludingly, we arrive to the picture of an essentially rigid behaviour of the older oceanic lithosphere. The pattern of magnetic anomalies and fossil fracture zones does not suggest intra-plate deformations, but shows evidence for differential motions between parts of the major plates. This type of motion is described in terms of second order plate boundaries. These boundaries are not a stable feature, but seem to jump or migrate in position. The distribution of seismicity in older oceanic lithosphere supports the absence of large intra-plate deformations.

The way in which the history of seafloor spreading is recorded in the oceanic lithosphere, puts a limit to the accuracy and the further detailing of the reconstruction of the first order relative movement of the African and American plate. Uncertainties are related to the variability and the skewness of magnetic anomalies. The low amplitude of seafloor spreading anomalies near the equator is another factor. The variability of fracture zone topography in relation to changes in spreading direction implies uncertainties in the position of the fracture zone axes and in the identifications of changes in spreading direction. If more data, especially continuous seismic reflection and magnetic data, become available on the American plate and off the Cape Verde Islands, minor adjustments of the synthetic flowlines may follow. However, more data cannot help to remove the fundamental uncertainty with which a stage pole can be determined. Therefore, we estimate that the ellipses of confidence of the given stage poles will not be improved significantly anymore.

On the other hand, additional data are needed for a more accurate study of the evolution of the second order plate boundaries in the area. The differential motion in the New England area can be further established with a survey of the Mesozoic magnetic anomalies on the African plate, complementary to the surveys on the American plate. Because a differential motion during the Cretaceous Magnetic Quiet Period must also have affected the older crust on the American side, a comparison of the two magnetic anomaly patterns allows a more accurate determination of the differential pole.

For the Atlantic north of the Azores, an evaluation of the accuracy of the published reconstructions is necessary, as well as a further analysis of the recently published magnetic map of the Iberian plate. The preliminary reconstruction of the spreading pattern of the South Atlantic, presented in this study, gives a more accurate description of the flowlines than earlier reconstructions, but still is not very well constrained. Additional data are necessary to refine this reconstruction and study its accuracy. Only if the spreading histories of the northern and southern parts of the Atlantic are known to the same degree of precision as in the study area, detailed differential movements between North and South America and between Africa and Europe can be predicted with confidence.

References

Anonymous - NAVADO III Bathymetric, magnetic and gravity investigations HNMS Snellius 1964-1965, *Hydrographic Newsletter, special publication number* **3,** 1967.

Archambault M.F. - Evolution cinematique post-Eocene de l'Atlantique nord et central. Implications sur le fonctionnement des Acores et l'evolution du domaine Mediterraneen Occidental, Ph.D Thesis, *University Bretagne Occidentale,* pp 211, 1984.

Atwater T., MacDonald K.C. - Are spreading centres perpendicular to their transform faults?, *Nature,* **200,** 22-29, 1977.

Ball M.M., Harrison C.G.A. - Crustal plates in the Central Atlantic, *Science,* **167,** 1128-1129, 1970.

Balmino B., Moynet B., Sarrailh M., Vales N. - Free air gravity anomalies over the oceans from Seasat and GEOS 3 altimeter data, *EOS Trans. Am. Geophys. Un.,* **68,** 17-19, 1987.

Bonnin J. - Evolution geodynamique de la ligne Acores-Gibraltar, *Ph.D. Thesis, Paris VII,* pp 144, 1978.

Bougault H., Dmitriev L., Schilling J.G., Sobolev A., Joron J.L., Needham H.D. - MAR 14°N Triple Junction: Mantle heterogeneity from trace elements, in press, 1987.

Bowin C. - Caribbean gravity field and plate tectonics, *Geol. Soc. Am. spec. paper,* **169,** pp 79, 1976.

Brozena J.M. - Temporal and spatial variability of seafloor spreadinf processes in the Northern South Atlantic, *J. Geophys. Res.,* **91,** 497-510, 1986.

Buck W.R., Parmentier E.M. - Convection beneath young oceanic lithosphere: implications for thermal structure and gravity, *J. Geophys. Res.,* **91,** 1961-1974, 1986.

Cazenave A. - Thermal cooling of oceanic lithosphere: new constraints from geoid height data, *Earth Planet. Sci. Lett.,* **70,** 395-406, 1984.

Cazenave A., Lago B., Dominh K. - Geoid anomalies over the north-east Pacific fracture zones from satellite altimeter data, *Geophys. J. R. astr. Soc.,* **69,** 15-31, 1982.

Cazenave A., Lago B., Dominh K. - Thermal parameters of the oceanic lithosphere estimated from geoid height data, *J. Geophys. Res,* **88,** 1105- 1118, 1983.

Chase C.G. - Plate kinematics: The Americas, East Africa, and the rest of the world, *Earth Planet. Sci. Lett.,* **37,** 355-368, 1978.

Chapman M.E. - Techniques for interpretation of geoid anomalies., *J. Geophys. Res.,* **84,** 3793-3801, 1979.

Cochran J.R., Talwani M. - Free-air gravity anomalies in the world's oceans and their relationship to residual elevation, *Geophys. J. R. astr. Soc.,* **50,** 495-552, 1977.

Collette B.J. - Thermal contraction joints in a spreading seafloor as origin of fracture zones, *Nature,* **251,** 299-300, 1974.

Collette B.J. - Fracture zones in the North Atlantic: morphology and a model, *J. Geophys. Soc., London,* **143,** 763-774, 1986.

Collette B.J., Slootweg A.P., Verhoef J., Roest W.R. - Geophysical investigations of the floor of the Atlantic Ocean between 10° and 38° N (Kroonvlag-project), *Proc. Kon. Ned. Akad. Wet., series B,* **87,** 1-76, 1984.

Collette B.J., Verhoef J. - Mid-ocean ridge asthenospheric topography near transform fault intersections, *Terra Cognita,* **7,** 457, 1987.

Collette B.J., Verhoef J., Mulder A.F.J. - Gravity and a model of the Median Valley, *J. Geophys.*, **47,** 91-98, 1980.

Crough S.T. - Thermal origine of mid-plate hot-spot swells, *Geophys. J. R. astr. Soc.*, **55,** 451-469, 1978.

Crough S.T. - Geoid anomalies across fracture zones and the thickness of the lithosphere, *Earth Planet. Sci. Lett.*, **44,** 224- 230, 1979.

Crough S.T. - Mesozoic hot spot epeirogeny in eastern North America, *Geology,* **9,** 2-6, 1981.

Danobeitia-Canales J.J. - Estudio geofysico submarino en el area del Archipielago Canario, Ph.D. thesis, *Universidad Complutense, Madrid,* pp 168, 1985.

DBDB5 - Navoceano Digital Bathymetric Data Base (5-minute) Unclassified, *National Geophysical Data Center,* Boulder, Colorado, 1984.

DeMets C., Gordon G., Stein S., Argus D.F., Engeln J., Lundgren P., Quible D.G., Stein C., Weinstein S.A., Wiens D.A., Woods D.F. - NUVEL-1: A new global plate motion dataset and model, *EOS Trans. Am. Geophys. Un.*, **66,** 368-369, 1985.

Detrick R.S. jr. - An analysis of geoid anomalies across the Mendocino Fracture Zone: implications for thermal models of the lithosphere, *J. Geophys. Res.*, **86,** 11751-11762, 1981.

Detrick Jr. R.S., Purdy G.M. - The crustal structure of the Kane fracture zone from seismic refraction studies, *J. Geophys. Res.*, **85,** 3759- 3777, 1980.

Dewey J.F. - Finite plate implications: some implications for the evolution of rock masses at plate margins, *Am. J. Sci.*, **275- A,** 260-284, 1975.

Diament M. - Etude de la reponse isostatique en domain oceanique et applications a trois zones de fracture de l'Atlantique, *These doct. 3e cycle, Universite de Paris-Sud,* Paris, 1981.

Diamant M., Sibuet J.-C., Hadaoui A. - Isostasy of the Northern Bay of Biscay continental margin, *Geophys. J.R. astr. Soc.*, **86,** 893-908, 1986.

Dixon T.H., Naraghi M., McNutt M.K., Smith S.M. - Bathymetric prediction from SEASAT altimeter data, *J. Geophys. Res.*, **88,** 1563-1571, 1983.

Dixon T.H., Parke M.E. - Bathymetry estimates in the southern oceans from Seasat altimetry, *Nature,* **304,** 406-411, 1983.

Duncan R.A. - Age progressive volcanism in the New England Seamounts and the opening of the central Atlantic Ocean, *J. Geophys. Res.*, **89,** 9980-9991, 1984.

Fox P.J., Pitman III W.C., Shephard F. - Crustal plates in the Central Atlantic: Evidence for at least two poles of rotation, *Science,* **165,** 487-489, 1969.

Francheteau J. - Plate tectonics model of the opening of the Atlantic Ocean south of the Azores, in: Tarling D.H. & Runcorn S.K. (Eds.), *Implications of continental drift to the earth sciences,* Academic Press, New York, 197-202, 1973.

Francis T.J.G. - Serpentinisation faults and their role in the tectonics of slow spreading ridges, *J. Geophys. Res,* **86,** 11616- 11622, 1981.

Freedman A.P., Parsons B. - Seasat-derived Gravity over the Musicians Seamounts, *J. Geophys. Res.*, **91,** 8325-8340, 1986.

GEBCO - General Bathymetric Charts of the Oceans - sheet 5.07, *Hydrographic Chart Distribution Office,* Ottawa, 1982a.

GEBCO - General Bathymetric Chart of the Oceans, Sheet 5.08, *Hydrographic Chart Distribution Office,* Ottawa, 1982b.

Gibert D., Courtillot V. - Spectral analysis of Seasat data in the South Atlantic: geophysical and geodynamical consequences, *Terra Cognita,* **7,** 297, 1987.

Goldstein H. - *Classical Mechanics,* Addison-Wesley, Cambridge, Mass., pp 399, 1950.

Grimison N.L., Chen W.-P. - The Azores-Gibraltar Plate boundary: focal mechanisms, depths of earthquakes and their tectonic implications, *J. Geophys. Res.*, **91,** 2029-2047, 1986.

Haxby W.F. - Geotectonic imagery, in: Francheteau J., The ocean crust, *Sci. Am.*, **249,** 70-71, 1983a.

Haxby W.F. - Geotectonic Imagery from SEASAT, *Lamont-Doherty Geological Observatory of Columbia University,* Yearbook 1982- 1983, 12, 1983b.

Haxby W.F., Karner G.D., LaBreque J.L., Weissel J.K. - Digital images of combined oceanic and continental data sets and their use in tectonic studies, *EOS Trans. Am. Geophys. Un.*, **64,** 995-1004, 1983.

Haxby W.F., Weissel J.K. - Evidence for small-scale mantle convection from Seasat altimeter data, *J. Geophys. Res.*, **91,** 3507-3520, 1986.

Heirtzler J.R. (Ed.) - Relief of the Surface of the Earth, *Report MGG-2, National Geophysical Data Center,* 1985.

Heirtzler J.R., Dickson G.O., Herron E.M., Pitman III W.C., Le Pichon X. - Marine magnetic anomalies, geomagnetic field reversals, and motions of the ocean floor and continents, *J. Geophys. Res.*, **73,** 2119-2136, 1968.

Heiskanen W.A., Moritz H. - *Physical Geodesy,* W.H. Freeman, San Francisco, California, pp 364, 1967.

Hellinger S.J. - The uncertainties of finite rotations in plate tectonics, *J. Geophys. Res.*, **86,** 9312-9318, 1981.

IAGA Division I Working Group - International Geomagnetic Reference Fields: DGRF 1965, DGRF 1970, DGRF 1975 an IGRF 1980, *EOS Trans. Am. Geophys. Un.*, **62,** 1169, 1981.

IAGA Division I Working Group - International Geomagnetic Reference Field revision 1985, *Geophys. J. R. astr. Soc.*, **85,** 217-220, 1986.

Irving E., Irving G.A. - Apparent polar wander paths Carboniferous through Cenozoic and the assembly of Gondwana, *Geophys. Surv.*, **5,** 141-189, 1982.

Johnson G.L., Vogt P.R. - Mid-Atlantic Ridge from 47° to 51°N, *Geol. Soc. Am. Bull.*, **84,** 3443-3462, 1973.

Klitgord K.D., Schouten H. - Plate Kinematics of the Central Atlantic, in: Tucholke B.E. and Vogt P.R. eds., The Geology of North America: the Western North Atlantic Region, *Geol. Soc. America DNAG series,* **vol. M,** 351-378, 1986.

Kuijpers A., Schuttenhelm R.T.E., Verbeek J. (eds) - Geological studies in the Eastern Atlantic, *Mededelingen Rijks Geologische Dienst,* **38-2,** 31-232, 1984.

Ladd J.W. - Relative motion of South America with respect to North America and Caribbean tectonics, *Geol. Soc. Am. Bull.*, **87,** 969-976, 1976.

Lame D.B., Born G.H. - SEASAT measurement system evaluation: achievements and limitations, *J. Geophys. Res.*, **87,** 3175-3178, 1982.

Laughton A.S., Whitmarsh R.B., Rusby J.S.M., Somers M.L., Revie J., McCartney B.S. - A continuous East-West fault on the Azores-Gibraltar Ridge, *Nature,* **237,** 217-220, 1972.

Le Douaran S., Francheteau J. - Axial depth anomalies from 10 to 50° north along the Mid-Atlantic Ridge: correlation with other mantle properties., *Earth Planet. Sci. Lett.*, **54,** 29-47, 1981.

Le Mouel J.L., Galdeano A., Le Pichon X. - Remanent magnetization vector direction and the statistical properties of magnetic anomalies, *Geophys. J. R. Astr. Soc.*, **30,** 353-371, 1972.

Le Pichon X. - Sea-floor spreading and continental drift, *J. Geophys. Res.*, **73,** 3661-3697, 1968.

Le Pichon X., Fox P.J. - Marginal offsets, fracture zones, and the early opening of the North Atlantic, *J. Geophys. Res.*, **76,** 6294- 6308, 1971.

Le Pichon X., Francheteau J., Bonnin J. - Plate Tectonics, *Developments in Geotectonics* **6,** Elsevier, Amsterdam, pp 300, 1973.

Lorell J., Parke M.E., Scott J.F. - Seasat, Geophysical Data Record (GDR) users handbook, altimeter, *JPL Intern. Rep. 622-27, revision A,* Jet Propulsion Laboratory, Pasadena, California, 1980.

Louden K.E., Forsyth D.W. - Thermal conduction across fracture zones and the gravitational edge effect, *J. Geophys. Res.*, **81,** 1883-1902, 1976.

Louden K.E., White R.S., Potts C.G., Forsyth D.W. - Structure and seismotectonics of the Vema Fracture Zone, Atlantic Ocean, *J. Geol. Soc., London,* **143,** 795-805, 1986.

Lowrie W., Alvarez W. - One hundred million years of geomagnetic polarity history, *Geology,* **9,** 392-397, 1981.

Marsh F.G., Brenner A.C., Beckley B.D., Martin T.V. - Global mean sea surface based upon the Seasat altimeter data, *J. Geophys. Res.*, **91,** 3501-3506, 1986.

Marsh J.G., Martin Th.V. - The SEASAT altimeter mean sea surface model, *J. Geophys. Res.*, **87,** 3269-3280, 1982.

McKenzie D.P. - Speculations on the consequences and causes of plate motions, *Geophys. J. R. astr. Soc.*, **18,** 1-32, 1969.

McKenzie D.P., Sclater J.G. - Evolution of the Indian Ocean since the Late Cretaceous, *Geophys. J. R. astr. Soc.*, **24,** 437-528, 1971.

Menard H.W. - *Marine geology of the Pacific,* McGraw-Hill, New York, pp 271, 1964.
Menard H.W., Atwater T. - Changes in direction of sea floor spreading, *Nature,* **219,** 463-467, 1968.

Menard H.W., Atwater T. - Origin of fracture zone topography, *Nature,* **222,** 1037-1041, 1969.

Menard H.W., Chase T.E. - Fracture zones. *The Sea, vol* **4-1,** Wiley- Interscience, New York, 412-443, 1970.

Minster J.B., Jordan T.H. - Present-day plate motion, *J. Geophys. Res.*, **83,** 5331-5354, 1978.

Minster J.B., Jordan T.H., Molnar P., Haines E. - Numerical modelling of instantaneous plate tectonics, *Geophys. J. R. astr. Soc.*, **36,** 541-576, 1974.

Moritz H. - Geodetic Reference System 1980, *Bulletin Geodesique,* **38, 54,** 395-405, 1980.

Morgan W.J. - Rises, Trenches, Great Faults, and Crustal Blocks, *J. Geophys. Res.*, **73,** 1959-1982, 1968.

Morgan W.J. - Convection plumes in the lower mantle, *Nature*, **230,** 42, 1971.

Morgan W.J. - Hotspot tracks and the early rifting of the Atlantic, *Tectonophysics*, **94,** 123-129, 1983.

Mulder Th.F.A., Collette B.J. - Gravity anomalies over inactive fracture zones in the central North-Atlantic, *Mar. Geophys. Res.*, **6,** 383-394, 1984.

Mutter J.C., Detrick R.S., North Atlantic Transect Study Group - Multichannel seismic evidence for anomalously thin crust at Blake Spur Fracture Zone, *Geology*, **12,** 534-537, 1984.

Olivet J.L. - Nouveau modele d'evolution cinematique de l'Atlantique Nord et Central, *These d'etat*, Universite Paris VII, 1978.

Olivet J.-L., Bonnin J., Beuzart P., Auzende J.-M. - Cinematique de l'Atlantique Nord et Central, *CNEXO rapports scientifiques et techniques*, **n° 54,** pp 108, 1984.

Parson L.M., Searle R.C. - Strike-slip fault in slow-slipping transform faults - evidence from GLORIA surveys of Atlanis and Romanche Fracture Zone, *J. Geol. Soc., London*, **143,** 757-761, 1986.

Parsons B., Sclater J.G. - An analysis of the variation of ocean floor bathymetry and heat flow with age, *J. Geophys. Res.*, **82,** 803-828, 1977.

Patriat Ph., Segoufin J., Goslin J., Beuzart P. - Relative positions of Africa and Antarctica in the upper Cretaceous: Evidence for non-stationary behaviour of fracture zones, *Earth Planet. Sci. Lett.*, **75,** 204-214, 1985.

Perry R.K., Fleming H.S., Vogt P.R., Cherkis N.Z., Feden R.H., Thiede J., Strand J.E., Collette B.J. - Bathymetry and plate tectonic evolution, *Geol. Soc. Am., Map and chart series*, **MC-35,** , 1981.

Peter G., Dewald O.E., Bassinger B.G. - Caribbean Atlantic Geotraverse, NOAA-IDOE 1971, Report No 2, Magnetic Data, *NOAA Technical Report ERL 288-AOML 12*, Boulder, Colorado, 1973b.

Peter G., Merrill G., Bush S. - Caribbean Atlantic Geotraverse, NOAA-IDOE 1971, Report No 1, Project Introduction, Bathymetry, *NOAA Technical Report ERL 293-AOML 13*, Boulder, Colorado, 1973a.

Phillips J.D., Fleming H.S., Feden R.H., King W.F., Perry R.K. - Aeromagnetic study of the Mid-Atlantic Ridge near Oceanographer Fracture Zone, *Geol. Soc. Am. Bull.*, **86,** 1348- 1357, 1975.

Phillips J.D., Luyendijk B.P. - Central North Atlantic Plate Motions over the last 40 million years, *Science*, **170,** 727-729, 1970.

Pindell J., Dewey J.F. - Permo-Triassic reconstruction of Western Pangea and the evolution of the Gulf of Mexico/Caribbean Region, *Tectonics*, **1,** 179-211, 1982.

Pitman III W.C., Talwani M. - Sea-floor spreading in the North Atlantic, *Geol. Soc. Am. Bull.*, **83,** 619-646, 1972.

Purdy G.M., Rabinowitz P.D., Schouten H. - The Mid-Atlantic Ridge at 23° N: Bathymetry and magnetics, *in: Melson W.G., Rabinowitz P.D., et al., Init. Repts. DSDP*, **45,** Washington (U.S. Government Printing Office), 119- 128, 1978.

Purdy G.M., Rabinowitz P.D., Velterop J.J.A. - The Kane Fracture Zone in the central Atlantic Ocean, *Earth Planet. Sci. Lett.*, **45,** 429-434, 1979.

Rabinowitz P.D., Cande S.C., Hayes D.E. - The J-anomaly in the central North Atlantic ocean, in: Tucholke B.E., Vogt P.R., et al., *Init. Repts. DSDP*, **43,** Washington (U.S. Government Printing Office), 879-885, 1979.

Rabinowitz P.D., Purdy G.M. - The Kane Fracture Zone in the Western Central Atlantic Ocean, *Earth Planet. Sci. Lett.*, **33,** 21-26, 1976.

Rapp R.H. - The determination of geoid undulations and gravity anomalies from Seasat altimeter data, *J. Geophys. Res.*, **88,** 1552-1562, 1983.

Rapp R.H. - Gravity anomalies and sea surface heights derived from a combined GEOS 3/Seasat altimeter data set, *J. Geophys. Res.*, **91,** 4867-4876, 1986.

Robb J.M., Kane M.F. - Structure of the Vema Fracture Zone from Gravity and Magnetic Intensity profiles, *J. Geophys. Res.*, **80,** 4441- 4445, 1975.

Rodgers J., Sougy J. - The West African connection - Evolution of the central Atlantic Ocean and its continental margins, *Geology*, **12,** 635-636, 1984.

Roest W.R., Collette B.J. - The Fifteen Twenty Fracture Zone and the North American - South American plate boundary, *J. Geol. Soc., London*, **143,** 833-843, 1986.

Roest W.R., Searle R.C., Collette B.J. - Fanning of fracture zones and a three-dimensional model of the Mid-Atlantic Ridge, *Nature*, **308,** 527-531, 1984.

Rohr K., Twigt W. - Mesozoic complementary crust in the North Atlantic, *Nature*, **283,** 758-761, 1980.

Rona P.A. - Asymmetric fracture zones and sea-floor spreading, *Earth Planet. Sci. Lett.*, **30,** 109-116, 1976.

Rona P.A., Gray D.F. - Structural behaviour of fracture zones symmetric and asymmetric about a spreading axis: Mid-Atlantic Ridge (Latitude 23° N to 27° N), *Geol. Soc. Am. Bull.*, **91,** 485-494, 1980.

Sandwell D.T. - Thermomechanical evolution of oceanic fracture zones, *J. Geophys. Res.*, **89,** 11401-11413, 1984.

Sandwell D.T. - Thermal stress and the spacing of transform faults, *J. Geophys. Res.*, **91,** 6405-6417, 1986.

Sandwell D.T., Schubert G. - Geoid height-age relation from SEASAT altimeter profiles across the Mendocino Fracture Zone, *J. Geophys. Res.*, **87,** 3949-3958, 1982a.

Sandwell D.T., Schubert G. - Lithospheric flexure at fracture zones, *J. Geophys. Res.*, **87,** 4657-4667, 1982b.

Savostin L.A., Sibuet J.-C., Zoneshain L.P., Le Pichon X., Roulet M.-J. - Kinematic evolution of the Tethys Belt from the Atlantic ocean to the pamirs since the Triassic, *Tectonophysics*, **123,** 1-35, 1986.

Schouten J.A. - A fundamental analysis of magnetic anomalies over oceanic ridges, *Mar. Geophys. Res.*, **1,** 111-144, 1971.

Schouten H., Dick H.J.B., Klitgord K.D. - Migration of mid-ocean ridge volcanism, *Nature*, in press.

Schouten H., Klitgord K.D. - The memory of the accreting plate boundary and the continuity of fracture zones, *Earth Planet. Sci. Lett.*, **59,** 255-266, 1982.

Schouten H., Klitgord K.D., Whitehead J.A. - Segmentation of mid-ocean ridges, *Nature*, **317,** 225-229, 1985.

Sclater J.G., Francheteau J. - The implications of terrestrial heat flow observations on current tectonic and geochemical models of the crust and upper mantle of the earth, *Geophys. J. R. astr. Soc.*, **67,** 747- 754, 1970.

Sclater J.G., Hellinger S., Tapscott C. - The paleobathymetry of the Atlantic Ocean from Jurassic to present, *J. Geol.*, **85,** 509-552, 1977.

Searle R.C. - Side-scan sonar studies of North Atlantic fracture zones, *J. Geol. Soc. Lond.*, **136,** 283-292, 1979.

Searle R.C. - Tectonic pattern of the Azores spreading centre and triple junction, *Earth Planet. Sci. Lett.*, **51,** 415- 434, 1980.

Searle R.C., Laughton A.S. - Sonar studies of the Mid-Atlantic Ridge and the Kurchatov fracture zone, *J. Geophys. Res.*, **82,** 5313-5328, 1977.

Sibuet J.-C., Le Pichon X., Goslin J. - Thickness of the lithosphere deduced from gravity edge effects across the Mendocino Fault, *Nature,* **252,** 676- 679, 1974.

Sibuet J.-C., Mascle J. - Plate kinematic implication of Atlantic equatorial fracture zone trends, *J. Geophys. Res.*, **83,** 3401-3421, 1978.

Sibuet J.-C., Veyrat-Peiney B. - Gravimetric model of the Atlantic equatorial fracture zones, *J. Geophys. Res.*, **85,** 943-954, 1980.

Sinha M.C., Louden K.E. - The Oceanographer Fracture Zone - I. Crustal structure from seismic refraction studies, *Geophys. J. R. astr. Soc.*, **75,** 712-736, 1983.

Slootweg A.P. - Computer contouring with a digital filter, *Mar. Geophys. Res.*, **3,** 401-405, 1978.

Slootweg A.P. - Basement imaging with side-looking seismics, *Mar. Geophys. Res.*, **8,** 149-174, 1986.

Slootweg A.P., Collette B.J. - Crustal structure and spreading history of the central North Atlantic in the Cretaceous Magnetic Quiet Zone (African Plate), *Proc. Kon. Ned. Ak. Wet., Series B,* **88,** 251-302, 1985.

Srivastava S.P., Tapscott C.R. - Plate kinematics of the North Atlantic, in: Tucholke B.E., Vogt P.R., eds. The Geology of North America: the Western North Atlantic region, *Geol. Soc. Amer. DNAG series,* **vol. M,** 379-404, 1986.

Stein S., Engeln J., Wiens K., Fujita K., Speed R. - Subduction seismicity and tectonics in the Lesser Antilles arc, *J. Geophys. Res.*, **87,** 8642-8664, 1982.

Stein S., Gordon R.G. - Statistical tests of additional plate boundaries from plate motion inversions, *Earth Planet. Sci. Lett.*, **69,** 401-412, 1984.

Stock J.M., Molnar P. - Some geometrical aspects of uncertainties in combined plate reconstructions, *Geology,* **11,** 697-701, 1983.

Tapley B.D., Born G.H., Parke M.E. - The SEASAT altimeter data and its accuracy assessment, *J. Geophys. Res.*, **87, C,** 3179-3188, 1982.

Tucholke B.E., Houtz R.E., Ludwig W.J. - Sediment thickness and depth to basement in western North Atlantic Ocean Basin, *AAPG Bull.*, **66,** 1384- 1395, 1982.

Tucholke B.E., Schouten H. - Structural response of North Atlantic transforms to "extensional" shifts in pole of relative plate motion, *EOS Trans. Am. Geophys. Un.*, **67,** 1282, 1986.

Turcotte D.L. - Are transform faults thermal contraction cracks?, *J. Geoph. Res.*, **79,** 2573-2577, 1974.

Turcotte D.L., Oxburgh E.R. - Mid-plate Tectonics, *Nature,* **244,** 237-239, 1973.

Twigt W. - Magnetic anomalies over fracture zones in the Central North Atlantic Ocean, Ph.D. Thesis, *Geologica Ultraiectina,* **26,** Utrecht, pp 125, 1980.

Twigt W., Slootweg A.P., Collette B.J. - Topography and magnetic analysis of an area Southeast of the Azores (36° N, 23° W), *Mar. Geoph. Res.*, **4,** 91-104, 1979.

Twigt W., Verhoef J., Rohr K., Mulder Th.F.A., Collette B.J. - Topography, magnetics and gravity over the Kane Fracture Zone in the Cretaceous Magnetic Quiet Zone (African Plate), *Proc. Kon. Ned. Ak. Wet., Series B,* **86,** 181-210, 1983.

Uchupi E., Phillips J.D., Prada K.E. - Origin and structure of the New England Seamount Chain, *Deep Sea Res.*, **17,** 483-494, 1970.

Van Andel T.H., Von Herzen R.P., Phillips J.D. - The Vema Fracture Zone and the tectonics of transverse shear zones in oceanic crustal Plates, *Mar. Geophys. Res.*, **1**, 261-283, 1971.

VandenBerg J. - Paleomagnetic data from the western Mediterranean: a review., *Geol. & Mijnbouw*, **58**, 161-174, 1979.

Verhoef J. - Geophysical study of the Atlantis-Meteor seamount complex, Ph.D. thesis, *Geologica Ultraiectina*, **38**, Utrecht, pp 153, 1984.

Verhoef J. - The Sedimentation pattern around the Atlantis-Meteor Seamount Complex: a model study, *Earth Planet. Sci. Lett.*, **73**, 117-128, 1985.

Verhoef J., Collette B.J. - A tear fault system beneath the Atlantic-Meteor Seamount Group, *Ann. Geophys.*, **1**, 199-206, 1983.

Verhoef J., Collette B.J. - A geophysical investigation of the Atlantis-Meteor Seamount Complex, *Proc. Kon. Ned. Ak. Wet., series B*, **88**, 427-479, 1985.

Verhoef J., Collette B.J., Miles P.R., Searle R.C., Sibuet J.-C., Williams C.A. - Magnetic anomalies in the northeast Atlantic Ocean, *Mar. Geophys. Res.*, **8**, 1-25, 1986.

Verhoef J., Duin E.J.Th. - A 3-dimensional analysis of magnetic anomalies over fracture zones in the Cretaceous Magnetic Quiet Zone (Madeira Abyssal Plain), *J. Geol. Soc. London*, **143**, 823-832, 1986.

Vine F.J., Matthews D.H. - Magnetic anomalies over oceanic ridges, *Nature*, **199**, 947-949, 1963.

Vogt P.R. - The Iceland phenomenon: imprints of a hot spot on the ocean crust, and implications for flow below the plates, *in: Geodynamics of Iceland and the North Atlantic area*, Kristjansson L., ed., Reidel, Dordrecht, 105-126, 1974.

Vogt P.R., Perry R.K. - North Atlantic Ocean: Bathymetry and plate tectonic evolution, *Geol. Soc. Am. Map and Chart Series*, **MC-35**, pp 21 1981.

Vogt P.R., Tucholke B.E. - The New England Seamounts: Testing origins, in: Tucholke B.E., Vogt P.R., et al., 1979, *Init. Reps. DSDP*, **v. 43**, Washington D.C. (US Government Printing Office), 847-856, 1979.

Vogt P.R., Zondek B., Fell P.W., Cherkis N.Z., Perry R.K. - Seasat altimetry, the North Atlantic Geoid, and evaluation of shipborne subsatellite profiles, *J. Geophys. Res.*, **89**, 9885-9903, 1984.

Von Herzen R.P., Detrick R.S., Crough S.T., Epp D., Fohn U. - Thermal origin of the Hawaiian swell: heat flow evidence and thermal models., *J. Geophys. Res.*, **87**, 6711- 6723, 1982.

Watts A.B., Cochran J.R., Patriat P., Doucoure M. - A bathymetry and altimetry profile across the Southwest Indian Ridge crest at 31°S latitude, *Earth Planet. Sci. Lett.*, **73**, 129-139, 1985.

Whitmarsh R.B., Calvert A.J. - Crustal structure of Atlantic fracture zones: I - Charlie-Gibbs FZ, *Geophys. J. R. astr. Soc.*, **85**, 107-138, 1986.

White R.S., Detrick R.S., Sinha M.C., Cormier M.H. - Anomalous seismic crustal structure of oceanic fracture zones, *Geophys. J. R. astr. Soc.*, **79**, 779-798, 1984.

White J.V., Sailor R.V., Lazarewicz A.R., LeSchack A.R. - Detection of seamount signatures in SEASAT altimeter data using matched filters, *J. Geophys. Res.*, **88**, 1541- 1551, 1983.

Wilson J.T. - A new class of faults and their bearing on continental drift, *Nature*, **73**, 1959-1982, 1965.

Acknowledgements

This thesis was produced in the Department of Marine Geophysics, Vening Meinesz Laboratorium, State University of Utrecht, The Netherlands.

I am very much indebted to Prof.Dr. B.J. Collette (Head of the Department) for his continuous inspiring support. His advice and criticism have been of great value throughout the study.

Many thanks are due to my former colleagues at the department of marine geophysics, Jaap Verhoef, Peter Slootweg and Juan Danobeitia. Joop Hoofd assisted with the conversion and the processing of the Seasat data and he improved the FELIX database and presentation system. Ad Stolk spent much time in making final illustrations. Henk van der Meer and Dick Verweij are thanked for their efforts during the seagoing expeditions.

The Seasat data were obtained from Dr. J.G. Marsh of the NASA Goddard Space Flight Center. Prof. Dr. R. Rummel is thanked for his intermediary.

The surveys of the Mid-Atlantic Ridge in 1975 and 1977, and that of the Fifteen Twenty Fracture Zone in 1982 were of particular importance for the recognition of the plate boundary between North and South America. They were carried out as part of the Vaarplan-project of the Netherlands Council of Oceanic Research (formerly: the Netherlands Commission for Sea Research). The board of directors of the Nedlloyd Rederijdiensten B.V. made it possible to collect data on board the MV Nedlloyd Hollandia that were essential for the present study.

The research described in this thesis was supported by the Netherlands Foundation for Earth Science Research (AWON) with financial aid from the Netherlands Organization for the Advancement of Pure Research (ZWO).

Samenvatting

De geschiedenis van het uiteengaan van de kontinenten rond de Atlantische Oceaan is vastgelegd in strukturen in de oceaanbodem. De afdeling mariene geofysika van het Vening Meinesz Laboratorium heeft zich in de afgelopen jaren toegelegd op het verzamelen en interpreteren van gegevens in het centrale gedeelte van de Noordatlantische Oceaan, o.a. met het Kroonvlag- en het Vaarplan- projekt. De nadruk lag op het bestuderen van de topografie en de magnetische signatuur van frakturezones en het voorkomen van vulkanische gebergten. Een eerste interpretatie van deze gegevens werd bemoeilijkt door een tekort aan waarnemingen ten Westen van de Midatlantische Rug. In 1984 werd daarom het Nedlloyd projekt uitgevoerd aan boord van het ms. Nedlloyd Hollandia.

De huidige studie beoogt het geven van een nauwkeurige rekonstruktie van de beweging van de kontinenten rond de Noordatlantische Oceaan tussen de 10e en de 40e breedtegraad. Daarbij worden ook de tweede-orde-effekten bestudeerd.

Hoofdstuk 2 beschrijft de gebruikte gegevens en geeft een toelichting op de verwerking tot basisdokumenten. De onderzoekingen op zee bestonden uit het meten van de diepte van de oceaan en van de struktuur van het oceanisch grondgebergte, dat dikwijls met sedimenten is bedekt, met behulp van kontinue seismische-reflektiemethoden. De topografie van de oceaanbodem wordt gekenmerkt door grote breukzones (frakturezones) die de fossiele sporen vormen van de transformbreuken die de Mid-atlantische Rug doorsnijden. Frakturezones geven informatie over de richting van de beweging van de kontinenten. De afwijkingen van de zwaartekracht over frakturezones zijn sterk gerelateerd aan de topografie in het golflengte-bereik van 50-200 km.

Meting van het aardmagneetveld geeft indirekt informatie over de ouderdom van het betreffende gedeelte van de oceaan. Aangezien de ompolingen van het aardmagneetveld zijn vastgelegd in de oceaankorst op het moment van vorming op de spreidingsrug, ontstaat een patroon van magnetische anomalieën waarmee lijnen van gelijke ouderdom (isochronen) zijn te identificeren. Frakturezones geven ook aanleiding tot magnetische anomalieën, aangezien de korst aan beide zijden van de frakturezone verschillend van ouderdom is. Het is echter niet alleen het ouderdomskontrast dat een magnetische frakturezone anomalie veroorzaakt; ook in magnetisch rustige periodes, wanneer er geen ompolingen plaatsvinden, worden frakturezones gekenmerkt door magnetische anomalieën die duiden op een verhoogde magnetisatie aan de jonge zijde van de frakturezone-as. De magnetische gegevens werden verwerkt tot kontourkaarten. Bovendien kon gebruik worden gemaakt van de identifikaties van magnetische anomalieën welke werden gepubliceerd door Klitgord en Schouten (1986).

Naast de metingen op zee werden satellietwaarnemingen van de gemiddelde hoogte van het zeeoppervlak gebruikt. Deze gegevens werden verkregen van het NASA

Goddard Space Flight Center. De Seasat satelliet bevond zich in een bijna circulaire baan rond de aarde, op een hoogte van 800 km. Van juli tot oktober 1978 werd met de radar-hoogtemeter de afstand van de satelliet tot het zeeoppervlak gemeten. Na berekening van het gemiddelde van 10 metingen (1 seconde) wordt een nauwkeurigheid van ongeveer 10 cm bereikt. De afstand tussen de meetpunten bedraagt dan 7 km. Vervolgens wordt de hoogte van het zeeoppervlak ten opzichte van de referentie ellipsoïde berekend. Het zeeoppervlak reflekteert o.m. de grote lijnen van de struktuur van het oceanisch grondgebergte. De grote nauwkeurigheid van de metingen maakt het mogelijk ook de kortere golflengten (25-500 km) te benutten voor het bestuderen van het frakturezonepatroon. Na toepassing van een filter dat de metingen omrekent naar zwaartekrachts-anomalieën kunnen frakturezones zeer nauwkeurig worden geïdentificeerd. Op deze wijze worden de nog steeds schaarse waarnemingen aan boord van schepen geverifieerd en geëxtrapoleerd.

De morfologie van de fossiele breukzones wordt besproken in hoofdstuk 3. De typische topografie van Atlantische frakturezones ontstaat in het transformdomein op de Midatlantische Rug. In de diepe midden vallei (median valley) wordt de aldaar nieuw gevormde korst als het ware gelast aan de oudere, hoger liggende korst aan de overzijde van de transform. Zo ontstaat als een typische frakturezone- doorsnede een asymmetrische vallei met een hoge wal aan de oude zijde van de fossiele breuk. Dit reliëf is het spiegelbeeld van het reliëf dat men op grond van de ouderdom/diepte relatie zou verwachten. De topografie van frakturezones is niet op normale wijze isostatisch gekompenseerd. Zwaartekrachts-anomalieën gemeten over frakturezones tonen aan dat er een massatekort is onder het frakturezonedal en een overschot onder de hoge wal.

In hoofdstuk 4 wordt de methode van de rekonstruktie beschreven. Een onderscheid wordt gemaakt tussen separatiepolen, die worden gebruikt voor de rekonstruktie van vroegere plaat konfiguraties, en polen die de werkelijke beweging op ieder moment aangeven. Een derde type pool, de halfpool, wordt geïntroduceerd om het mogelijk te maken de rekonstruktie in gedeelten, voor verschillende tijdzones, uit te voeren. Halfpolen beschrijven de over een tijdzone geïntegreerde beweging van één plaat. De methode wordt verder uitgewerkt om breukrichtingen en magnetische isochronen te kunnen kombineren. Door een stapsgewijze benadering wordt het probleem beter gedefinieerd.

Het totale databestand vormt het meest komplete dat tot nu toe voor dit doel werd gebruikt en maakt het mogelijk een gedetailleerde rekonstruktie te maken van de geschiedenis van de opening van de centrale Noordatlantische Oceaan in de afgelopen 120 miljoen jaar. De rekonstruktie wordt beschreven in hoofdstuk 5. Het spreidingspatroon van dit gedeelte van de oceaan is erg symmetrisch en laat een aantal belangrijke veranderingen in de richting van de relatieve beweging tussen Noordamerika en Afrika zien. Kleinere richtingsveranderingen resulteerden in een geometrische aanpassing van transformbreuken en spreidingselementen aan de nieuwe richting. Bij grote veranderingen, zoals die aan het einde van de magnetisch rustige periode van het Krijt, traden aanpassingen op in de vorm van sprongen van de rug en verplaatsing van frakturezones. Deze reorganisaties van de spreidingsrug werden in het

model verwerkt door op vier plaatsen in het verleden een rugvorm te definiëren. De oorzaak van richtingsveranderingen in de beweging van de kontinenten moet buiten het studiegebied worden gezocht.

In de diskussie (hoofdstuk 6) worden de uitkomsten van de rekonstruktie besproken. Hierbij wordt de nadruk gelegd op tweede-orde afwijkingen van de eerste-orde relatieve beweging van de Noordamerikaanse en de Afrikaanse plaat. Deze afwijkingen kunnen het gevolg zijn van het zich niet star gedragen of het breken van lithosfeerplaten.

Een eerste type tweede-orde afwijking wordt gevonden in de waaiering van transformbreukrichtingen. Deze waaiering is kleiner dan eerder werd verondersteld en bedraagt 1-2°. Het is een lokaal effekt, dat geen meetbare gevolgen heeft in de sporen van fossiele frakturezones. De verklaring voor dit fenomeen moet worden gezocht in thermische krimp in het horizontale vlak. Deze thermische krimp is ook verantwoordelijk voor het feit dat de transformbreuken zich als slenk strukturen manifesteren.

Het andere type tweede-orde afwijkingen wordt beschreven in termen van tweede-orde plaatgrenzen. Deze grenzen gaan gepaard met relatief kleine deformaties in de oceanische korst. Afhankelijk van de positie van de differentiële pool kunnen er evenwel grote konsequenties zijn op globale schaal. De analyse van het databestand gaf aanleiding tot de veronderstelling van een fossiele plaatgrens ter hoogte van de New England Seamounts. Voorts was het mogelijk de geschiedenis van de plaatgrens tussen Noord- en Zuidamerika en die tussen Afrika en de Iberische Plaat nader te bestuderen.

De ontdekking van het feit dat de tweede-orde plaatgrens tussen Noord- en Zuidamerika zich sinds ongeveer 10 miljoen jaar nabij de frakturezone op 15° 20' N (Fifteen Twenty Frakturezone) bevindt, leidde tot de konklusie dat deze plaatgrens zich vóór die tijd zuidelijker moet hebben bevonden. Uit de analyse van de Seasat gegevens in de equatoriale Atlantische Oceaan blijkt dat de plaatgrens 40 miljoen jaar geleden nabij de evenaar lag en zich vervolgens verplaatst heeft naar de huidige positie vlak ten noorden van de Fifteen Twenty Frakturezone. De pool die hoort bij de relatieve beweging tussen Noord- en Zuidamerika bevindt zich nabij de plaatgrens. Het gevolg van de differentiële beweging tussen beide platen is dat er rek op treedt in de jonge oceanische korst nabij de spreidingsas en kompressie in de oudere korst.

De plaatgrens tussen Noord- en Zuidamerika vertoont sterke gelijkenis met de Azoren-Gibraltar plaatgrens die gepaard gaat met rek nabij de Azoren en kompressie in de Middellandse Zee. Deze grens tussen Afrika en Eurazië is in zijn huidige vorm pas ongeveer 40 miljoen jaar aktief. Een eerste vergelijking van het hier gepresenteerde spreidingsmodel met waarnemingen op de Iberische Plaat bevestigt dat deze plaat in de periode van 80 tot 40 miljoen jaar geleden in essentie tot de Afrikaanse plaat behoorde.

Een analyse van frakturezone richtingen ten noorden en zuiden van de onderzeese vulkanische gebergteketen van de New England Seamounts laat zien dat deze keten is ontstaan als gevolg van differentiële bewegingen in de Noordamerikaanse plaat. Aldus ontstond een tweede-orde plaatgrens. Deze plaatgrens, die gepaard ging met rek in de oceanische korst, was aktief tussen 120 en 80 miljoen jaar geleden.

Voorts wordt een scenario getest volgens hetwelk het Atlantis-Meteor Seamount Complex en de Corner Seamounts eveneens het gevolg zouden zijn van een tweede-

orde plaatgrens. Daarbij blijkt dat een differentiële beweging van 10-20 km niet kan worden uitgesloten. Het is met de huidige gegevens echter niet mogelijk een definitieve uitspraak te doen over de oorzaak van de rekbreuken die ten grondslag liggen aan het Atlantis-Meteor Seamount Complex.

Curriculum Vitae

De schrijver van dit proefschrift behaalde in 1976 het diploma atheneum-B aan het Dr. Knippenberg College te Helmond. In dat zelfde jaar werd begonnen met de studie natuurkunde aan de Rijksuniversiteit te Utrecht. In 1979 behaalde hij het kandidaatsexamen N2. Het doktoraal examen experimentele natuurkunde met bijvakken wiskunde en natuurkunde, sterrenkunde & samenleving werd in 1982 afgelegd. In 1984 werd een aanvullend doktoraal examen met groot bijvak fysika van de vaste aarde gedaan.

Vanaf januari 1983 is de auteur werkzaam bij de afdeling mariene geofysika van het Vening Meinesz Laboratorium van de Rijksuniversiteit Utrecht. In de periode vanaf 1979 werd deelgenomen aan vijf zeegaande expedities.

PLATE I

Filtered Basement Topography

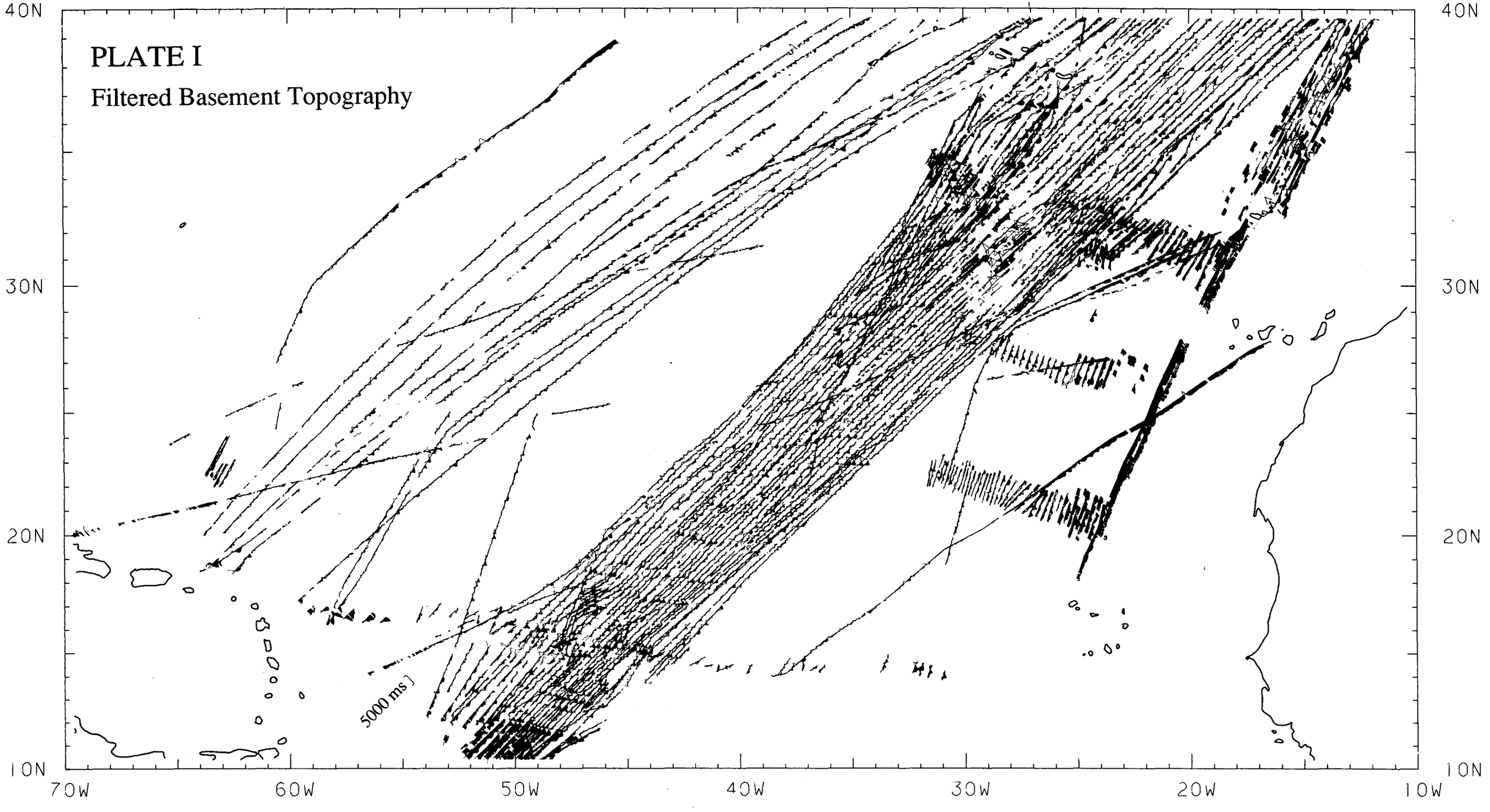

PLATE II

Shaded Basement Relief

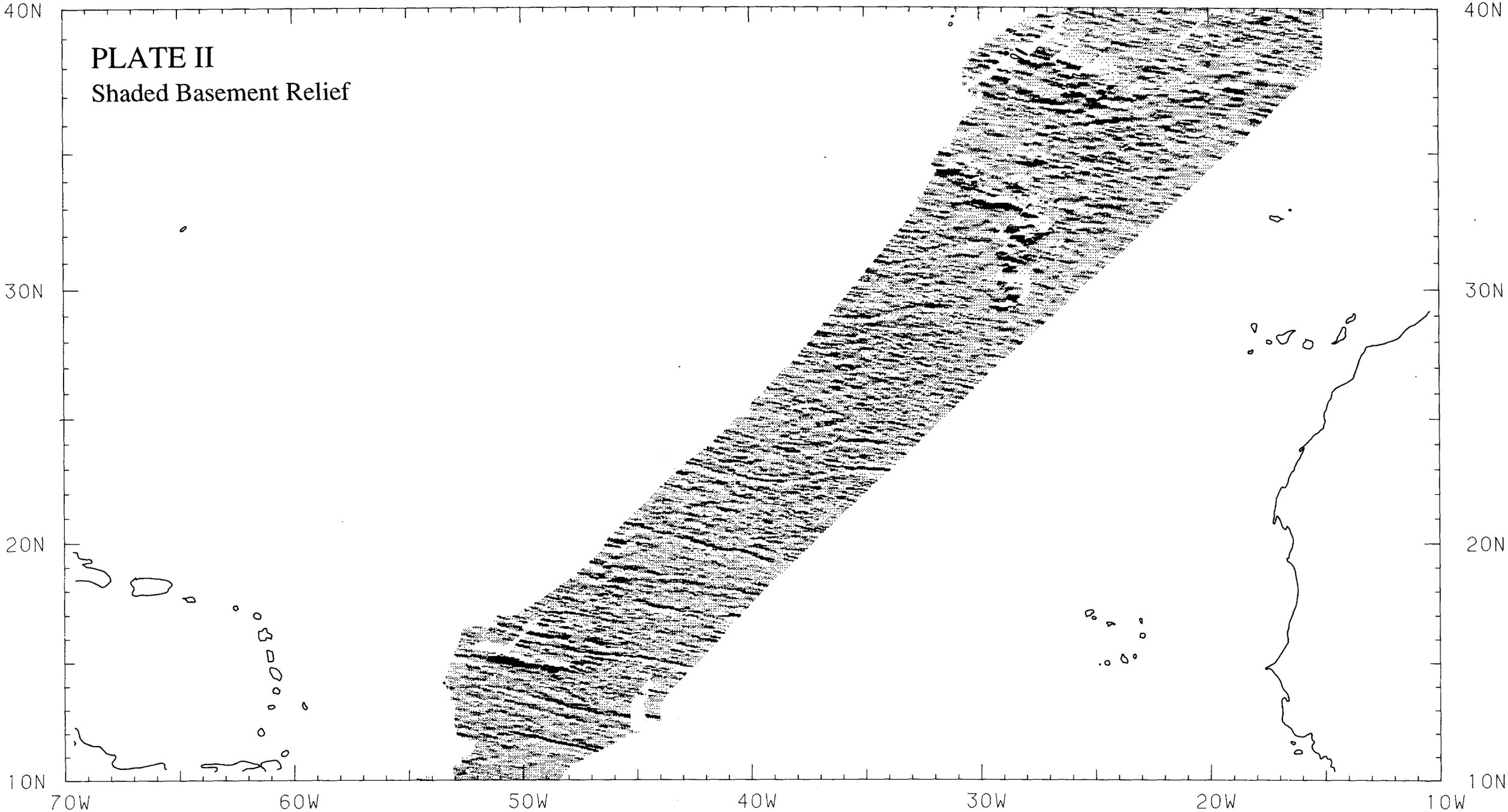

70W 60W 50W 40W 30W 20W 10W

40N

30N

20N

10N

m
0
500
1000
1500
2000
2500
3000
3500
4000
4500
5000
5500
6000

PLATE III
Bathymetry

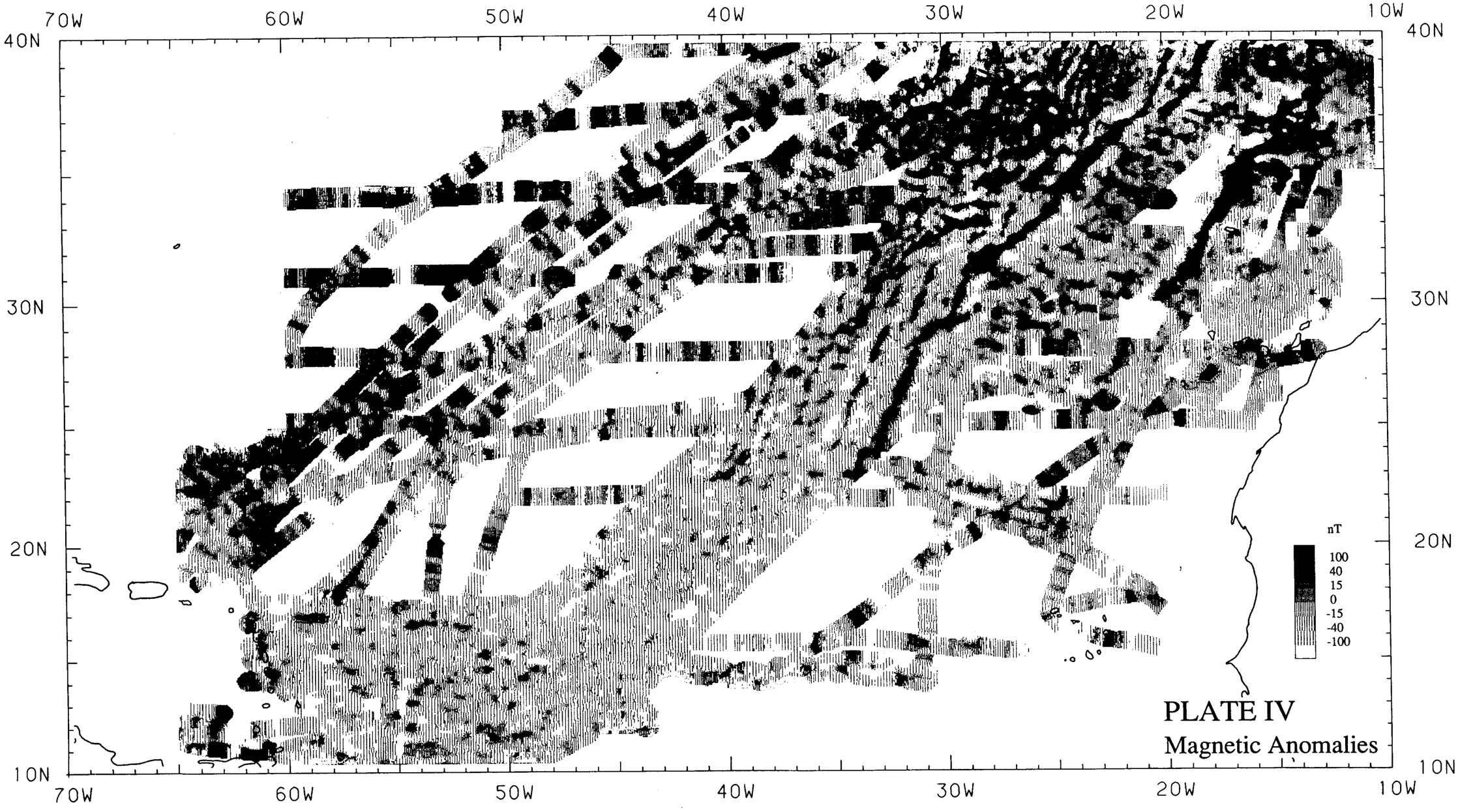
70W
60W
50W
40W
30W
20W
10W
40N
30N
20N
10N
nT
100
40
15
0
-15
-40
-100
PLATE IV
Magnetic Anomalies

PLATE V

Shaded Magnetic Anomalies

Reduced to the Pole

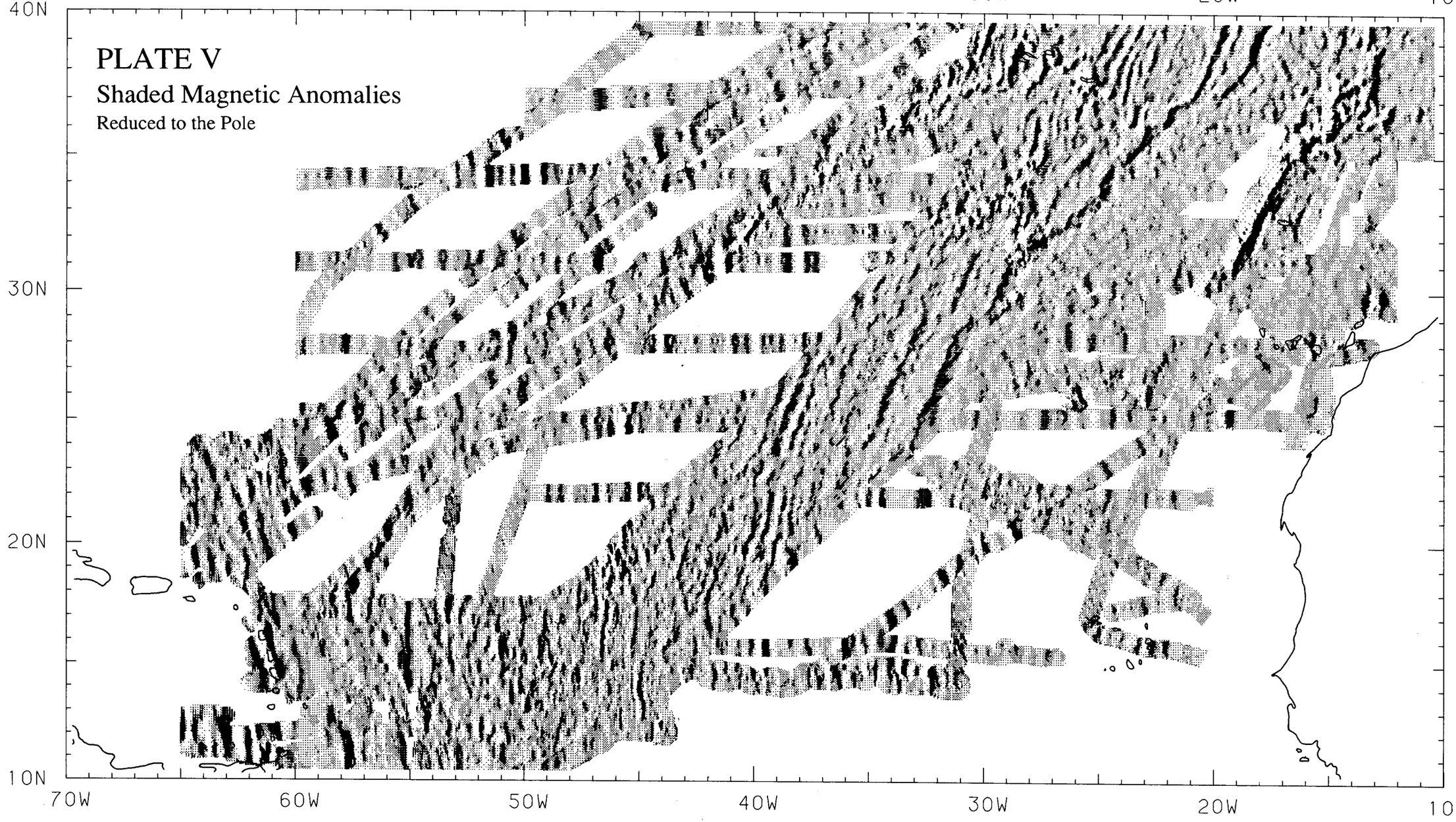

70W 60W 50W 40W 30W 20W 10W

40N 30N 20N 10N

M0 33 25 13 13 25 33 M0

+ M4
× M0
⊙ 34
△ 33
+ 32
× 30/31
⊙ 25
△ 24
+ 21
× 20
⊙ 13
△ 6
+ 5
• earthquake

PLATE VI

Magnetic Anomaly Identifications

after Klitgord and Schouten (1986)

PLATE VII

Free-air Gravity Anomalies

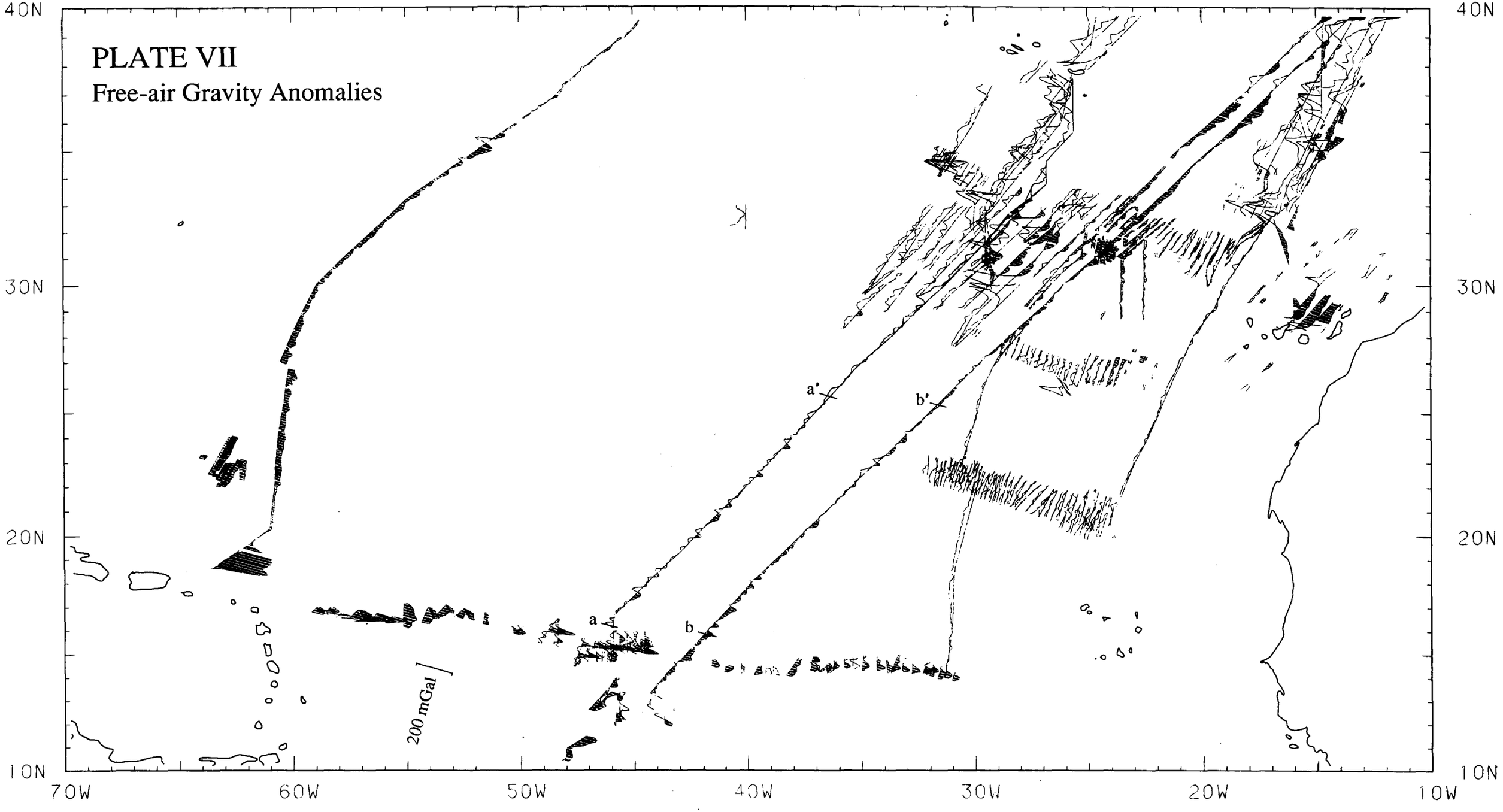

PLATE VIII

Filtered Gravity Anomalies

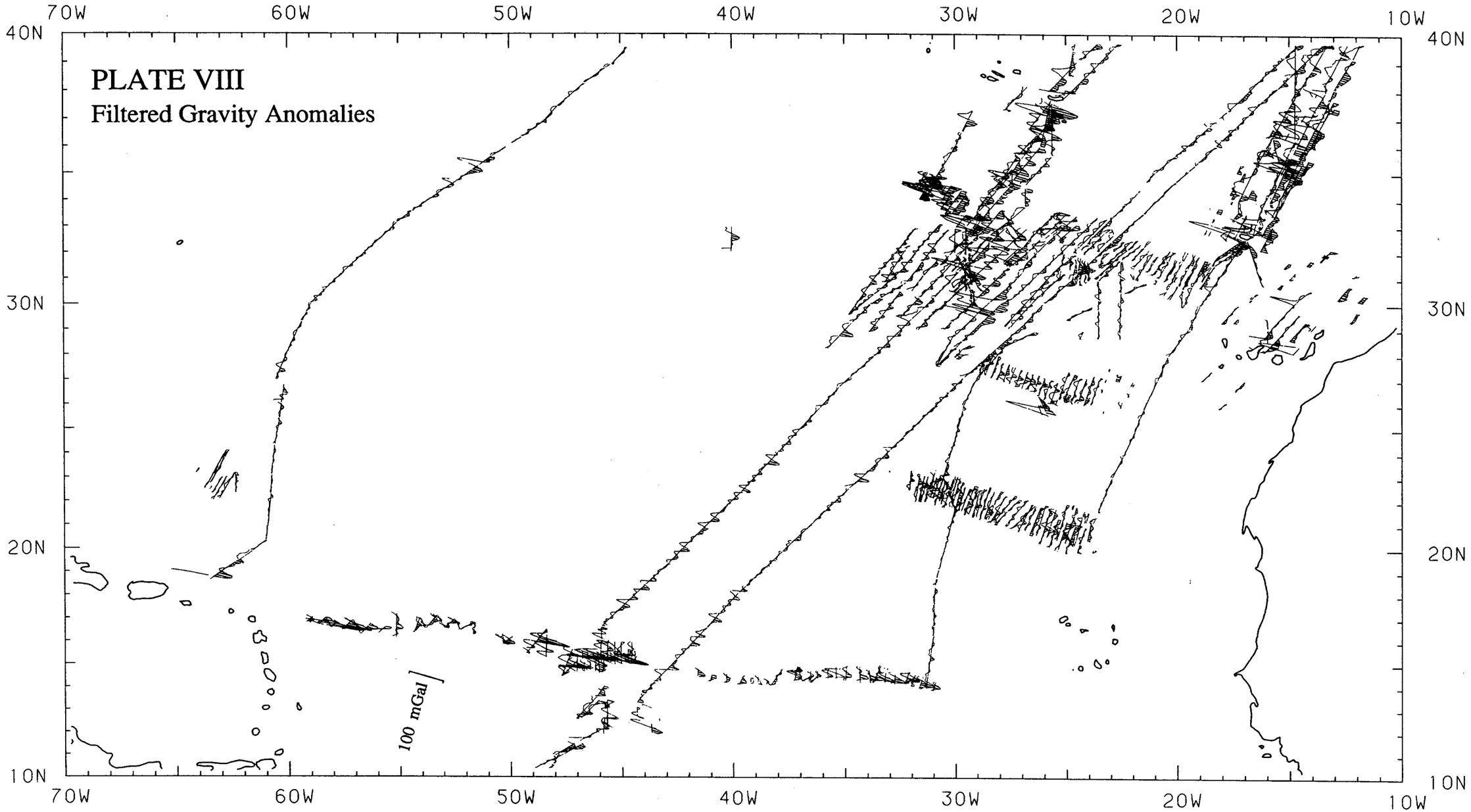

70W 60W 50W 40W 30W 20W 10W

40N 30N 20N 10N

[100 mGal

PLATE IX

Seasat along-track Gravity

descending revolutions

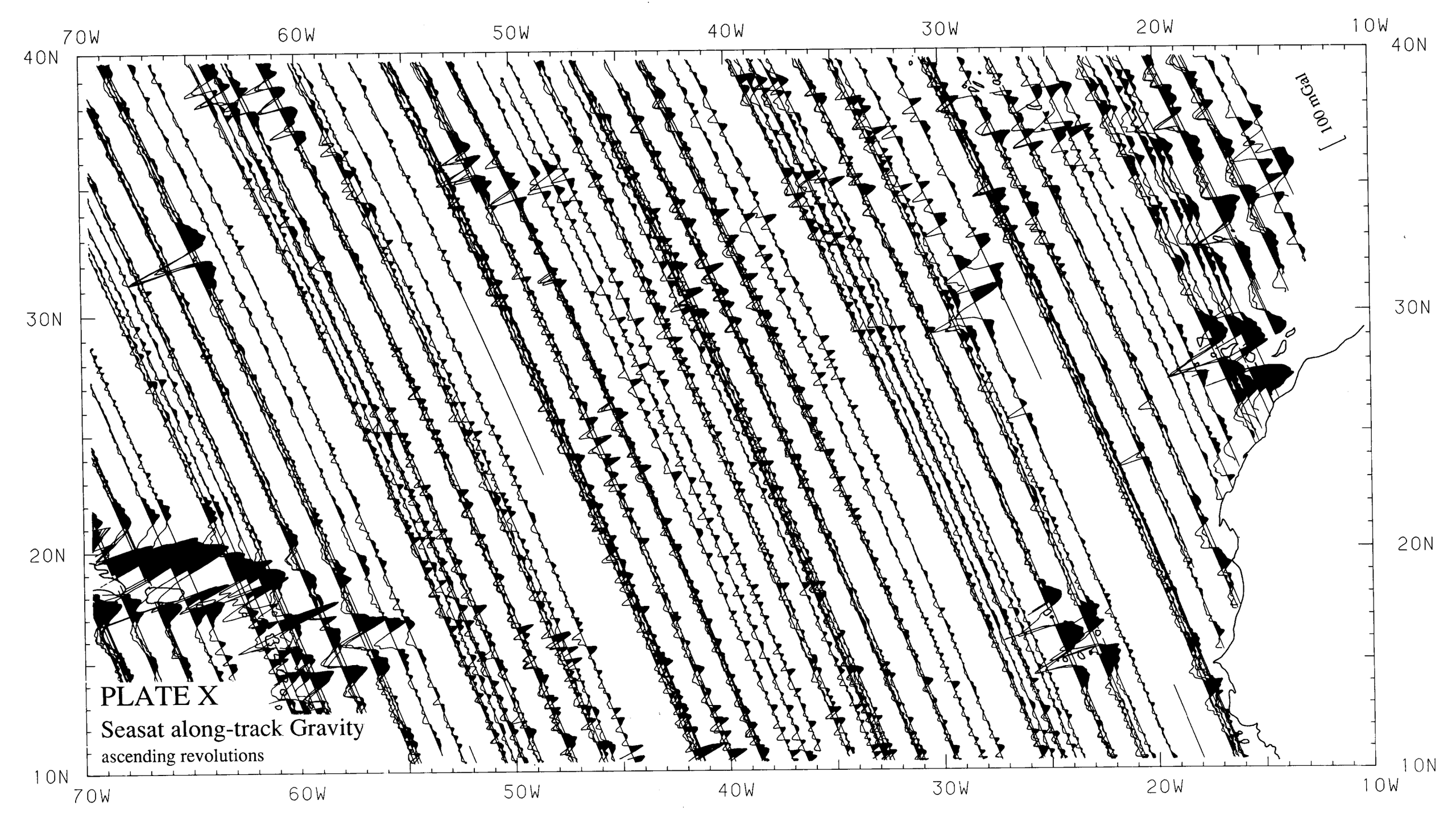
70W
60W
50W
40W
30W
20W
10W
40N
30N
20N
10N
100 mGal
PLATE X
Seasat along-track Gravity
ascending revolutions

PLATE XI

Generated Fracture Zone Segments

after Collette et al. (1984)

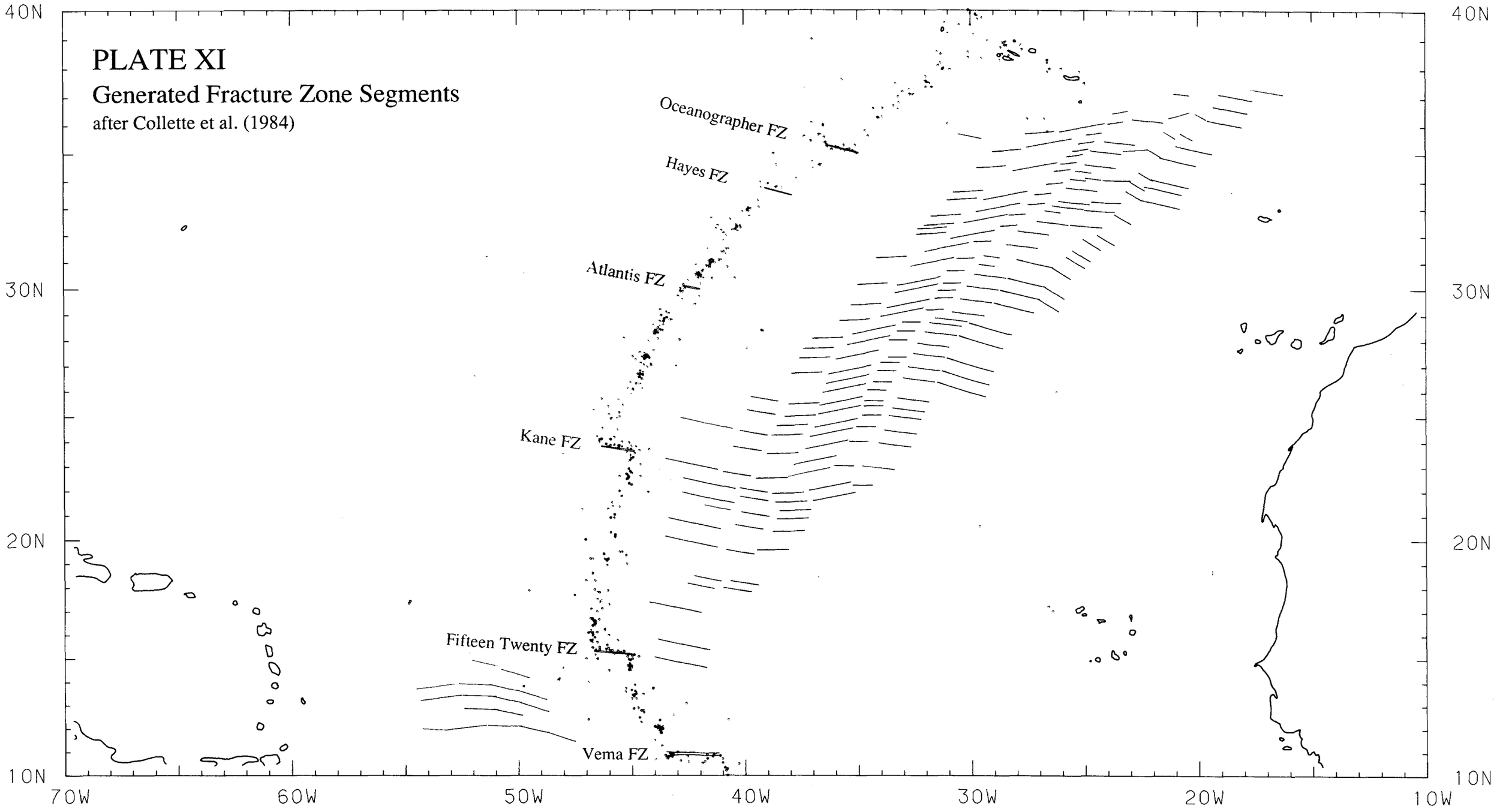

70W 60W 50W 40W 30W 20W 10W

40N 30N 20N 10N

M0 33 30/31 25 21 20 13 6 5 5 6 13 20 21 25 30/31 33 M0

PLATE XII

Synthetic Flowline and Isochron Pattern